CHAPTER V

RESULTS AND DISCUSSION

In this research, the investigation of the influence of surface acidity on the activity of 25wt%V_2O_5/TiO_2, 5wt%W-25wt%V_2O_5/TiO_2, and 3wt%K-25wt% V_2O_5/TiO_2 catalysts in selective catalytic reduction of NO with ammonia have been carried out. The results are divided into four sections. The characterization of the catalysts is reported in section 5.1. Section 5.2 shows the catalytic behavior of the catalysts. The effect of tungsten and potassium loading is given in section 5.3. Finally, section 5.4 explains the effect of SO_2 on the SCR activity.

5.1 Catalyst characterization

5.1.1 Determination of composition of catalyst and surface area

The real compositions of 25wt%V_2O_5/TiO_2, 5wt%W-25wt%V_2O_5/TiO_2, and 3wt%K-25wt%V_2O_5/TiO_2 which are determined by atomic adsorption spectroscopy (AAS) and BET surface area are summarized in Table 5.1.

Table 5.1 The composition of the catalysts and their BET surface areas.

Catalyst	V (wt%)	W (wt%)	K (wt%)	Surface area (m^2/g)
TiO_2	-	-	-	11.88
25wt%V_2O_5/TiO_2	23	-	-	9.87
5wt%W-25wt%V_2O_5/TiO_2	23	3.5	-	10.78
3wt%K-25wt%V_2O_5/TiO_2	23	-	2.5	12.44
V_2O_5	100	-	-	10.40

The data in table 5.1 demonstrates that when tungsten and potassium are added, the surface area of both catalysts slightly changes. Thus, tungsten and potassium loading barely affect the fluctuation of surface area.

5.1.2 X-ray Diffraction (XRD) and FT-IR analysis

X-ray Diffraction is a technique which can identify the crystal structure. The XRD patterns for the pure TiO_2 (anatase) support and crystalline V_2O_5 structures are shown in figures 5.1 and 5.2, respectively, and used as reference. Figure 5.3 presents the XRD pattern of 25wt%V_2O_5/TiO_2. Comparison of figure 5.3 with the reference patterns (figures 5.1 and 5.2), it is apparent that both crystalline vanadia and titania (anatase) are found on 25wt%V_2O_5/TiO_2 catalyst. Figures 5.4 and 5.5 show the XRD patterns of 5wt%W-25wt%V_2O_5/TiO_2 and 3wt%K-25wt%V_2O_5/TiO_2, respectively. When adding potassium and tungsten in 25wt%V_2O_5/TiO_2, a difference between spectra can not be observed. This means that the amount of both potassium and tungsten on 25wt%V_2O_5/TiO_2 surface may be not enough to be detected by XRD or both potassium and tungsten do not form as crystalline structure on the 25wt%V_2O_5/TiO_2 based catalyst.

The functional group on the 25wt%V_2O_5/TiO_2-based catalysts can be identified by using Fourier Transform Infrared Spectroscopy in the wavelength of 400 – 4000 cm^{-1}.

The IR spectra of pure TiO_2 (anatase) support and V_2O_5 are presented in figures 5.6 and 5.7. The major bands of pure TiO_2 (anatase phase) appear near 640 cm^{-1}, and 860 cm^{-1}, whereas the bands of V_2O_5 present at 490 cm^{-1}, 610 cm^{-1}, 833 cm^{-1}, and 1022 cm^{-1}. The bands at 1022 cm^{-1} and 833 cm^{-1} have been assigned to the V=O and V-O-V species, respectively [Charr *et al.* 1988]. Figure 5.8 shows the IR spectrum of 25wt%V_2O_5/TiO_2. Comparing the spectrum with the reference spectra, the band near 1022 cm^{-1} and 860 cm^{-1} can be observed. It can be concluded that the important species on 25wt%V_2O_5/TiO_2 surface are the V=O and V-O-V species. The IR spectra of 5wt%W-25wt%V_2O_5/TiO_2 and 3wt%K-25wt%V_2O_5/TiO_2 are shown in figures 5.9 and 5.10, respectively. When compared to the IR spectrum of 25wt%V_2O_5/TiO_2, a difference between spectra can not be detected. This can be suggested that the amount of tungsten and potassium loading may be not enough to be detected by FT-IR. Thus, no new band can be observed.

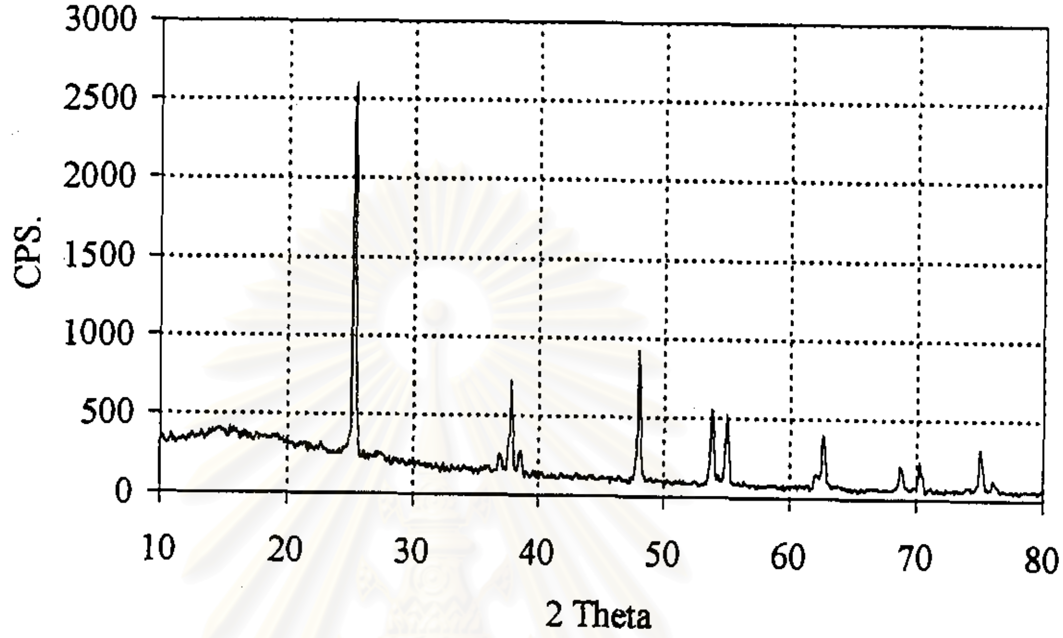

Figure 5.1 XRD pattern of pure TiO_2 support

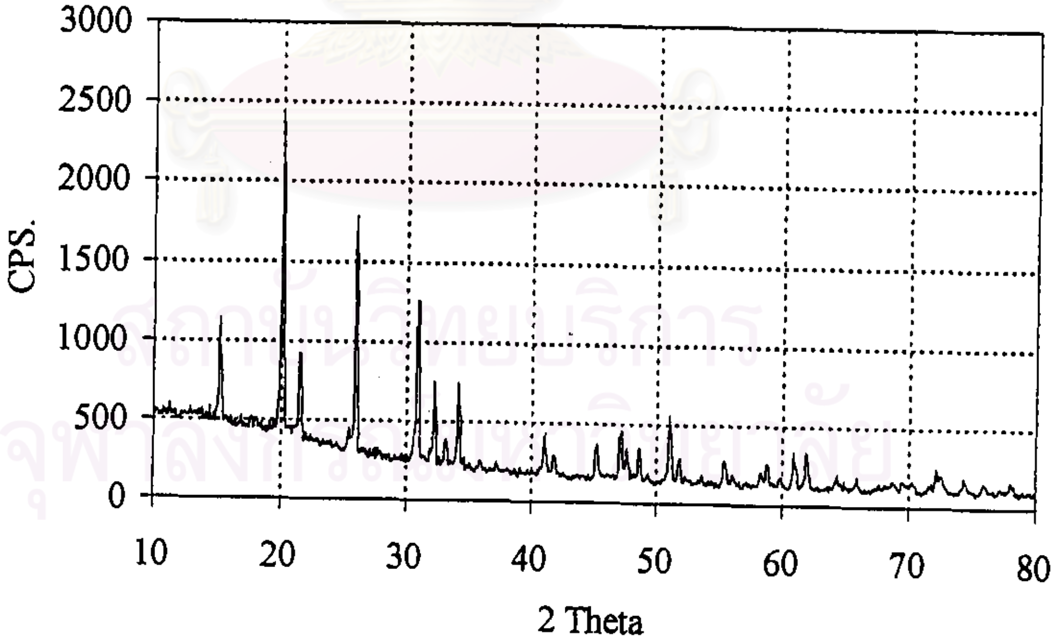

Figure 5.2 XRD pattern of pure V_2O_5

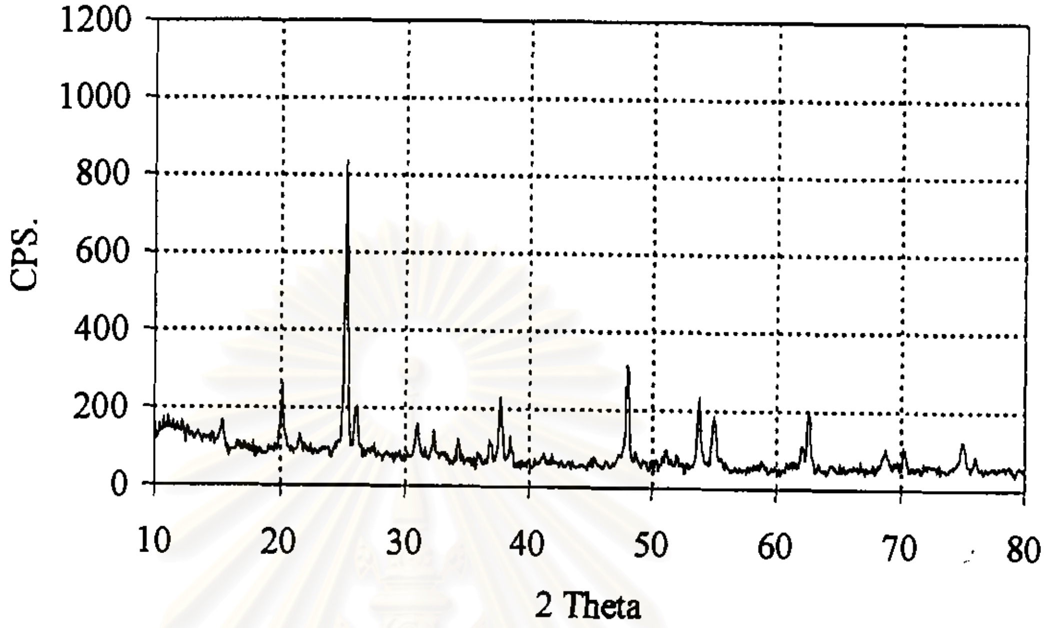

Figure 5.3 XRD pattern of 25wt%V_2O_5/TiO_2

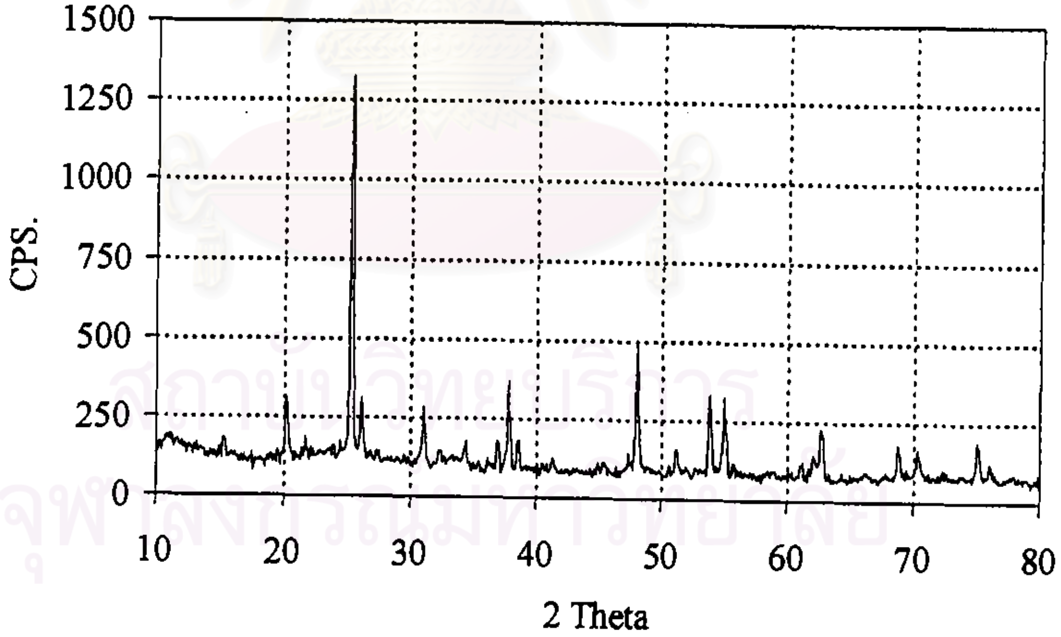

Figure 5.4 XRD pattern of 5wt%W-25wt%V_2O_5/TiO_2

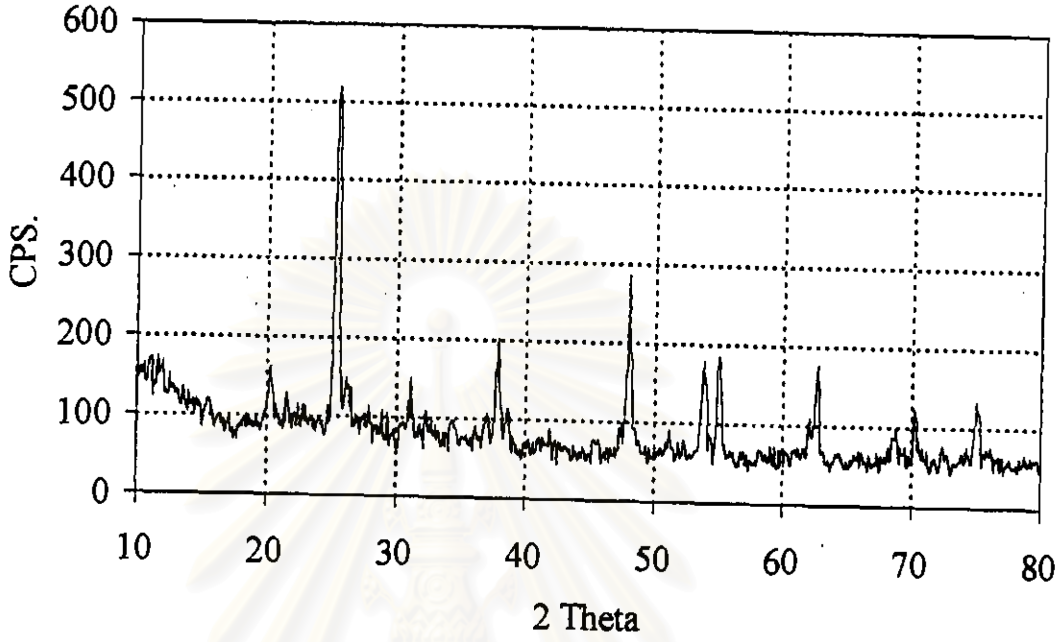

Figure 5.5 XRD pattern of 3wt%K-25wt%V_2O_5/TiO_2

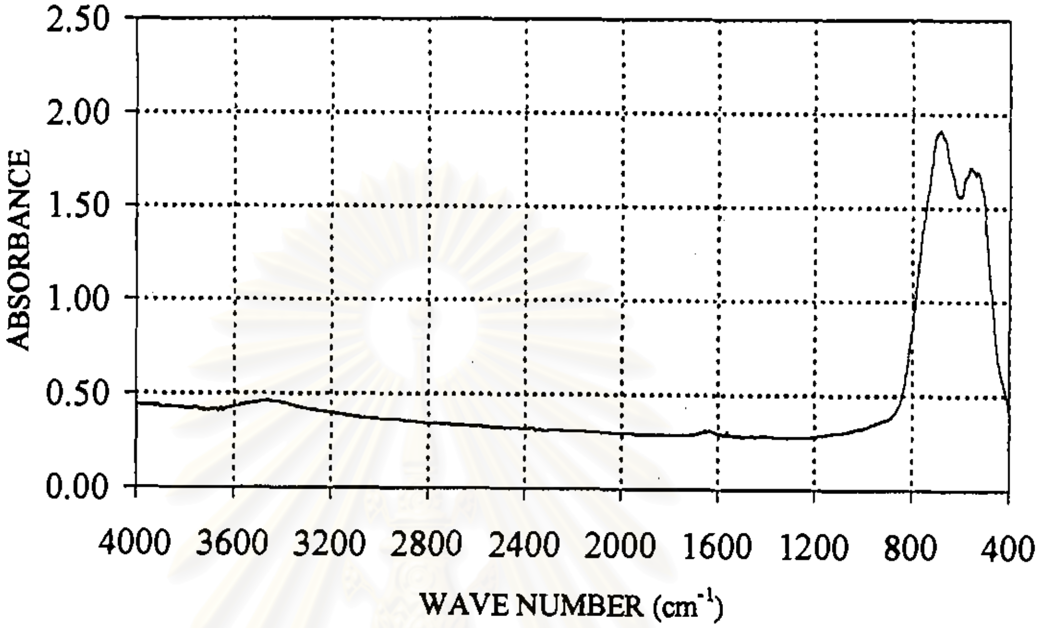

Figure 5.6 IR spectrum of pure TiO_2 support

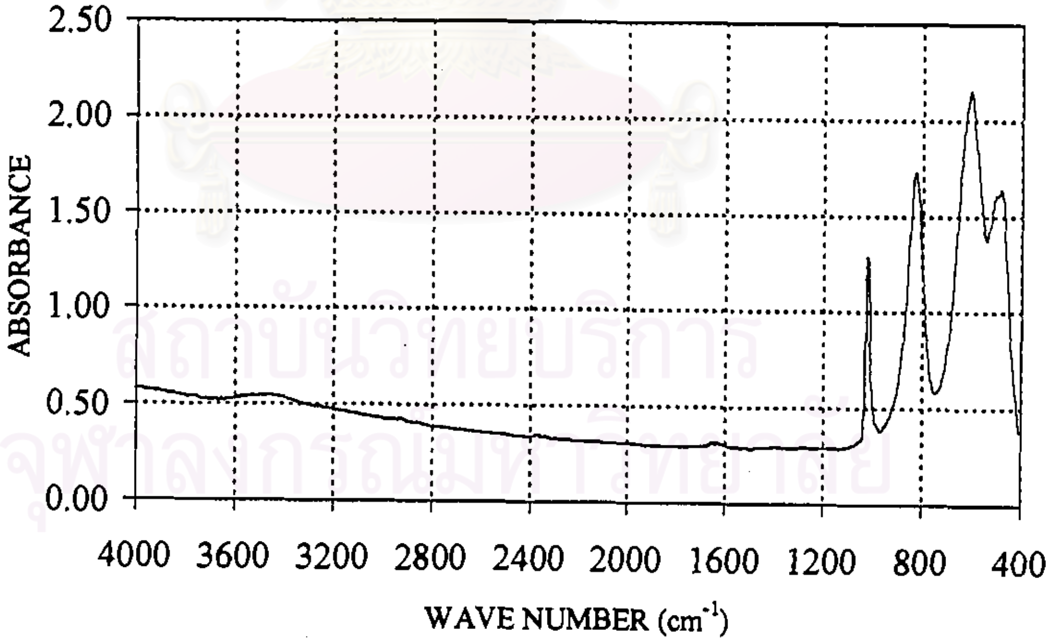

Figure 5.7 IR spectrum of pure V_2O_5

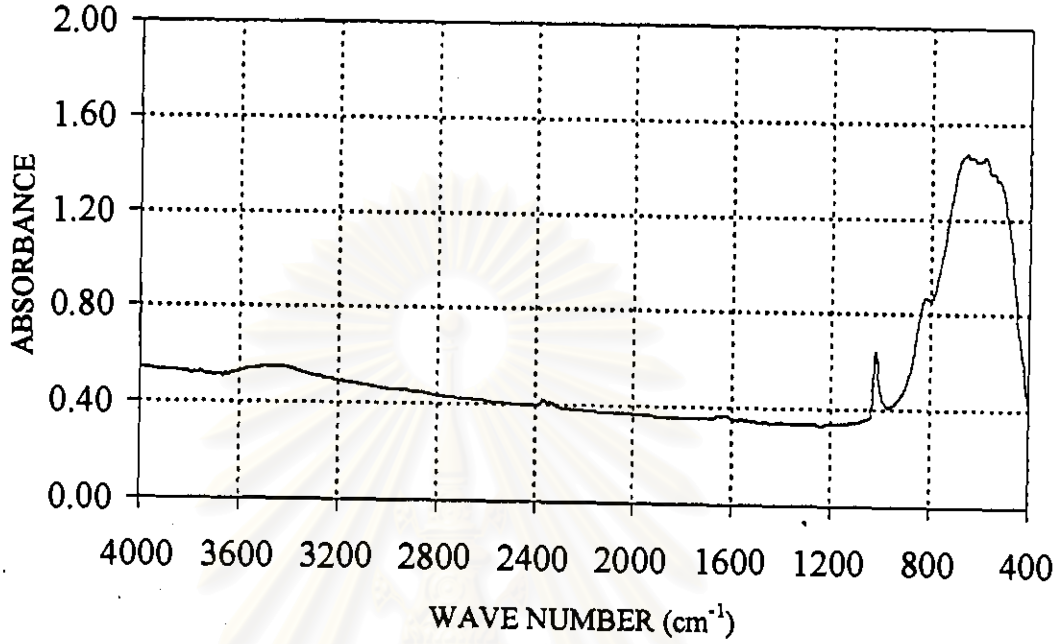

Figure 5.8 IR spectrum of 25wt%V_2O_5/TiO_2

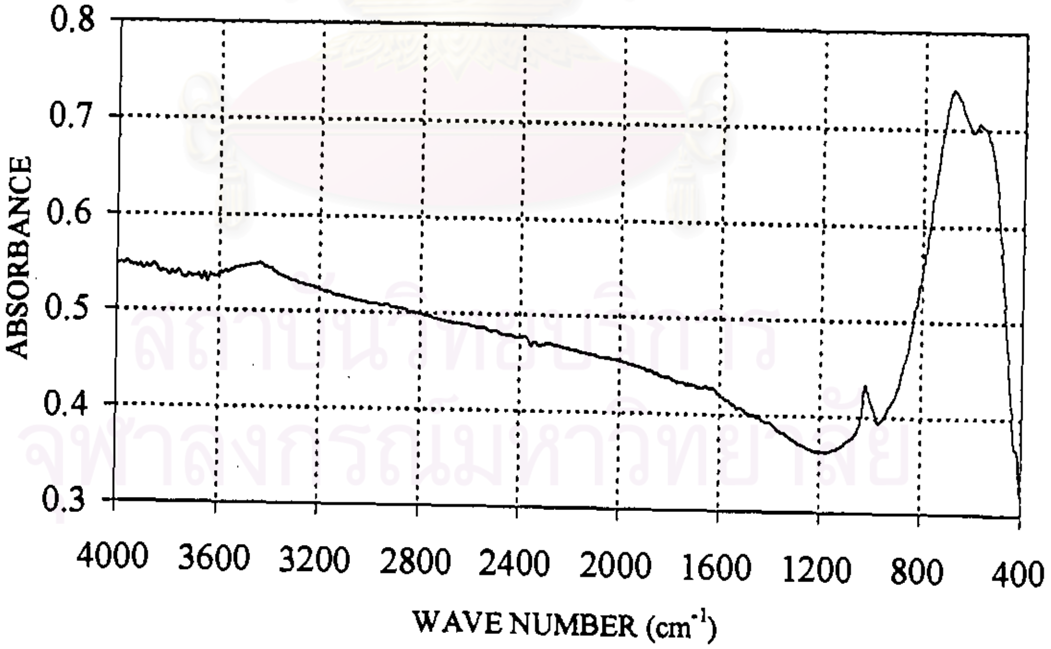

Figure 5.9 IR spectrum of 5wt%W-25wt%V_2O_5/TiO_2

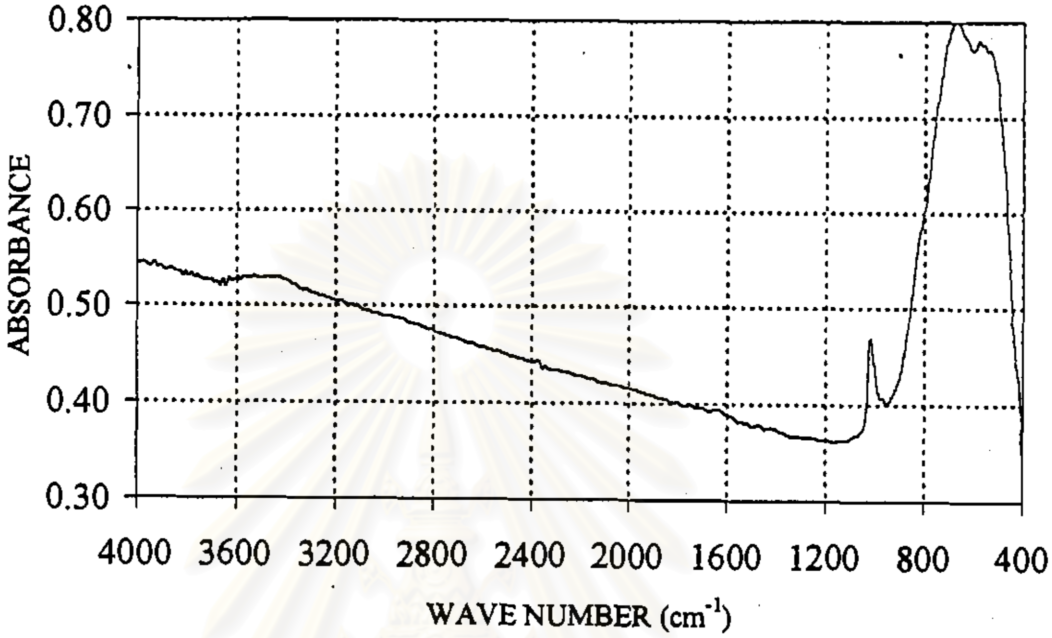

Figure 5.10 IR spectrum of 3wt%K-25wt%V_2O_5/TiO_2

5.1.3 Surface acidity

As discussed earlier, the surface acid properties of the catalysts involve in the selective catalytic reduction path of NO by NH_3. In a further experiment, the pyridine adsorption was used in order to investigate the nature of acid site on the surface.

- Pure TiO_2 support

Figure 5.11 shows the IR spectra obtained from adsorbed pyridine on pure TiO_2 support at room temperature up to 250 °C. It is cleared from the present work and other published works [Barrow *et al.* 1956, Gill *et al.* 1961] that the spectrum of the adsorbed pyridine at room temperature shows the band at 1445 cm^{-1} and the band near 1600 cm^{-1} due to coordinatively adsorbed pyridine on Lewis acid sites. The weaker band around 1480 cm^{-1} is ascribed to proton acidity [Parry 1963], while both the band at 1540 cm^{-1} and 1640 cm^{-1} representative of pyridium ions adsorbed on Brönsted acid sites can not be observed. This suggests that on pure TiO_2 support only Lewis acid site presents. After heating under evacuation at room temperature up to 250 °C, it can be observed that the adsorbed band of coordinated pyridine (1445 cm^{-1}) gradually decreases until hardly detectable at 250 °C. Figure 5.12(A) shows the percentage of the decrease of pyridine adsorbed on Lewis acid sites (the band at 1445 cm^{-1}) at various temperatures on pure TiO_2 support, whereas the amount of desorbed pyridine (the band at 1445 cm^{-1}) at different temperatures on pure TiO_2 support is shown in figure 5.12(B). The amount of desorbed pyridine at various temperatures is the amount and strength of acid site which is Lewis acid site of pure TiO_2 support. It is found that at temperature below 150 °C, the amount of desorbed pyridine is much more than that at higher temperatures. This means that most of acid sites on pure TiO_2 support is weak Lewis acid site.

The IR spectra of pyridine adsorption on pure TiO_2 support after preadsorption by SO_2, and evacuation at different temperature, are shown in figure 5.13. In the same manner, the figure shows the presence of coordinatively adsorbed pyridine (1445 cm^{-1} and 1600 cm^{-1}). By comparing the IR spectra of pure TiO_2 support with and without SO_2 predesorption at room temperature, IR spectrum of pure TiO_2 support with preadsorption by SO_2 shows remarkable difference. Lewis acid sites of pure TiO_2 support with preadsorption by SO_2 increase more evidently than that of pure TiO_2 support without SO_2 preadsorption while there is no difference of proton acidity on both samples. It is equivalent to saying that preadsorption by SO_2 increases Lewis acid sites on pure TiO_2 support. Figure 5.14(A) shows the percentage of the decrease of pyridine adsorbed on Lewis acid sites (1445 cm^{-1}) at various temperatures on pure TiO_2 support after preadsorption by SO_2 and figure 5.14(B) shows the amount of pyridine desorbed from Lewis acid site at different temperatures on pure TiO_2 after SO_2 preadsorption. From figures 5.14(A) and 5.14(B), it can be illustrated that adsorbed pyridine at lower temperature especially below 150 °C is released more enormously while that at higher temperature, though decreased but not rapidly. Additionally, only weak Lewis acid sites are observed on pure TiO_2 support with preadsorption by SO_2 similar to pure TiO_2 support without preadsorption. This means that preadsorption by SO_2 promotes the amount of weak Lewis acid site not strong Lewis acid site.

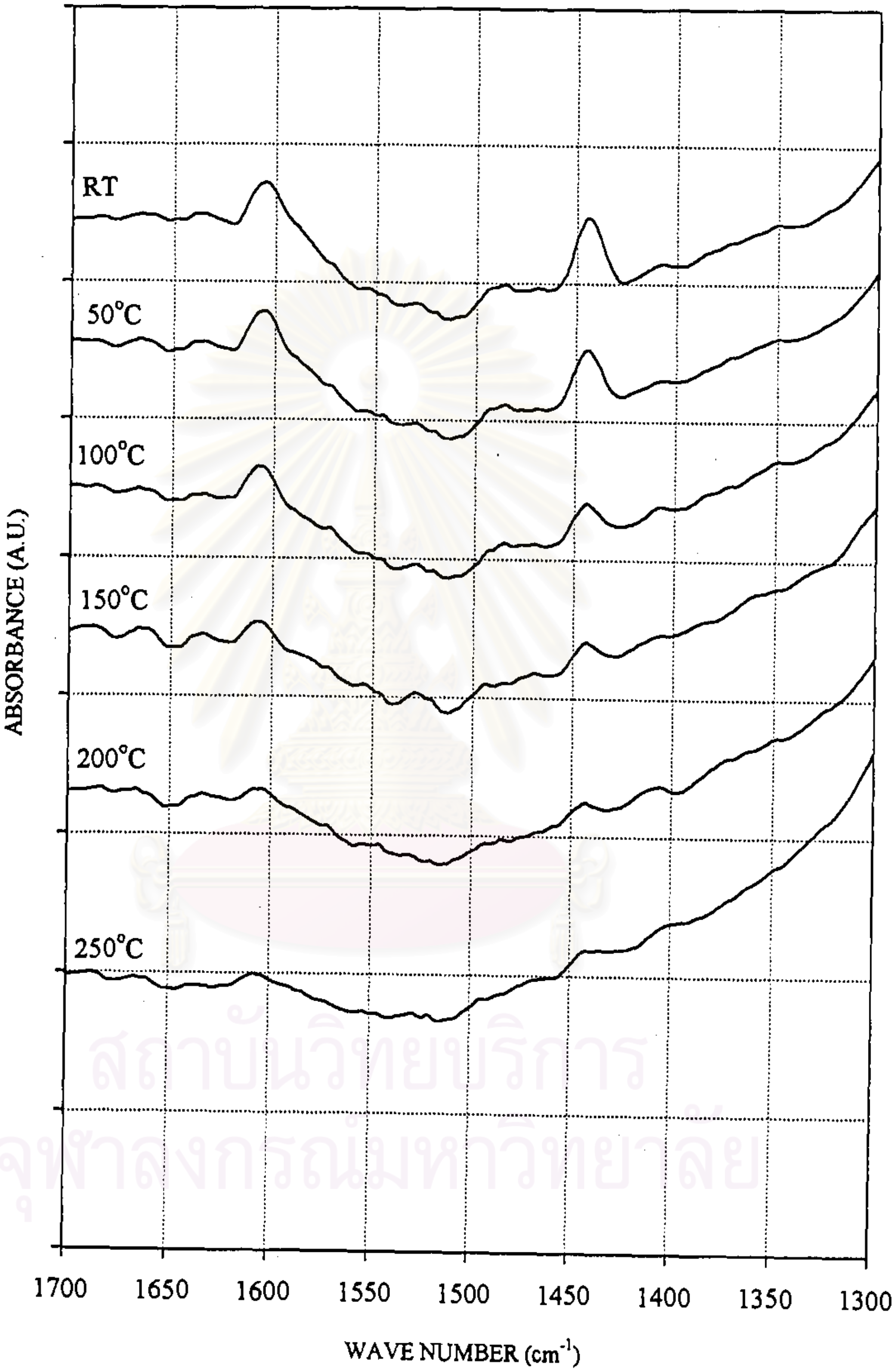

Figure 5.11 Pyridine adsorption on pure TiO_2 support

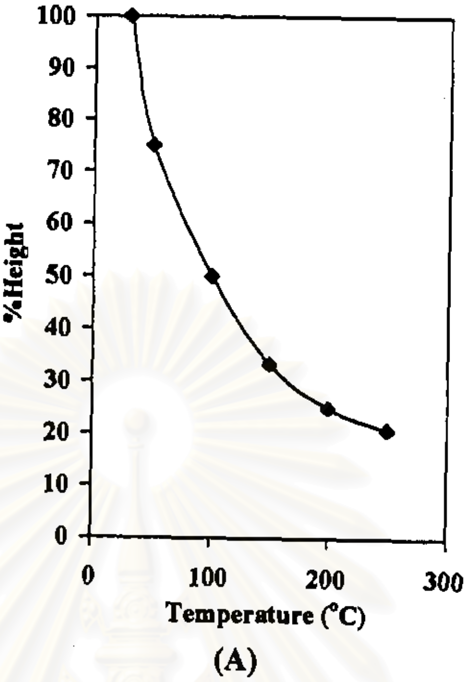

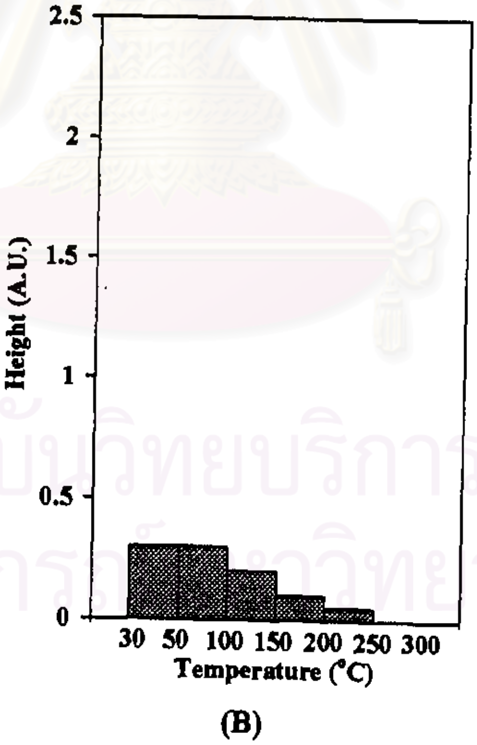

Figure 5.12 (A) The percentage of the band height of pyridine adsorbed on Lewis acid site of pure TiO_2 support at various temperatures

(B) The amount of pyridine desorbed from Lewis acid site of pure TiO_2 support at various temperatures

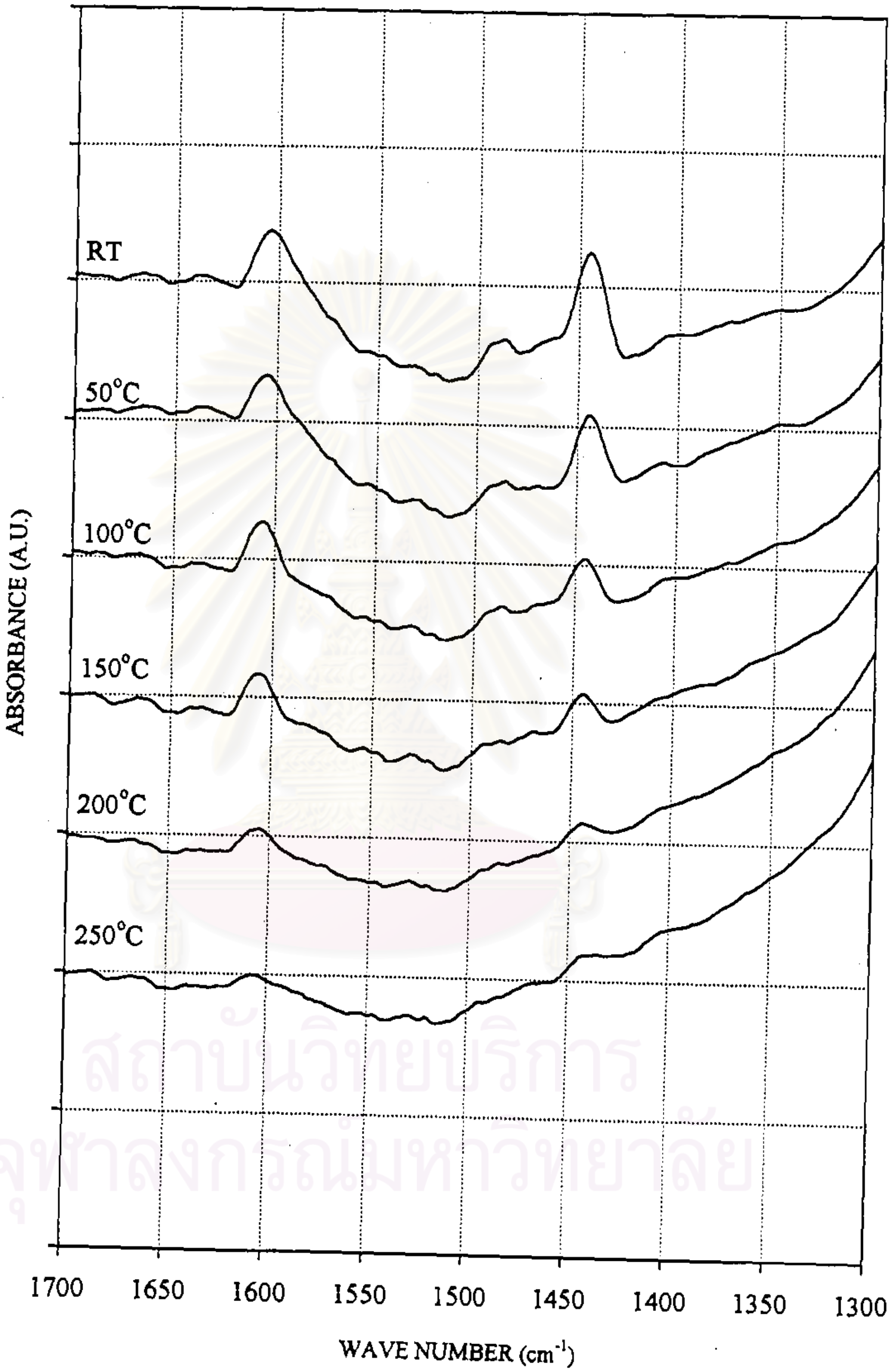

Figure 5.13 Pyridine adsorption on pure TiO_2 support after SO_2 preadsorbtion

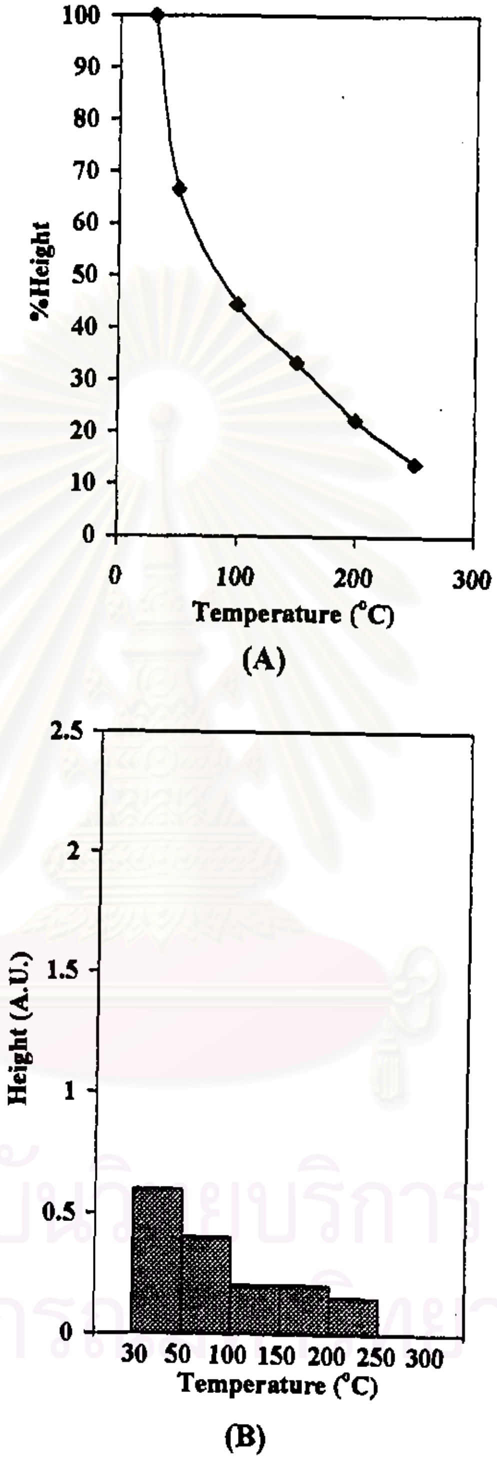

Figure 5.14 (A) The percentage of the band height of pyridine adsorbed on Lewis acid site of pure TiO_2 support after SO_2 preadsorption at various temperatures

(B) The amount of pyridine desorbed from Lewis acid site of pure TiO_2 support after SO_2 preadsorption at various temperatures

- **Fresh 25wt%V_2O_5/TiO_2**

The IR spectra of pyridine adsorption on fresh 25wt%V_2O_5/TiO_2 catalyst at various temperatures are shown in figure 5.15. Comparison between the adsorbed pyridine spectra of fresh 25wt%V_2O_5/TiO_2 and pure TiO_2 support at room temperature is completely different. For fresh 25wt%V_2O_5/TiO_2, the band due to coordinatively adsorbed pyridine on Lewis acid site (1445 cm^{-1} and 1600 cm^{-1}) and proton acidity (1480 cm^{-1}) is much higher than that of pure TiO_2 support. Surprisingly, the bands due to adsorbed pyridium ions on Brönsted acid site (1540 cm^{-1} and 1640 cm^{-1}) are apparently observed while not found on pure TiO_2 support. It indicates that the increase of Lewis and Brönsted acid site is the result of vanadia loading. Figures 5.16(A) and 5.16(B) show the percentage of the decrease of pyridine adsorbed on Lewis and Brönsted acid sites on fresh 25wt%V_2O_5/TiO_2 at different temperatures. At low temperature pyridine adsorbed on both Lewis and Brönsted acid sites dramatically decrease, while at high temperature they slightly drop. The amount and strength of Lewis and Brönsted acid site on fresh 25wt%V_2O_5/TiO_2 is shown in Figure 5.16(C) and 5.16(D). The figures show that the amount of pyridine desorbed from Lewis acid sites at temperature below 150 °C is much more than the amount desorbed at higher temperature. In the case of Brönsted acid sites, the amount of desorbed pyridine is mainly found at 100-200 °C. After heating at 300 °C, the pyridine adsorbed on Lewis and Brönsted acid sites still appear, showing that a minor amount of pyridine adsorbed on both Lewis and Brönsted acid sites is strongly bonded.

Figure 5.17 shows the IR spectra of pyridine adsorption on fresh 25wt%V_2O_5/TiO_2 catalyst after SO_2 preadsorption. After evacuation at room temperature, the IR spectrum shows again the presence of both Lewis acid sites (1445 cm^{-1} and 1600 cm^{-1}) and Brönsted acid sites (1540 cm^{-1} and 1640 cm^{-1}). A comparison between the IR spectra at room temperature of fresh 25wt%V_2O_5/TiO_2 after and before SO_2 preadsorption (figure 5.15), showing that the intensity of the band belongs to pyridinium ions adsorbed on Brönsted acid sites (1540 cm^{-1}) and coordinatively adsorbed pyridine (1445 cm^{-1}) increase. This means that SO_2

preadsorption increases the amount of both Lewis and Brönsted acid sites at various temperatures. Figures 5.18 shows the decrease of pyridine adsorbed on Lewis and Brönsted acid site and the amount of pyridine desorption from Lewis and Brönsted acid site. Comparison between figure 5.18 and figure 5.16 shows that both the number and strength of Lewis and Brönsted acid sites increase when the catalyst is preadsorbed by SO_2.

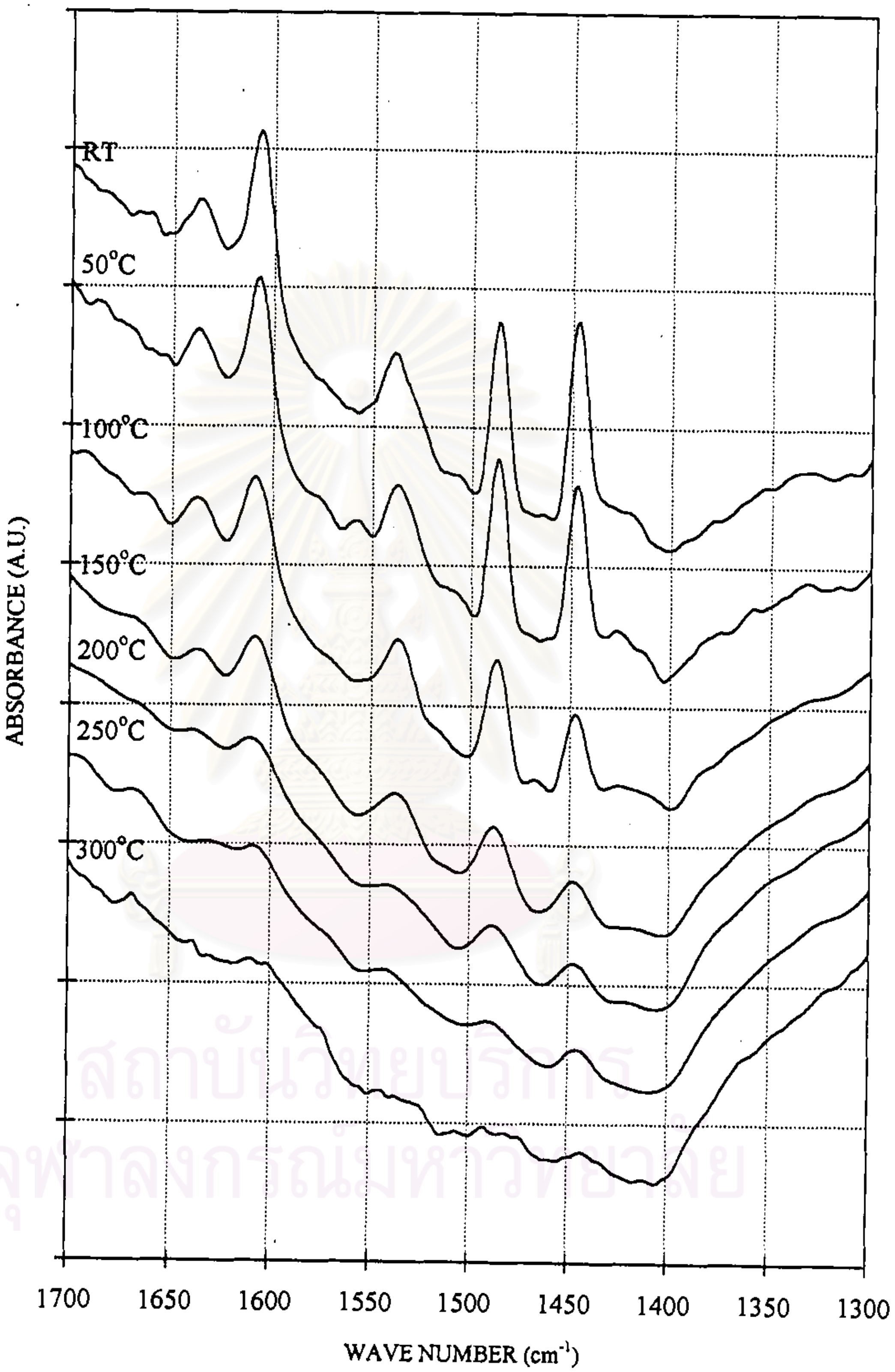

Figure 5.15 Pyridine adsorption on fresh 25wt%V_2O_5/TiO_2

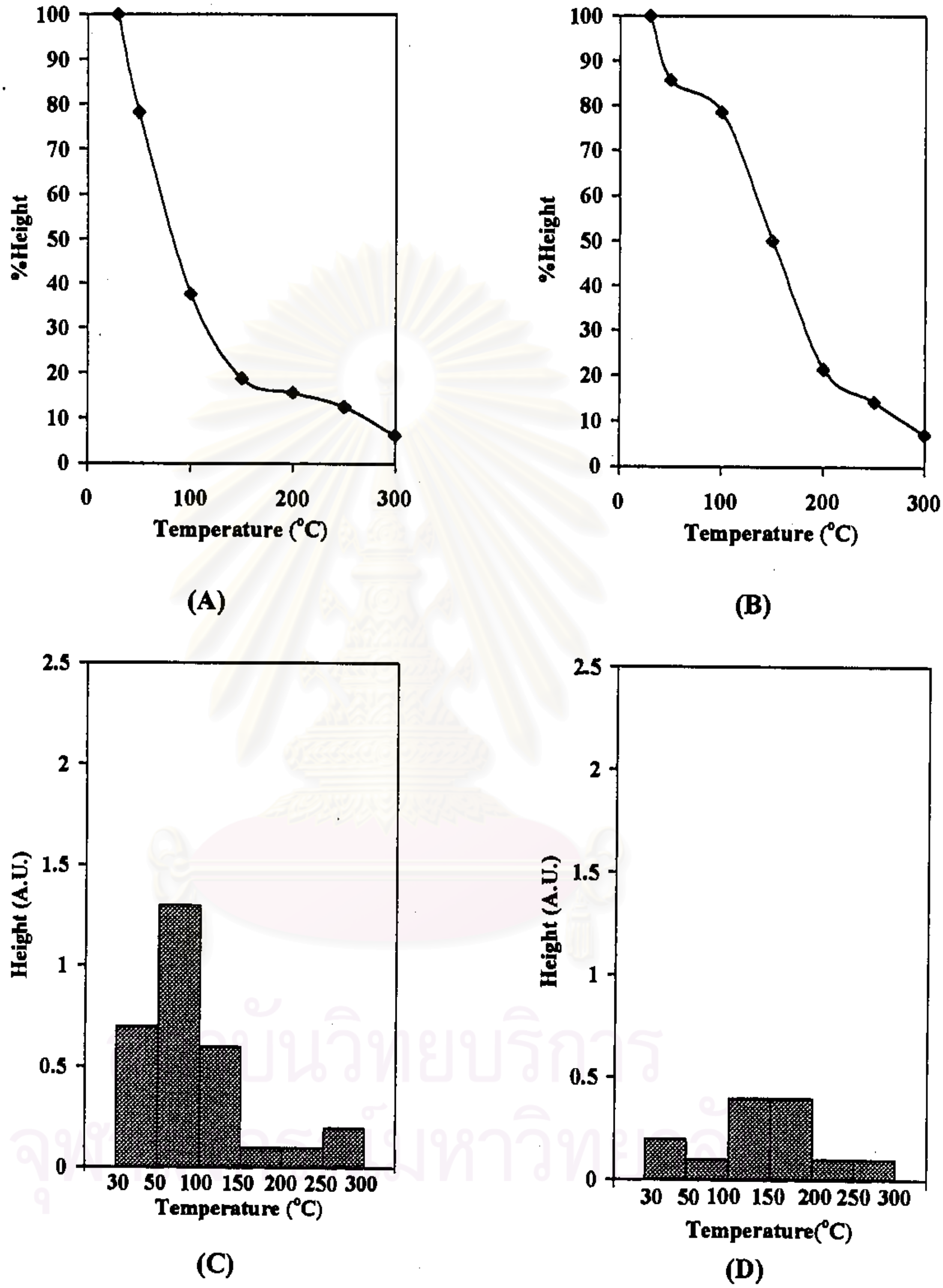

(A)

(B)

(C)

(D)

Figure 5.16 The percentage of the band height of pyridine adsorbed on Lewis (A) and Brönsted (B) acid site and the amount of pyridine desorbed from Lewis (C) and Brönsted (D) acid site on fresh 25wt%V_2O_5/TiO_2

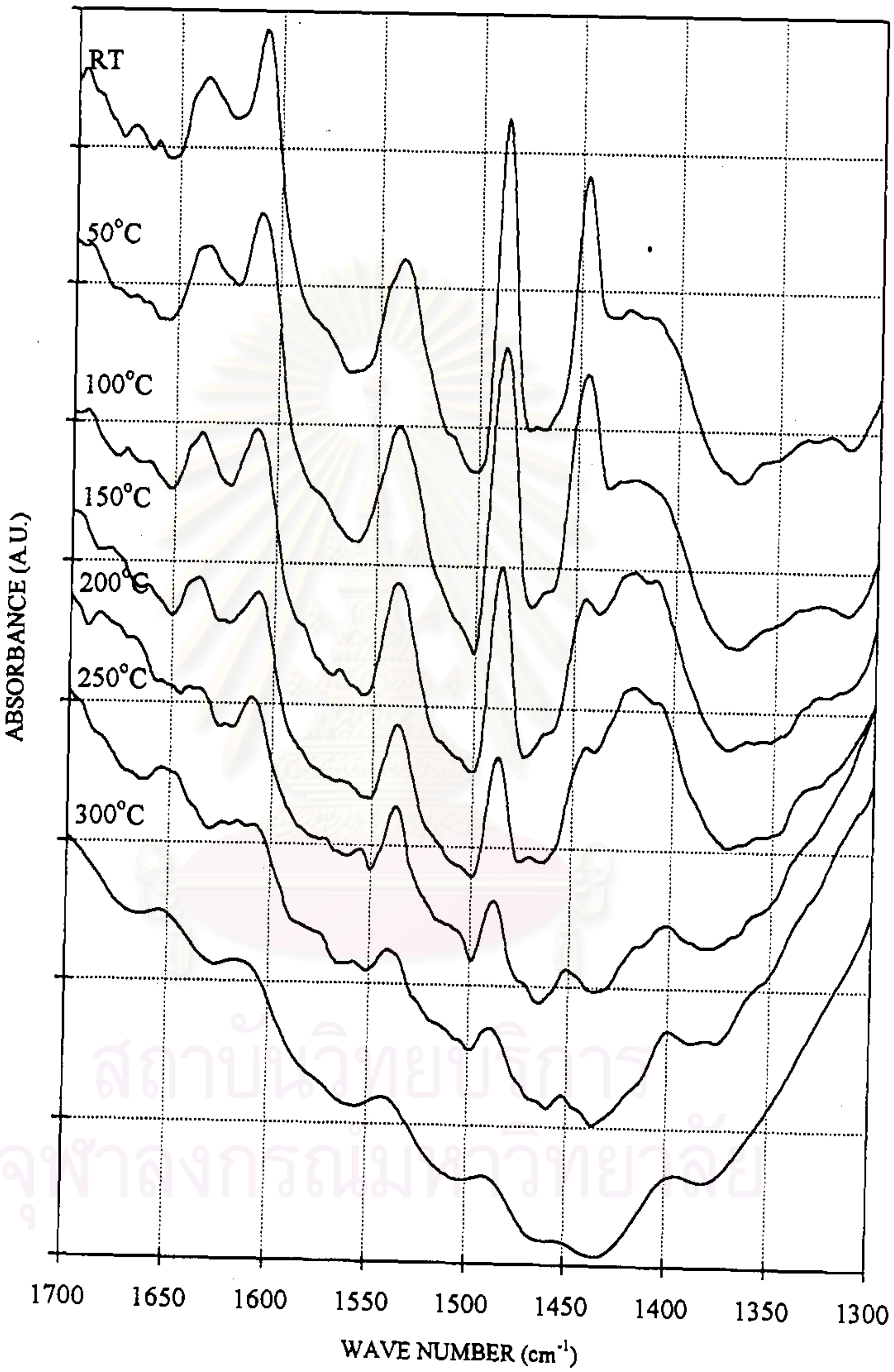

Figure 5.17 Pyridine adsorption on fresh 25wt%V_2O_5/TiO_2 after SO_2 preadsorption

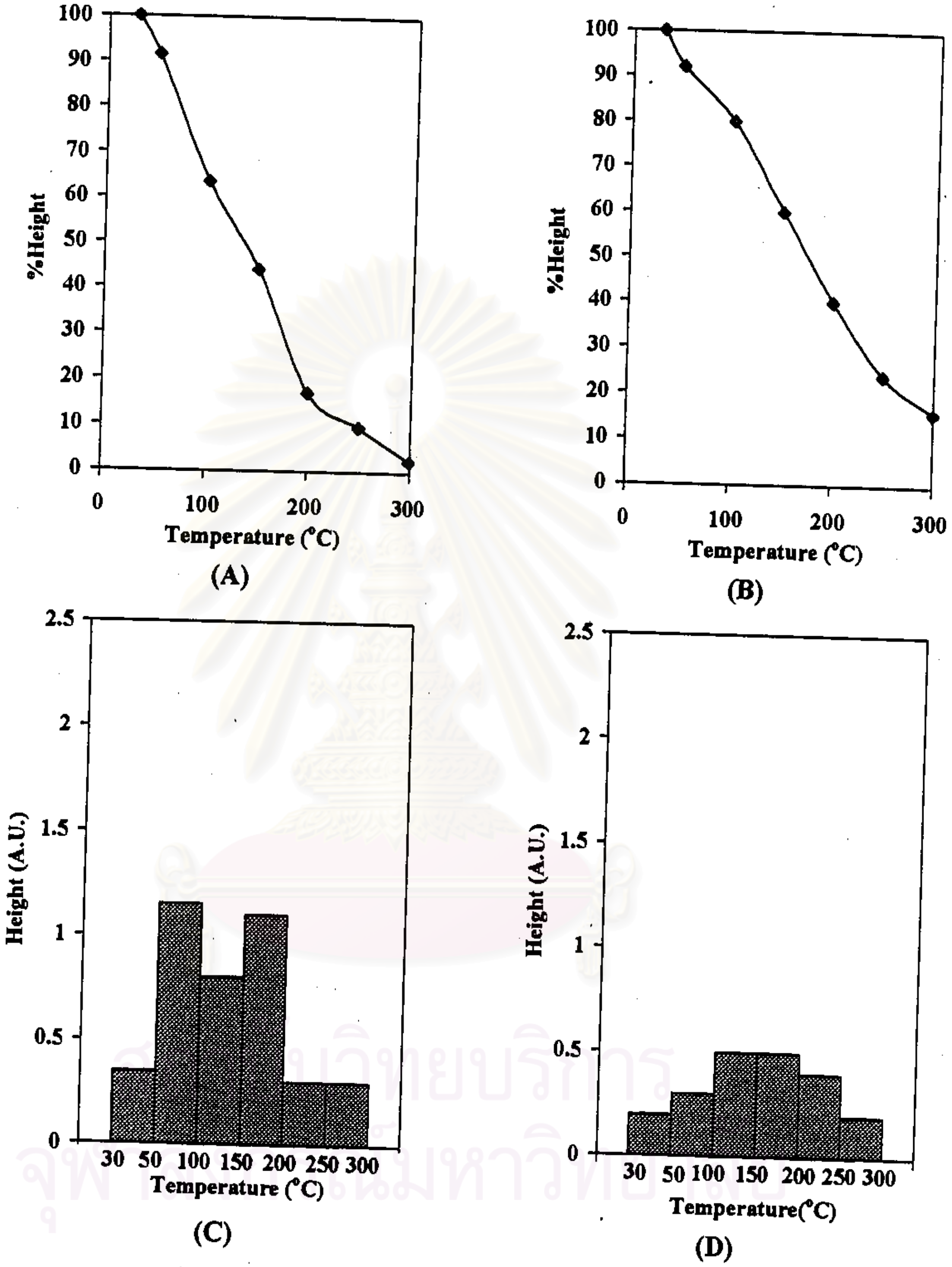

(A)

(B)

(C)

(D)

Figure 5.18 The percentage of the band height of pyridine adsorbed on Lewis (A) and Brönsted (B) acid site and the amount of pyridine desorbed from Lewis (C) and Brönsted (D) acid site on fresh 25wt%V_2O_5/TiO_2 after SO_2 preadsorption

- Fresh 5wt%W-25wt%V_2O_5/TiO_2

Figure 5.19 shows IR spectra obtained from pyridine adsorption on fresh 5wt%W-25wt%V_2O_5/TiO_2 at room temperature up to 300 °C. The main bands (1445 cm^{-1}, 1480 cm^{-1}, 1540 cm^{-1}, 1600 cm^{-1}, and 1640 cm^{-1}) which can be observed on fresh 25wt%V_2O_5/TiO_2 are also presented on fresh 5wt%W-25wt%V_2O_5/TiO_2, and these bands significantly increase in intensity. It means that the increase of both Lewis and Brönsted acid site is due to tungsten loading. The drop of pyridine adsorbed on Lewis and Brönsted acid site after heating up to 300 °C can be seen in figure 5.20(A). Figure 5.20(A) presents that at the low temperature, the pyridine adsorbed on Lewis acid site (1445 cm^{-1}) can desorb rapidly, while that adsorbed on Brönsted acid site does not change significantly at room temperature to 100 °C. When the desorption temperature is higher than 100 °C, subsequently, the pyridine adsorbed on Brönsted acid site dramatically drop. These results suggest that on fresh 5wt%W-25wt%V_2O_5/TiO_2, Brönsted acid sites are stronger than Lewis acid site. Figure 5.20(B) shows the amount of pyridine desorbed from Lewis and Brönsted acid site at various temperatures. By comparing with fresh 25wt%V_2O_5/TiO_2 (figure 5.16), the substantially increase of the amount of pyridine desorbed from Lewis acid sites can be observed at all temperature ranges. While the amount of pyridine desorbed from Brönsted acid site, especially, at high temperature significantly go up too. It can be concluded that tungsten loading not only increases the amount of both Brönsted and Lewis acid sites, but increases the acid strength of them as well.

The IR spectra of pyridine adsorption over fresh 5wt%W-25wt%V_2O_5/TiO_2 after preadsorption by SO_2 is shown in figure 5.21. Comparison of the spectra of fresh 5wt%W-25wt%V_2O_5/TiO_2 with and without SO_2 preadsorption (Figure 5.19), after SO_2 preadsorption, the surface of this catalyst moderately decreases in Lewis acid site (1445 cm^{-1}), while Brönsted acid site is increased. The result is different from SO_2 preadsorption on both fresh 25wt%V_2O_5/TiO_2 and pure TiO_2 support which found that SO_2 increase both Lewis and Brönsted acid sites. Figures 5.22(A) shows the decrease of pyridine adsorption on Lewis and Brönsted acid site. It has been found that the adsorbed pyridine on Lewis acid site is rapidly declined in the temperature ranges 50 °C-200 °C and marginally decreased at higher temperature. In the case of pyridine adsorbed on Brönsted acid site compared with that on fresh 5wt%W-25wt%V_2O_5/TiO_2 before SO_2 preadsorption, at low temperature, after SO_2 preadsorption the adsorbed pyridine on Brönsted acid site decreases more than that before SO_2 preadsorption. The amount of pyridine desorbed from Lewis and Brönsted acid site on fresh 5wt%W-25wt%V_2O_5/TiO_2 at different temperatures is shown in figure 5.22(B). At low temperature, the pyridine desorbed on both Lewis and Brönsted acid site significantly increase more than that at high temperature. While Brönsted acid site, after preadsorption by SO_2, is increased in a weak and strong acid sites.

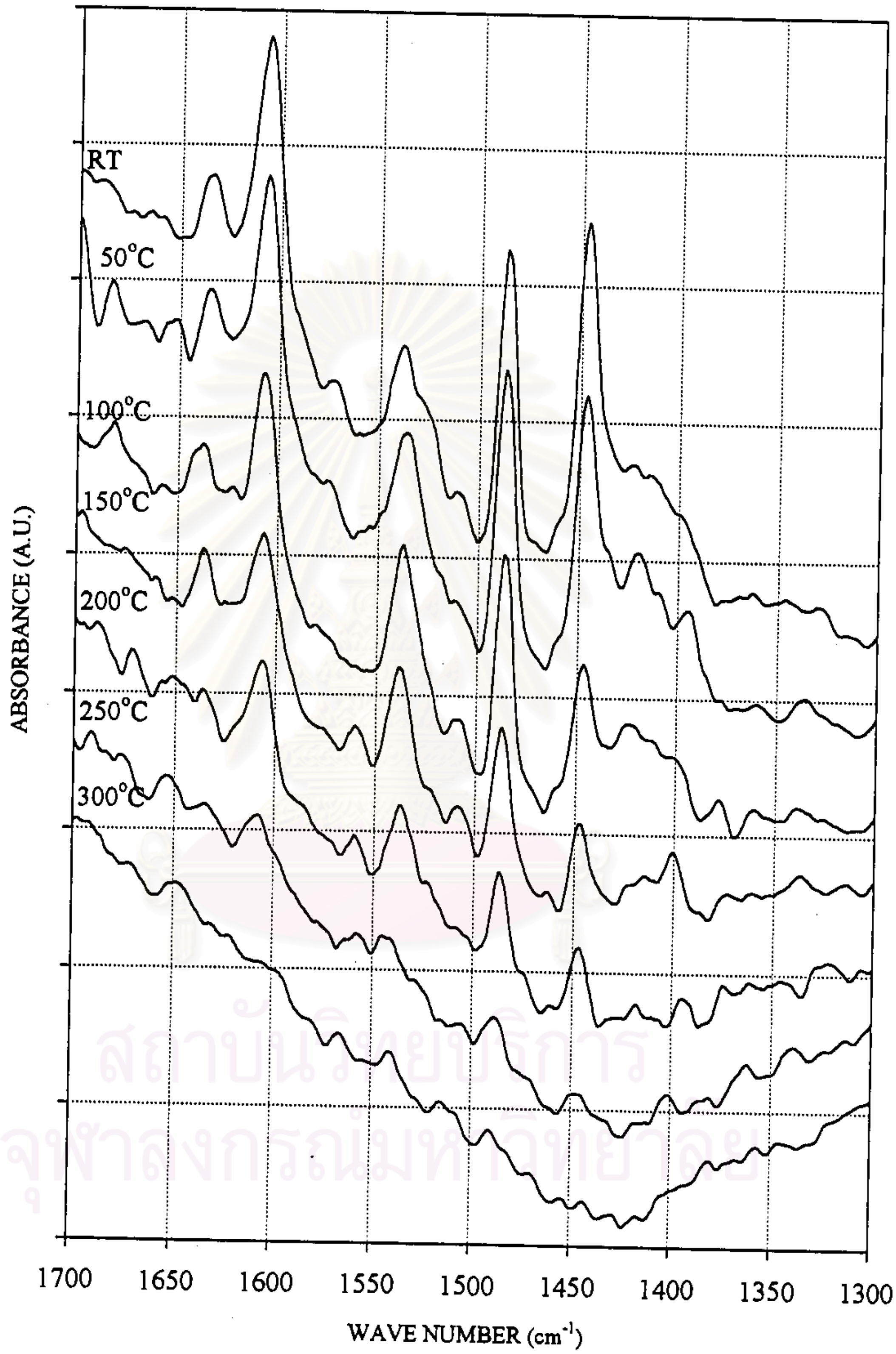

Figure 5.19 Pyridine adsorption on fresh 5wt%W-25wt%V_2O_5/TiO_2

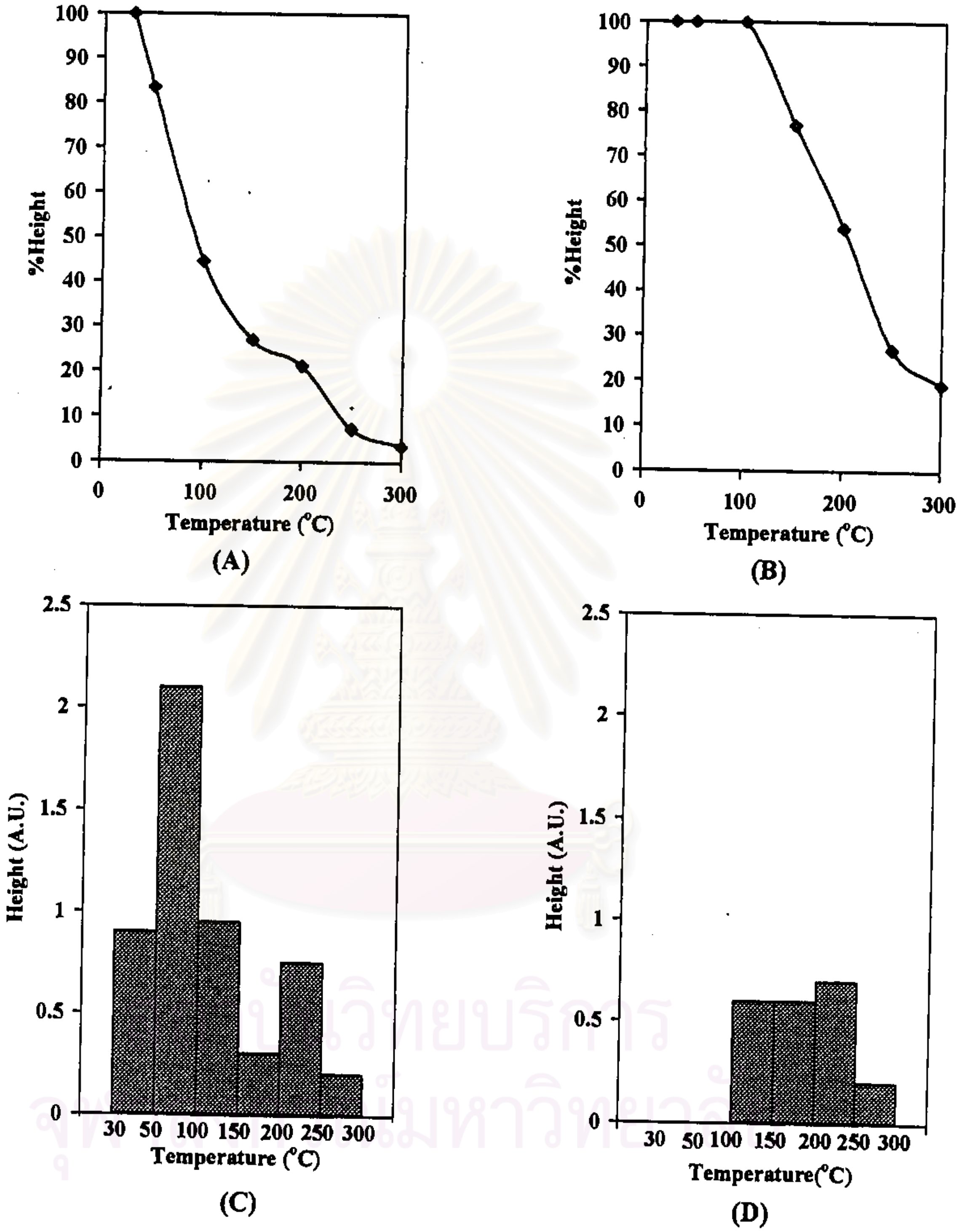

(A)

(B)

(C)

(D)

Figure 5.20 The percentage of the band height of pyridine adsorbed on Lewis (A) and Brönsted (B) acid site and the amount of pyridine desorbed from Lewis (C) and Brönsted (D) acid site on fresh 5wt%W- 25wt%V_2O_5/TiO_2

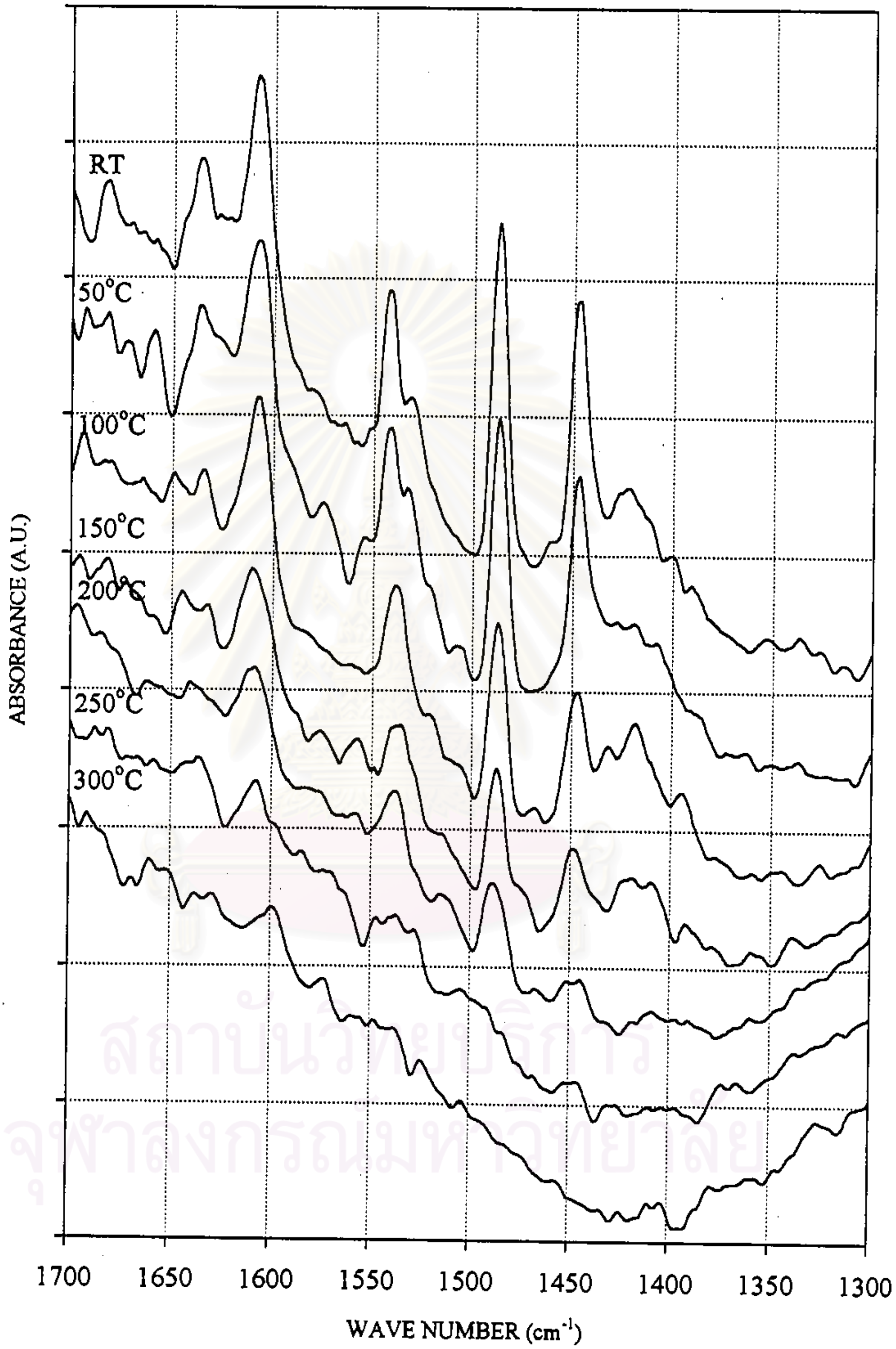

Figure 5.21 Pyridine adsorption on fresh 5wt%W-25wt%V_2O_5/TiO_2 after SO_2 preadsortion

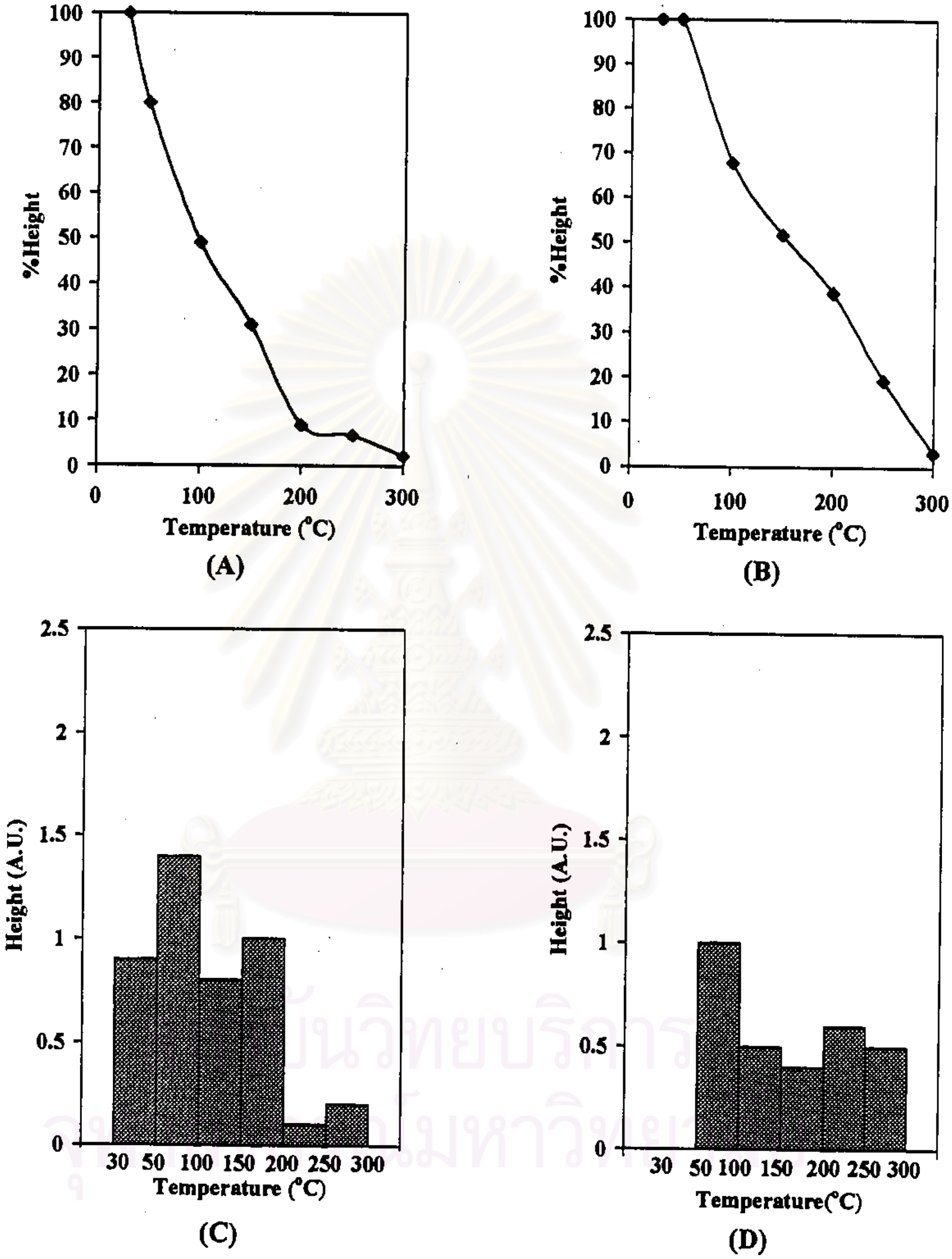

Figure 5.22 The percentage of the band height of pyridine adsorbed on Lewis (A) and Brönsted (B) acid site and the amount of pyridine desorbed from Lewis (C) and Brönsted (D) acid site on fresh 5wt%W - 25wt%V_2O_5/TiO_2 after SO_2 preadsorption

- Fresh 3wt%K-25wt%V_2O_5/TiO_2

Figure 5.23 illustrates IR spectra of adsorbed pyridine on fresh 3wt%K-25wt%V_2O_5/TiO_2. Comparison of the spectra at room temperature with fresh 25wt%V_2O_5/TiO_2, the intensity of pyridine adsorption (the bands 1540 cm^{-1}, 1640 cm^{-1}, 1445 cm^{-1} and 1600 cm^{-1}) steeply goes down, particularly, that belongs to pyridine adsorbed on Brönsted acid site. This means that both acid sites are significantly reduced by potassium loading. Figures 5.24 shows the amount of pyridine desorbed from Lewis and Brönsted acid site at different temperature. The figure shows that Lewis acid site has more a weak bond than a strong bond, whereas the amount of weak and strong Brönsted acid site is similar.

Figure 5.25 shows the spectra of pyridine adsorbed on fresh 3wt%K-25wt%V_2O_5/TiO_2 after SO_2 preadsorption at various temperatures. Comparing of the spectra at room temperature with that of fresh 3wt%K-25wt%V_2O_5/TiO_2 before SO_2 preadsorption, the figure clearly exhibits that SO_2 preadsorption dramatically increases Brönsted acid site, whereas Lewis acid site is decreased. Figure 5.26 presents the amount and strength of Lewis and Brönsted acid site of fresh 3wt%K-25wt%V_2O_5/TiO_2 after SO_2 preadsorption. Comparing with fresh 3wt%K-25wt%V_2O_5/TiO_2 before SO_2 preadsorption, shows that the decrease of Lewis acid site is belongs to a weak acid site while a strong acid site is relatively constant. In the case of Brönsted acid site both weak and strong acid site increase.

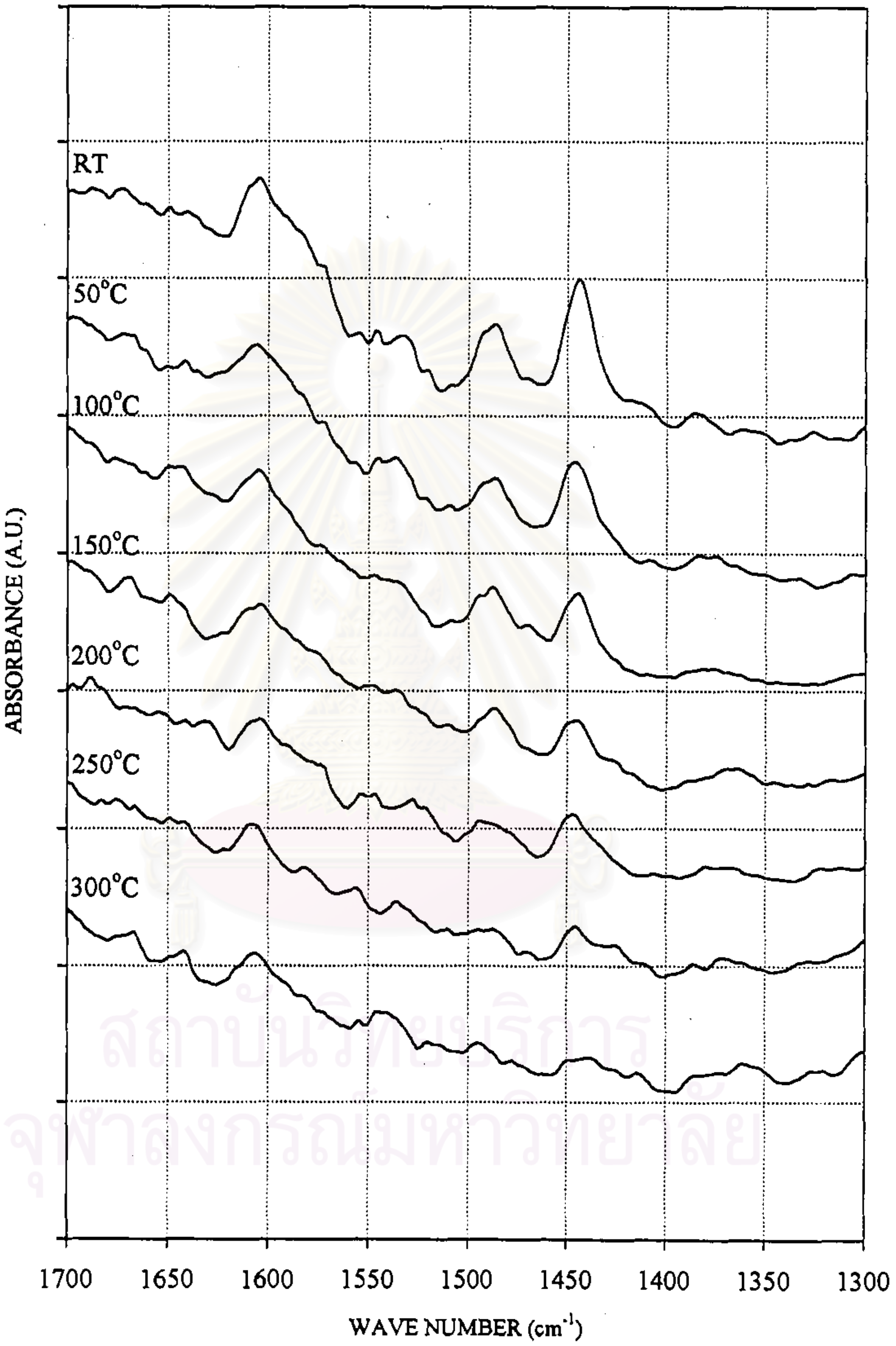

Figure 5.23 Pyridine adsorption on fresh 3wt%K-25wt%V_2O_5/TiO_2

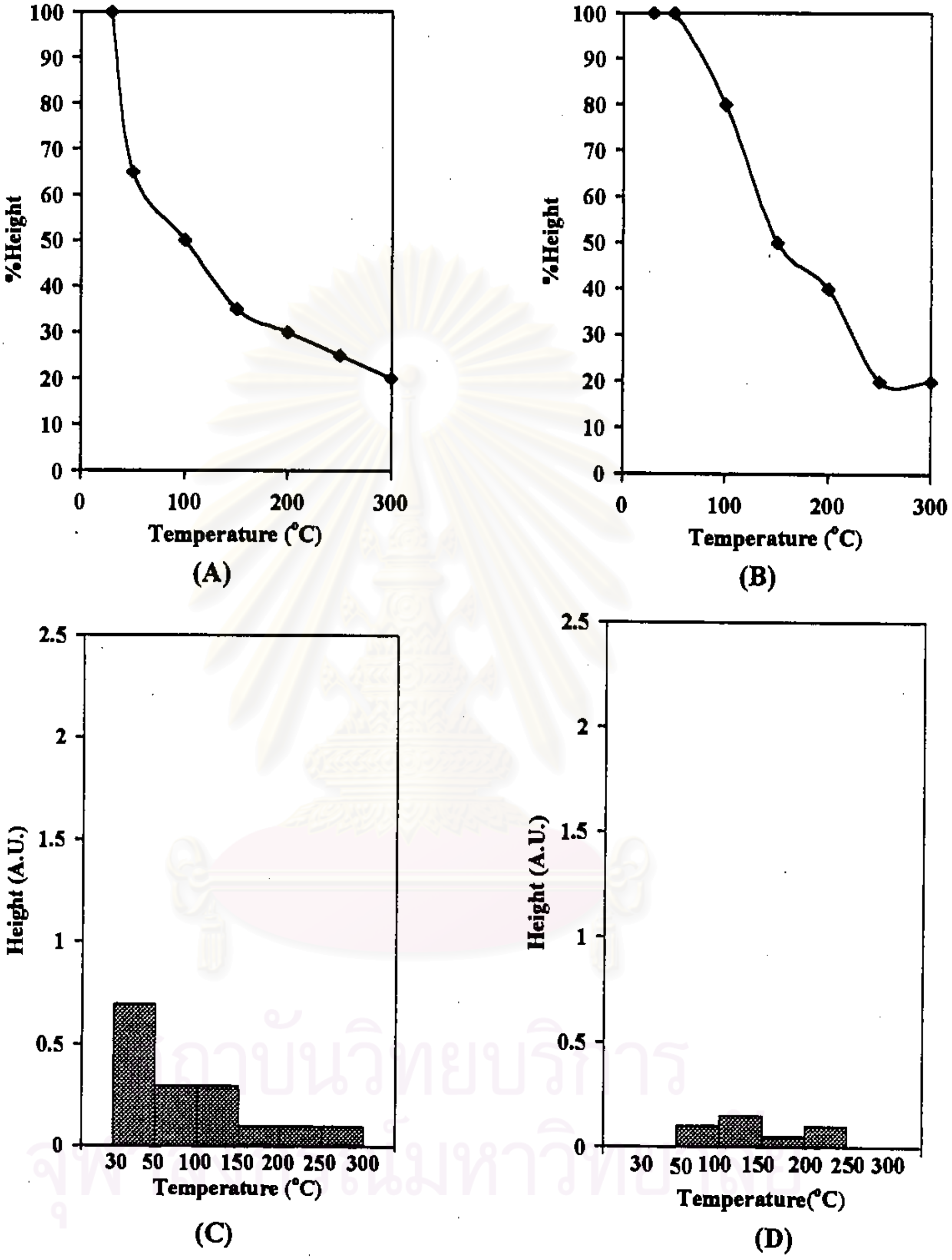

Figure 5.24 The percentage of the band height of pyridine adsorbed on Lewis (A) and Brönsted (B) acid site and the amount of pyridine desorbed from Lewis (C) and Brönsted (D) acid site on fresh 3wt%K- 25wt%V_2O_5/TiO_2

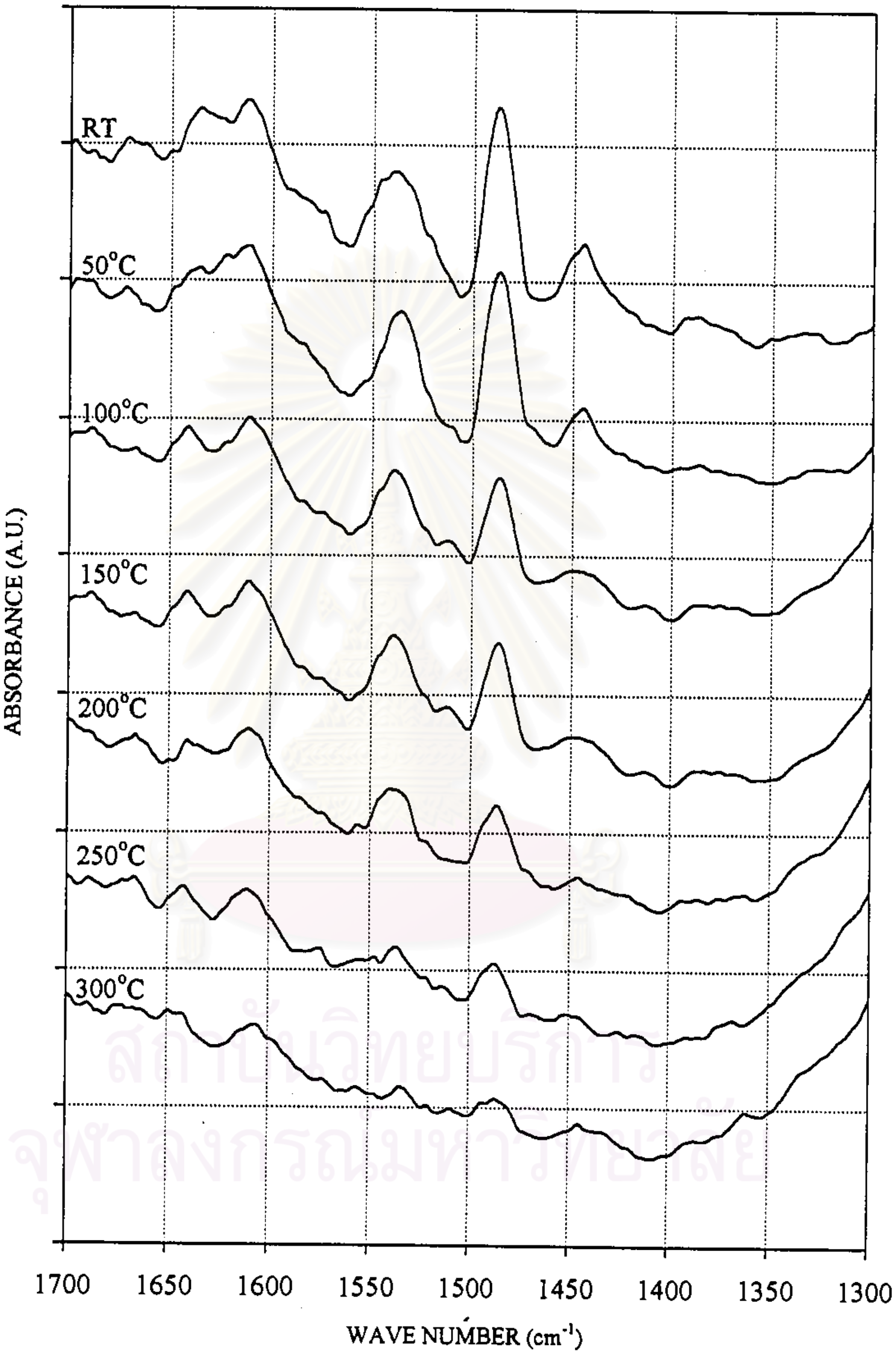

Figure 5.25 Pyridine adsorption on fresh 3wt%K-25wt%V_2O_5/TiO_2 after SO_2 preadsorption

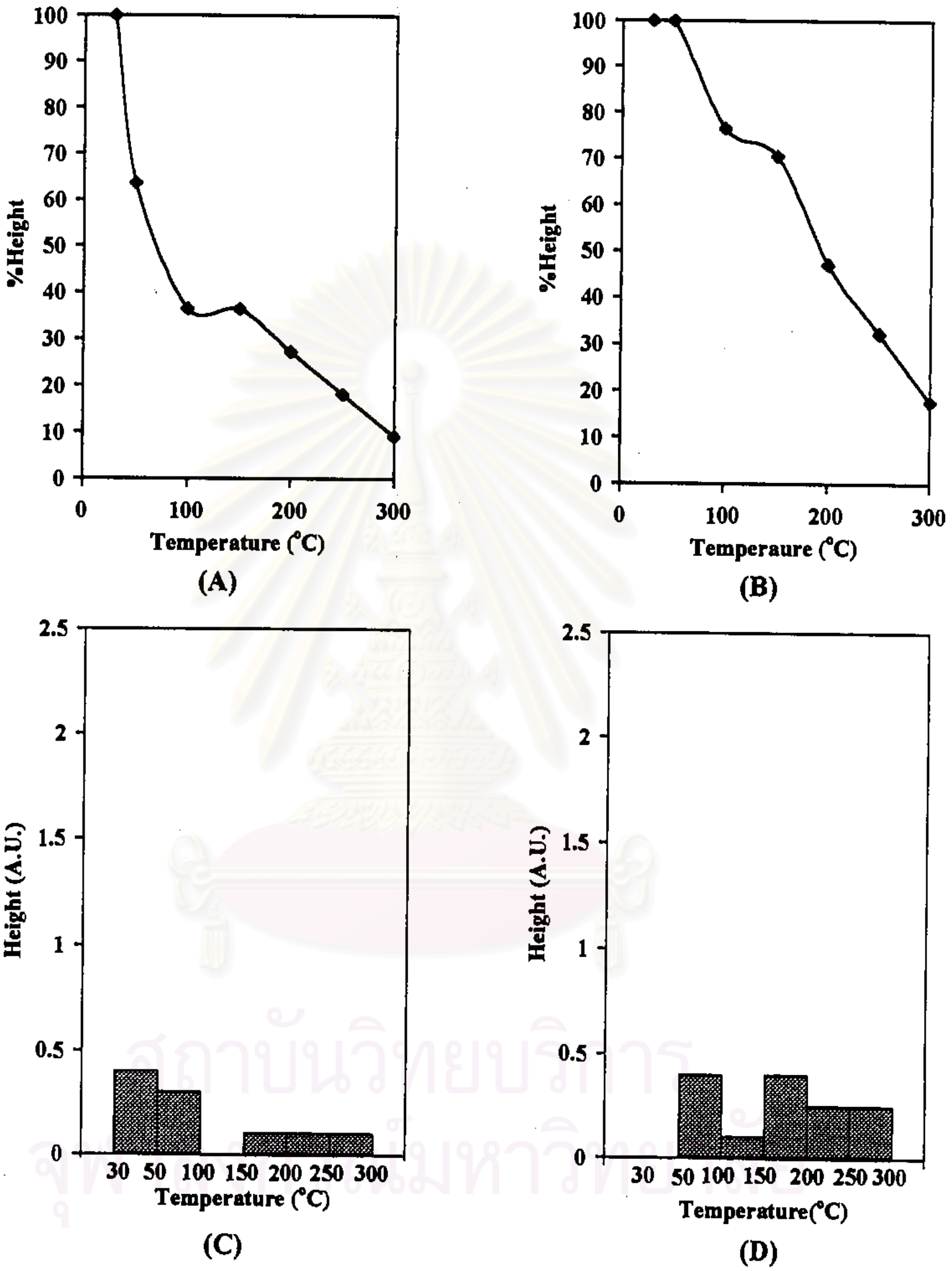

Figure 5.26 The percentage of the band height of pyridine adsorbed on Lewis (A) and Brönsted (B) acid site and the amount of pyridine desorbed from Lewis (C) and Brönsted (D) acid site on fresh 3wt%K - 25wt%V_2O_5/TiO_2 after SO_2 preadsorption

5.2 The catalytic behavior of the catalysts

In this section, the catalytic behavior of 25wt%V_2O_5/TiO_2 based catalysts, including 5wt%W-25wt%V_2O_5/TiO_2 and 3wt%K-25wt%V_2O_5/TiO_2 under various feed compositions; NO+NH_3, NO+NH_3+O_2, and NH_3+O_2 were investigated. In case of NO self-decomposition and NO oxidation, it was found that the NO conversions are very low compared with the reactions having NH_3. Therefore, both reactions are insignificant for further study. The previous research by Teratrakoonwichaya (1997) had noticed that the influence of homogeneous uncatalyzed gas-phase reaction and activity of pure TiO_2 support on the SCR reaction are negligible. Hence, the effect of homogeneous reaction and support will not be considered in following study.

- 25wt%V_2O_5/TiO_2

A comparison of the 25wt%V_2O_5/TiO_2 catalyst activity between the SCR reaction with O_2 and without O_2 at various temperatures is shown figure 5.27. At the reaction temperatures below 400 °C, NO conversion of 25wt%V_2O_5/TiO_2 in the presence of O_2 is higher than that in the absence of O_2. As for the temperatures above 350 °C, NO conversion of the SCR reaction with the presence of O_2 dramatically drops, whereas that without the presence of O_2, NO conversion still increases slightly and reach a maximum NO conversion near 50% at 500 °C. In the presence of O_2, the maximum NO conversion is about 90% at 300 °C. The result can be concluded that the presence of O_2 in feed composition promotes the SCR reaction at reaction temperatures below 350 °C.

At high reaction temperatures, the rapid decrease of NO conversion can be explained using the results shown in figure 5.28. Figure 5.28 presents the NH_3 oxidation of 25wt%V_2O_5/TiO_2. It is found that at temperature above 350°C, oxygen preferred to reacts with NH_3 to produce NO (and H_2O) and the maximum NO production (about 60%) is occurred at 500 °C. This result relates to the previous diminishing of NO conversion at high reaction temperature; oxygen in feed composition promotes NH_3 oxidation, preferably one with the SCR reaction.

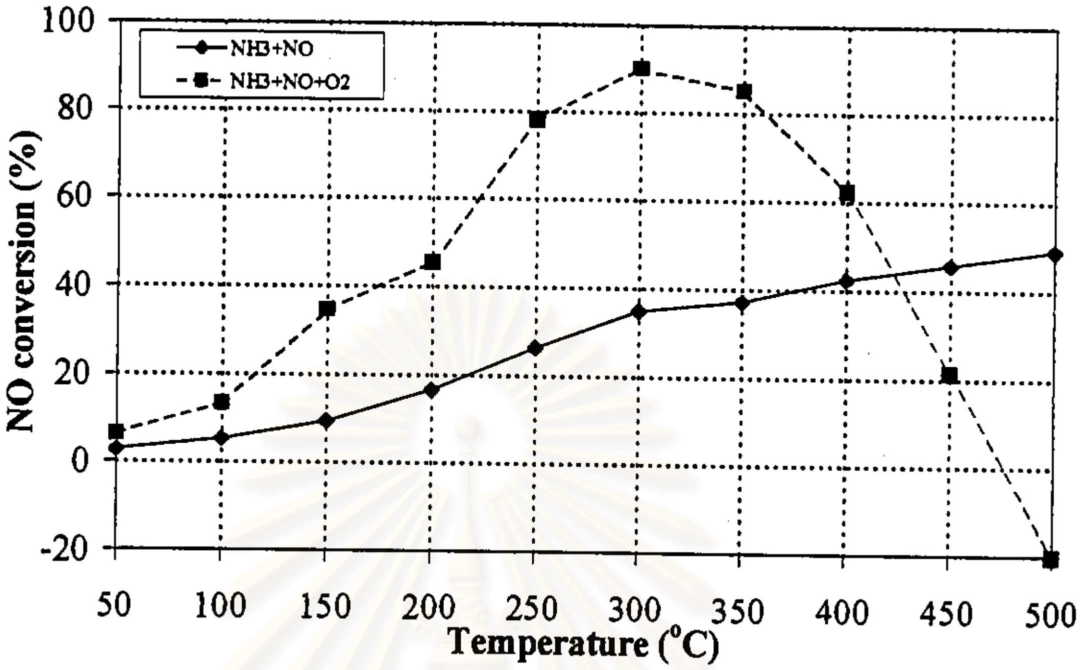

Figure 5.27 SCR activity of 25wt%V_2O_5/TiO_2 with and without O_2

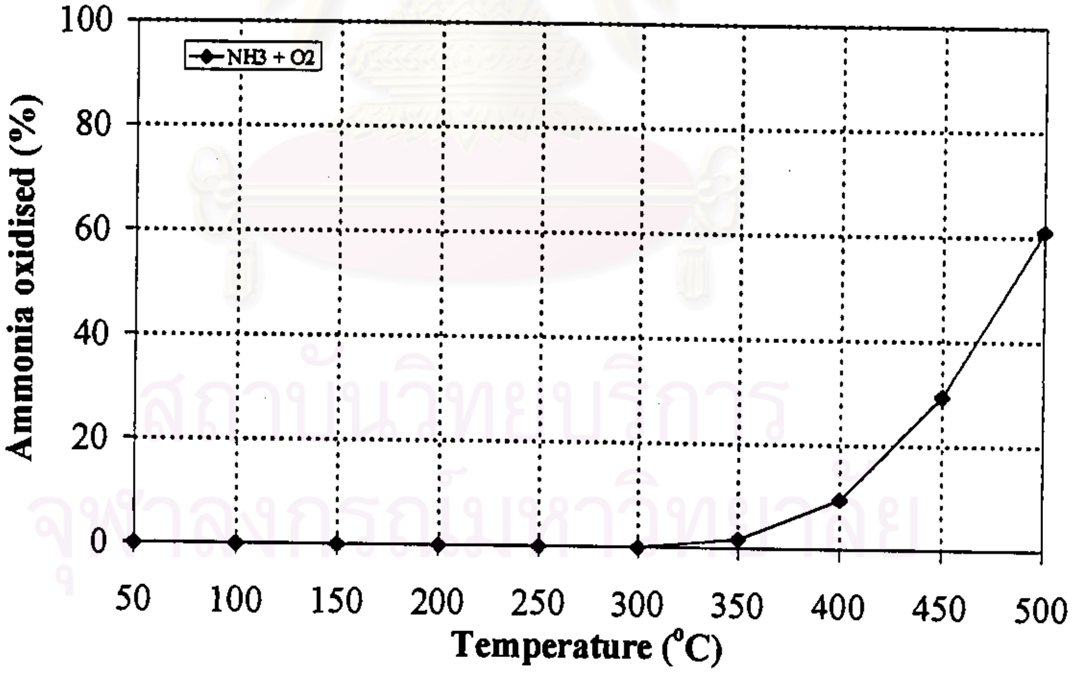

Figure 5.28 Ammonia oxidation of 25wt%V_2O_5/TiO_2

- 5wt%W-25wt%V_2O_5/TiO_2

Figure 5.29 demonstrates the NO conversion of 5wt%W-25wt%V_2O_5/TiO_2 with various feed components (NH_3+NO, and NH_3+NO+O_2). In the absence of O_2 in feed component, the NO conversion increases up to a maximum near 62% at around 350 °C and can maintain this conversion up to 500 °C. While in the presence of O_2, NO conversion increases with increasing temperature until the maximum NO conversion is reached about 98% at temperature around 300 °C. Between 300 °C and 400 °C, on 5wt%W-25wt%V_2O_5/TiO_2, NO conversion gradually declines and at higher temperature NO conversion is dramatically fallen. This effect suggests that the decrease of NO conversion at higher temperature is also caused by the direct oxidation of ammonia to nitric oxide (as shown in figure 5.30) as the same as the reaction on 25wt%V_2O_5/TiO_2. Figure 5.30 shows that the NH_3 oxidation increases up to a maximum about 70% at 500 °C.

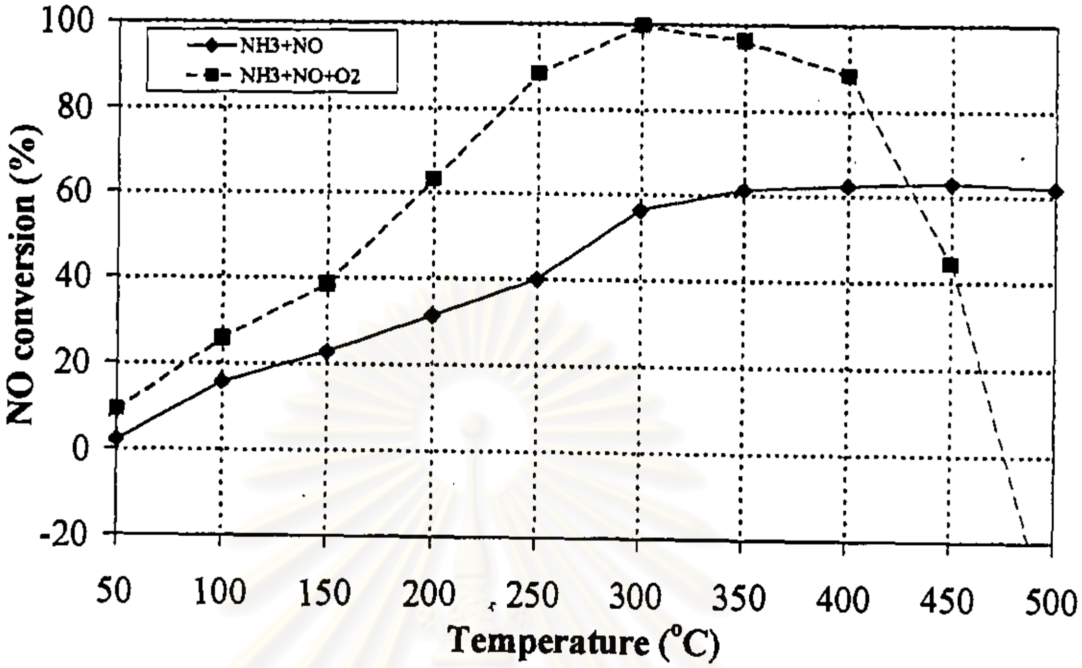

Figure 5.29 SCR activity of 5wt%W-25wt%V_2O_5/TiO_2

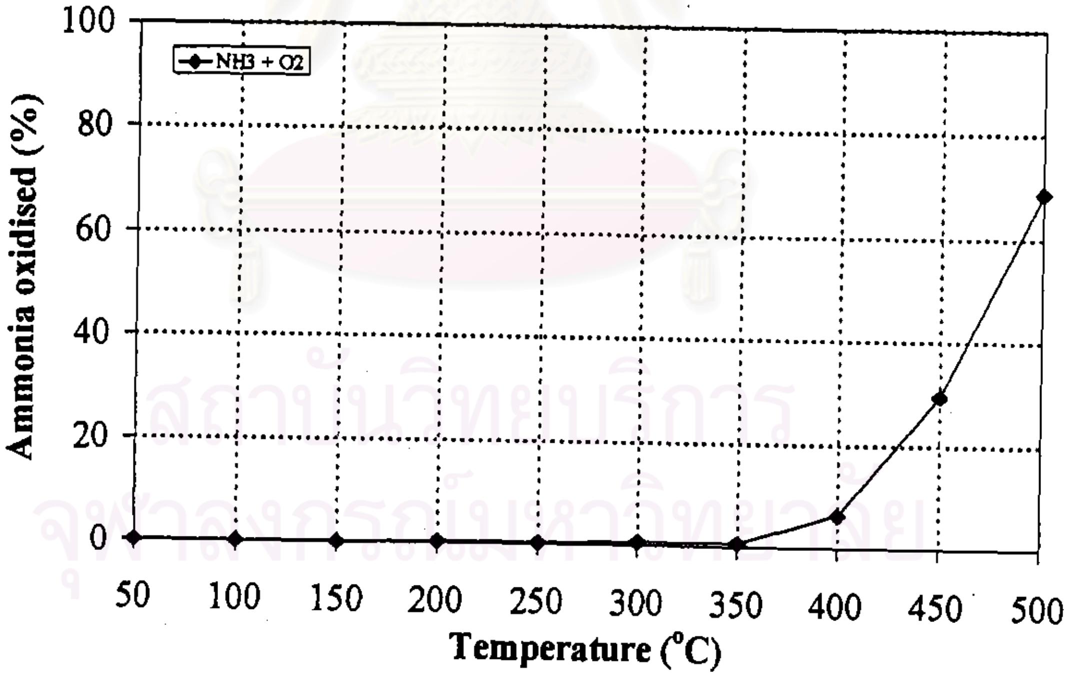

Figure 5.30 Ammonia oxidation of 5wt%W-25wt%V_2O_5/TiO_2

- 3wt%K-25wt%V_2O_5/TiO_2

Figure 5.31 shows the SCR activity of 3wt%K-25wt%V_2O_5/TiO_2 with the presence of O_2 and without the presence of O_2 at 50-500 °C. Under the absence of O_2 in feed gas, NO conversion increases significantly with rising temperature and reaches a maximum about 38% at 500 °C. As for the presence of O_2, NO conversion also increases with increasing temperature and at 500 °C, rises up to a maximum nearly 58%. When compared to the reaction without the presence of O_2, it is observed that NO conversion is clearly increased at various temperatures. NH_3 oxidation was tested (as shown in figure 5.32), and found that it can be marginally observed at high temperature. This result indicates that 3wt%K-25wt%V_2O_5 suppress substantially the NH_3 oxidation at high temperature. Thus, the SCR activity on 3wt%K-25wt%V_2O_5 continuously increases in the reaction temperature region above 350 °C.

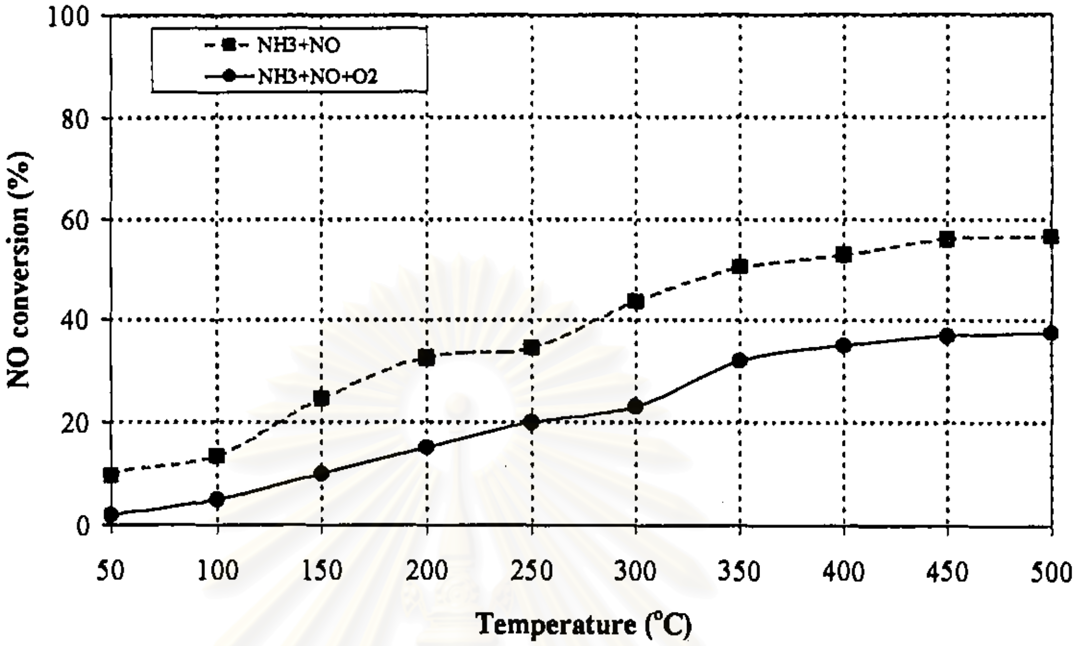

Figure 5.31 SCR activity of 3wt%K-25wt%V_2O_5/TiO_2

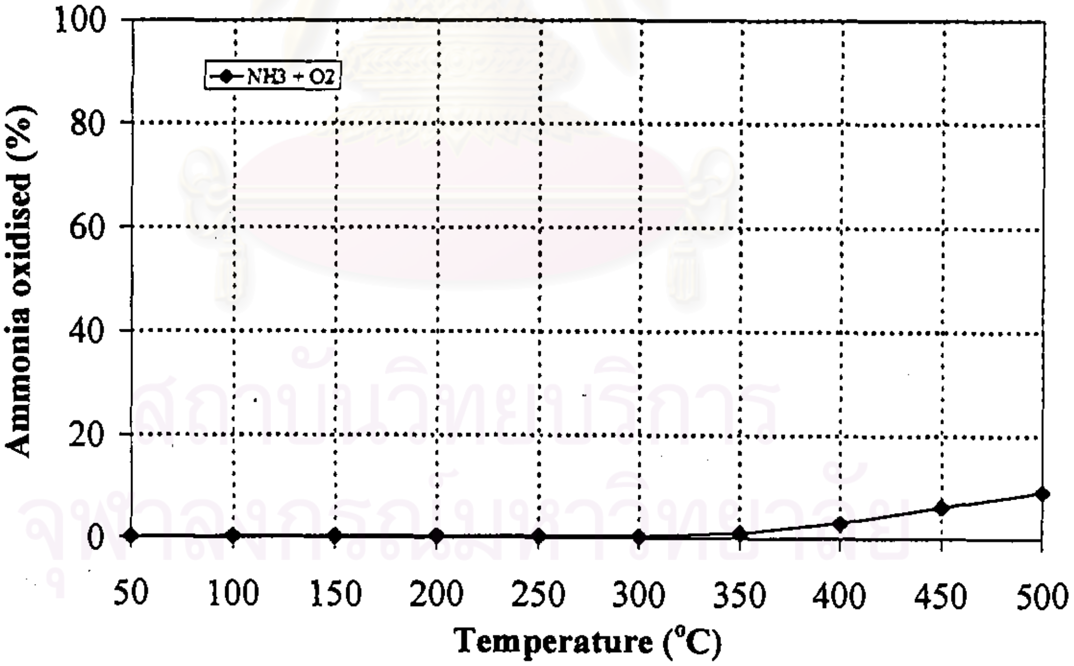

Figure 5.32 Ammonia oxidation of 3wt%K-25wt%V_2O_5/TiO_2

5.3 The effect of tungsten and potassium loading

The 25wt%V_2O_5/TiO_2 is a based-catalyst for this study. Because it give the optimum activity for SCR reaction (Teratrakoonwichaya, 1996). In this section, the effect of tungsten and potassium loading on the activity of SCR reaction is compared. The reaction conditions are 500 ppm NO, 500 ppm NH_3, and 2vol% O_2 at the reaction temperature range from 50 – 500 °C.

Figure 5.33 presents the SCR activity of 25wt%V_2O_5/TiO_2 5wt%W-25wt% V_2O_5/TiO_2, and 3wt%K-25wt%V_2O_5/TiO_2 catalysts at various reaction temperatures. It is found that comparing catalytic performance of the three catalysts at reaction temperature below 400 °C follow the following order 5wt%W-25wt%V_2O_5/TiO_2 > 25wt%V_2O_5/TiO_2 > 3wt%K-25wt%V_2O_5/TiO_2. The conversion shown in figure 5.33 can be explained using changes in surface acidity as shown previously in section 5.1.3. When tungsten is loaded to 25wt%V_2O_5/TiO_2, it results in catalyst that both amount and strength of Lewis and Brönsted acidity increase. It can conclude that NO conversion on 5wt%W-25wt%V_2O_5/TiO_2 is higher than NO conversion on 25wt%V_2O_5/TiO_2 due to the increase of both the number and strength of either/both Lewis or/and Brönsted acid sites. While potassium is added on 25wt%V_2O_5/TiO_2, both Lewis and Brönsted acid site on the surface of the catalyst decrease. Thus, the decrease of NO conversion on 3wt%K-25wt%V_2O_5/TiO_2 is due to a decline in surface acid site on 3wt%K-25wt%V_2O_5/TiO_2.

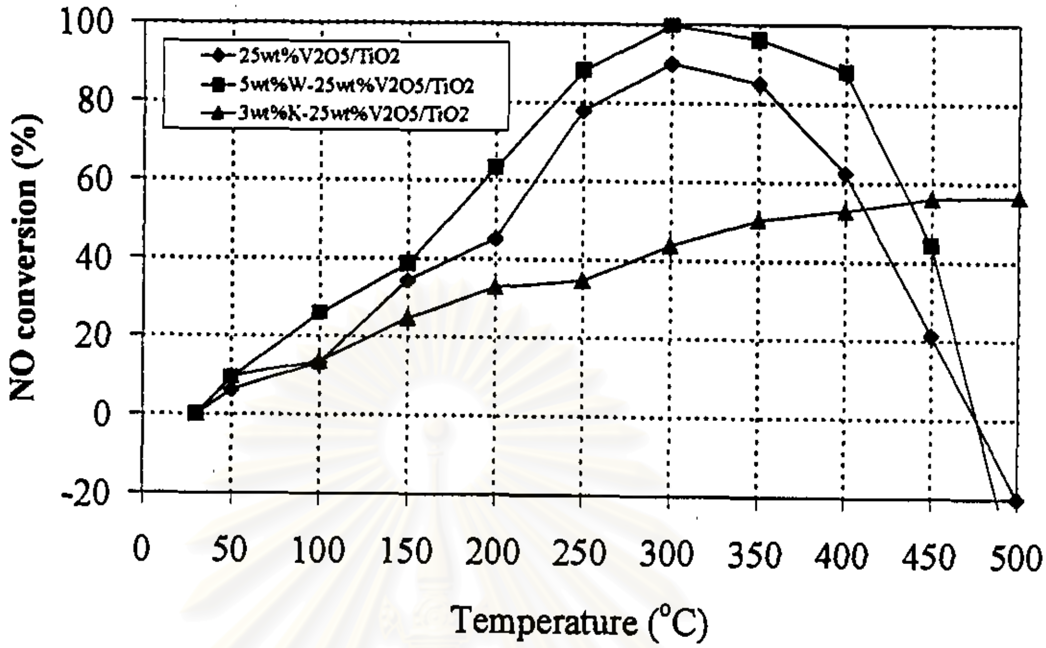

Figure 5.33 SCR activity of 25wt%V_2O_5/TiO_2, 5wt%W-25wt%V_2O_5/TiO_2, and 3wt%K-25wt%V_2O_5/TiO_2

5.4 The effect of SO_2

This section demonstrates the effect of SO_2 on 25wt% V_2O_5/TiO_2, 5wt%W-25wt%V_2O_5/TiO_2 and 3wt%K-25wt%V_2O_5/TiO_2 catalysts in the temperature range from 50 to 500 °C. The component of feed gas is NO 500 ppm, NH_3 500 ppm, O_2 2 vol%, and SO_2 50 ppm.

- 25wt%V_2O_5/TiO_2

Figure 5.34 shows NO conversion of 25wt%V_2O_5/TiO_2 in the reaction temperature range of 50 - 500 °C with and without SO_2 in the feed composition. At the reaction temperature below 150 °C, the SCR reactions with and without SO_2 give the similarity of NO conversion pattern. When the reaction temperature increases up to 300 °C, NO conversion of the SCR reaction with SO_2 reaches 95% of the highest NO conversion. As for the SCR reaction without SO_2, it is given 90% of maximum NO conversion at the same temperature of 300 °C. In contrast at higher temperature and with the presence of SO_2, NO conversion rapidly decreases and it is much more decrease than the NO conversion in the reaction without SO_2. From section 5.2 it can be concluded that at high temperature in the reaction without SO_2 on 25wt%V_2O_5/TiO_2, the NH_3 oxidation is more highly occurred than the SCR reaction loading to the decrease of NO conversion. In the case of the reaction with SO_2, it is possible to say that SO_2 in the feed gas improves the SCR reaction at the temperature below 300 °C. Some literatures [Saur *et al.* 1986 and Matralis *et al.* 1993] suggest that this is due to the occurrence of surface sulphate or (TiO_3) S=O on the catalyst surface which increases acid sites to catalyst and promotes the SCR reaction. At high temperature, NH_3 may prefer to react with SO_2 rather than NO which results in the formation of ammonium(bi)sulphates that depositing on active site resulting in deactivation or SO_2 promotes NH_3 oxidation which occurs well at high temperature. Therefore, NO conversion is dramatically decreased. When the spent catalyst obtained from the presence of SO_2 atmosphere is characterized by using FT-IR, the bands of NH_4SO_4 or $(NH_4)_2SO_2$ (as shown in appendix B) can not be detected. Consequently, the reason of decrease of NO conversion at high temperature may be caused by NH_3 oxidation. In the further experiment, the study of effect of various reaction temperatures on changing of catalyst acidity, especially, at the low temperature range shows that the SCR activity of 25wt%V_2O_5/TiO_2 with and without SO_2 is little different. While at high temperature, the SCR activity of 25wt%V_2O_5/TiO_2 with SO_2 is more decreased than that without SO_2. Thus, 25wt%V_2O_5/TiO_2 is further tested in the reaction at temperatures of 200 °C and 450 °C with and without SO_2 and then the spent 25wt%V_2O_5/TiO_2 catalysts are characterized by using pyridine adsorption technique which will show how changing of acidity of the catalyst is affected. The results of the experiments are described in detail below.

The spent catalysts of 25wt%V_2O_5/TiO_2, in case of the reaction without SO_2 at temperatures of 200 °C and 450 °C were characterized by using pyridine adsorption technique. The results are shown in figures 5.35 – 5.36 (200 °C) and figures 5.37 – 5.38 (450 °C). It is found that the spent catalysts obtained from both reaction temperatures have the same amount and strength of both Lewis and Brönsted acid sites and is similar to that of fresh 25wt%V_2O_5/TiO_2. From this result it can be concluded that the amount and strength of 25wt%V_2O_5/TiO_2 dose not change with reaction temperature. In the case of reaction with SO_2 at temperature of 200 °C and 450 °C, the pyridine adsorption results are shown in figures 5.39 – 5.40 (200 °C) and figures 5.41 – 5.42 (450 °C), respectively. The spent catalyst at reaction temperature 200 °C (as shown in figures 5.39 and 5.40) is compared with the spent catalyst at reaction temperature 450 °C (as shown in figures 5.41 and 5.42). It is found that the spent 25wt%V_2O_5/TiO_2 at 200 °C has much less amount and strength of Lewis and Brönsted acid sites than the spent 25wt%V_2O_5/TiO_2 at 450 °C. The spent 25wt%V_2O_5/TiO_2 at 450 °C compared with fresh 25wt%V_2O_5/TiO_2 after SO_2 preadsorption had lower amount and strength of acid site. From this result it can be concluded that SO_2 results in the changing of acidity of 25wt%V_2O_5/TiO_2 at various temperatures.

The different SCR activity on 25wt%V_2O_5/TiO_2 with and without SO_2 can be explained using changes in acidity of 25wt%V_2O_5/TiO_2. As shown in figure 5.34

previously at temperature of 200 °C, NO conversion of the reaction with SO_2 is slightly higher than in the reaction without SO_2. From results of acidity measurement of the catalyst, the amount of Lewis acid sites of the spent 25wt%V_2O_5/TiO_2 with SO_2 is more than that without SO_2 but the amount of Brönsted acid site of both spent catalysts is still the same. It can suggest that below 200 °C, SO_2 improves Lewis acid site which relates to enhance the SCR reaction activity. In case of high temperature (450 °C), NO conversion of the reaction with SO_2 is more dramatically decreased than that without SO_2. The amount of weak and strong Lewis acid site of the spent catalyst with SO_2 is much more than that without SO_2, while the number of their Brönsted acid sites are about the same. This result suggests that Lewis acid site in high temperature promotes more NH_3 oxidation reaction than SCR reaction. In case of the reaction with SO_2, it is clear that NO conversion is more rapidly decreased than that without SO_2 in that SO_2 enhances the amount and strength of Lewis acid site. Thus, NH_3 oxidation in the reaction with SO_2 is more well occur than NH_3 oxidation in the reaction without SO_2. Comparison of the amount and strength of acid sites on 25wt%V_2O_5/TiO_2 catalysts at various reaction temperatures are summarized in Table 5.2.

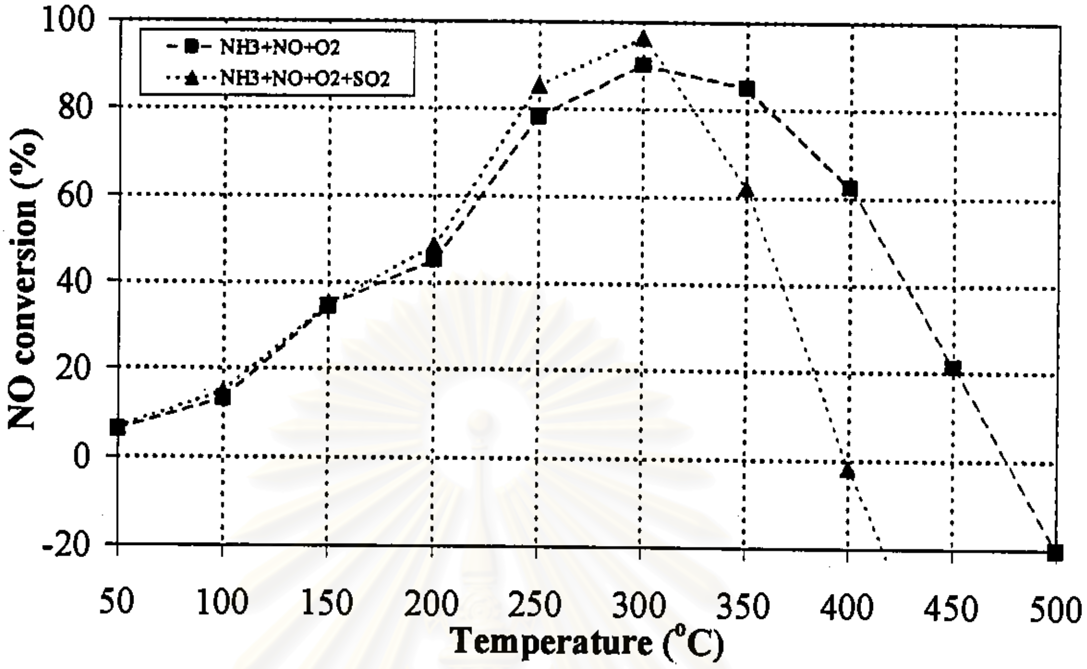

Figure 5.34 SCR activity of 25wt%V_2O_5/TiO_2

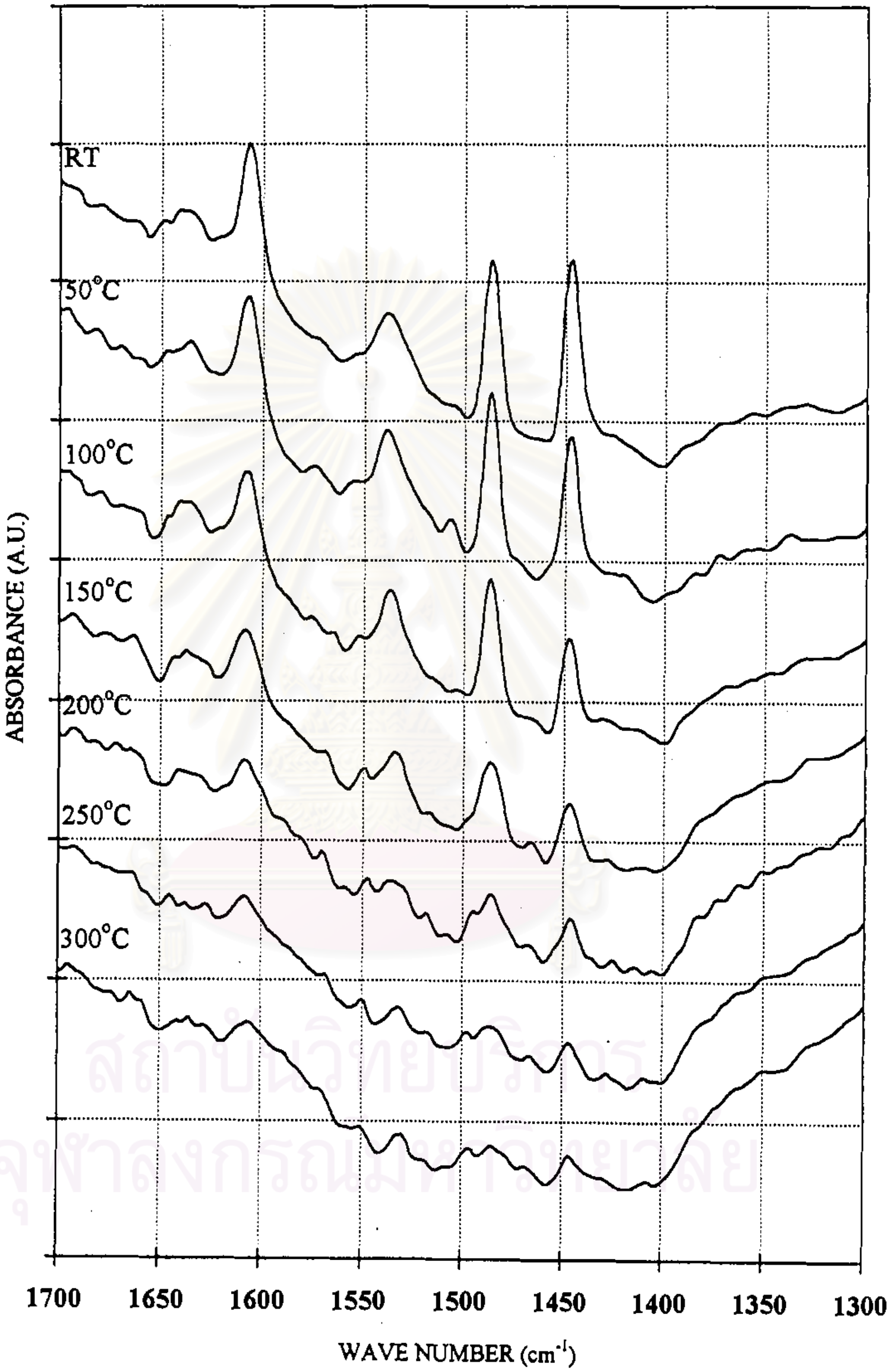

Figure 5.35 Pyridine adsorption on spent 25wt%V_2O_5/TiO_2 without SO_2 at 200°C

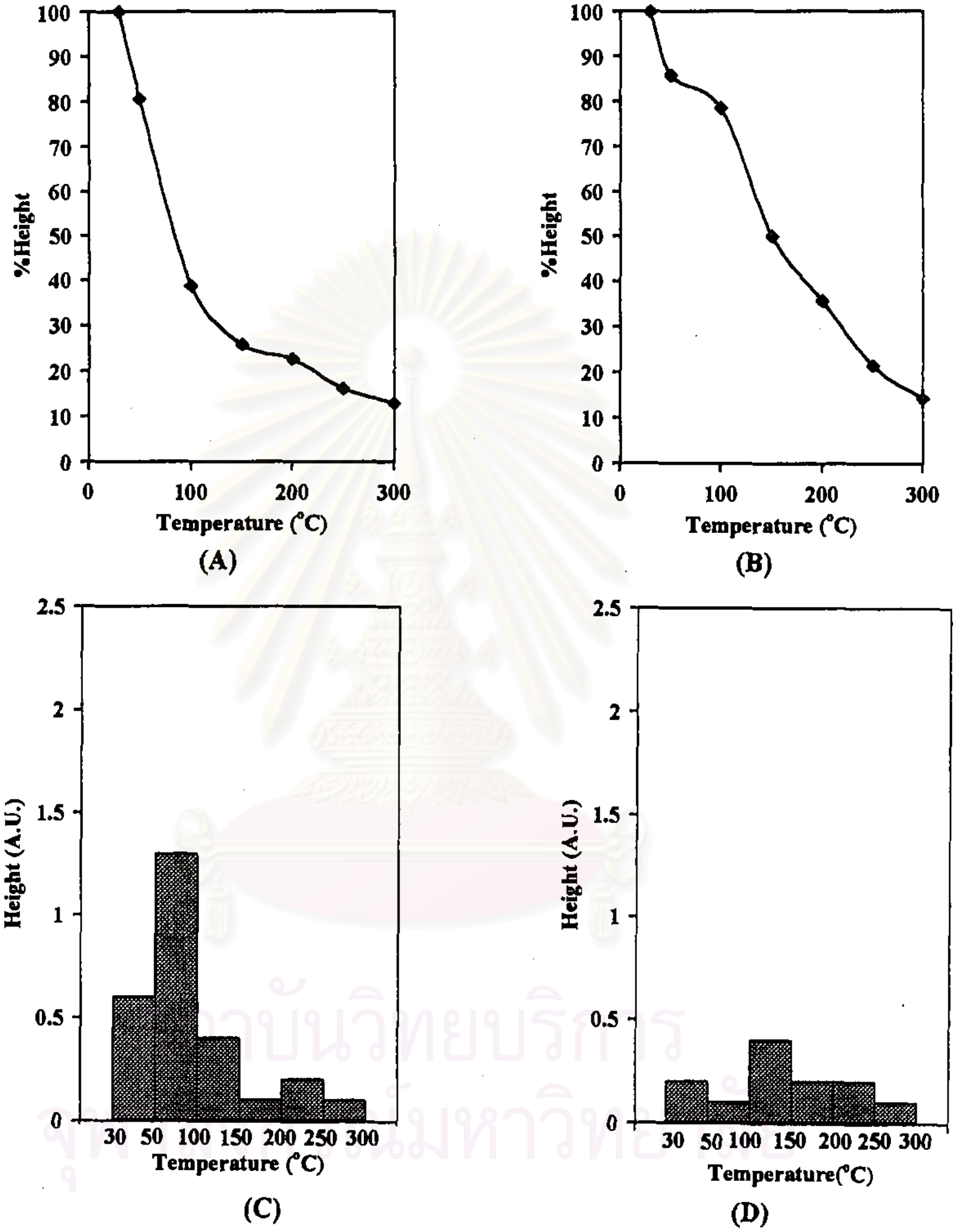

Figure 5.36 The percentage of the band height of pyridine adsorbed on Lewis (A) and Brönsted (B) acid site and the amount of pyridine desorbed from Lewis (C) and Brönsted (D) acid site on spent 25wt%V_2O_5/TiO_2 without SO_2 at 200 °C

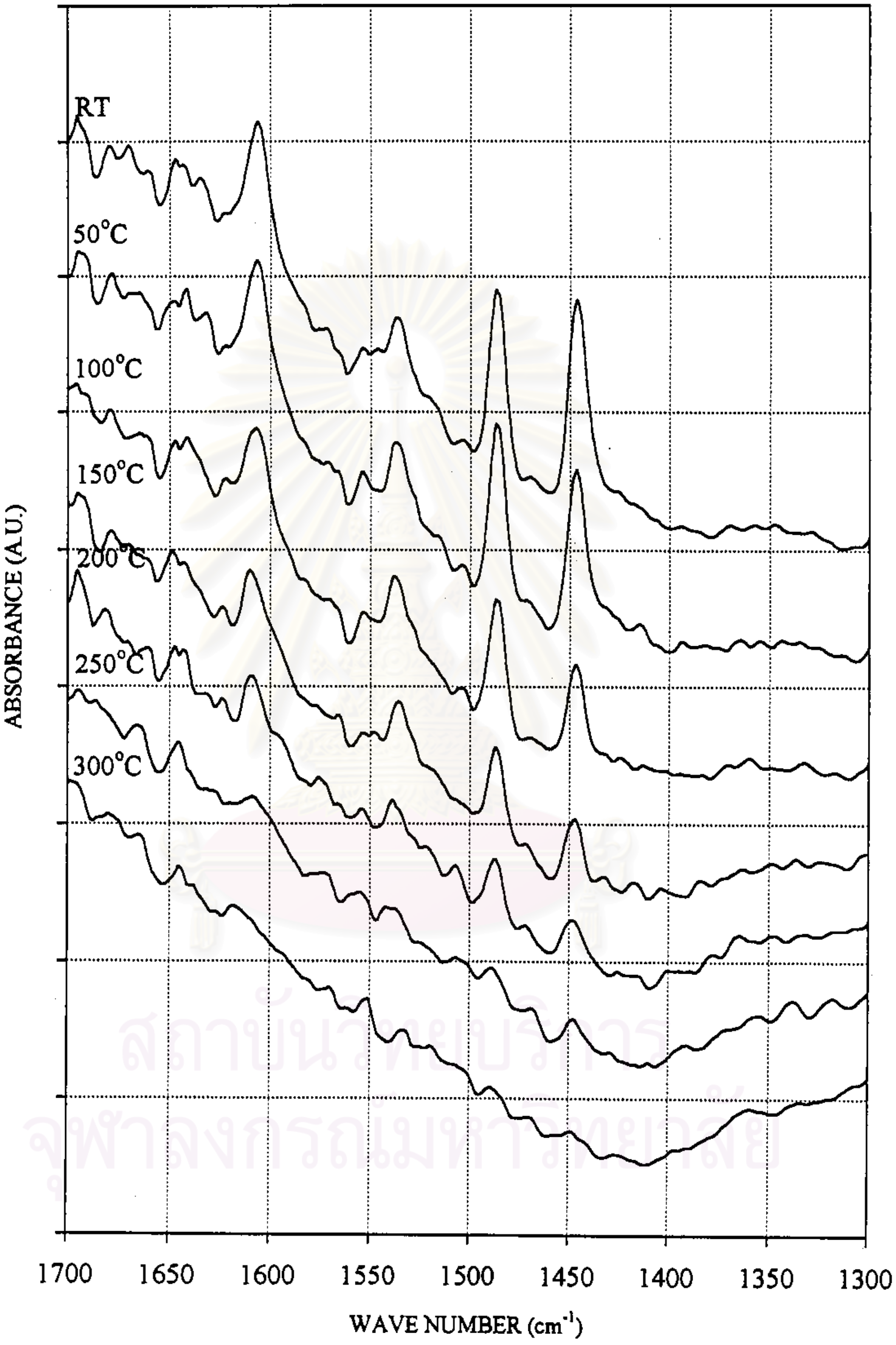

Figure 5.37 Pyridine adsorption on spent 25wt%V_2O_5/TiO_2 without SO_2 at 450°C

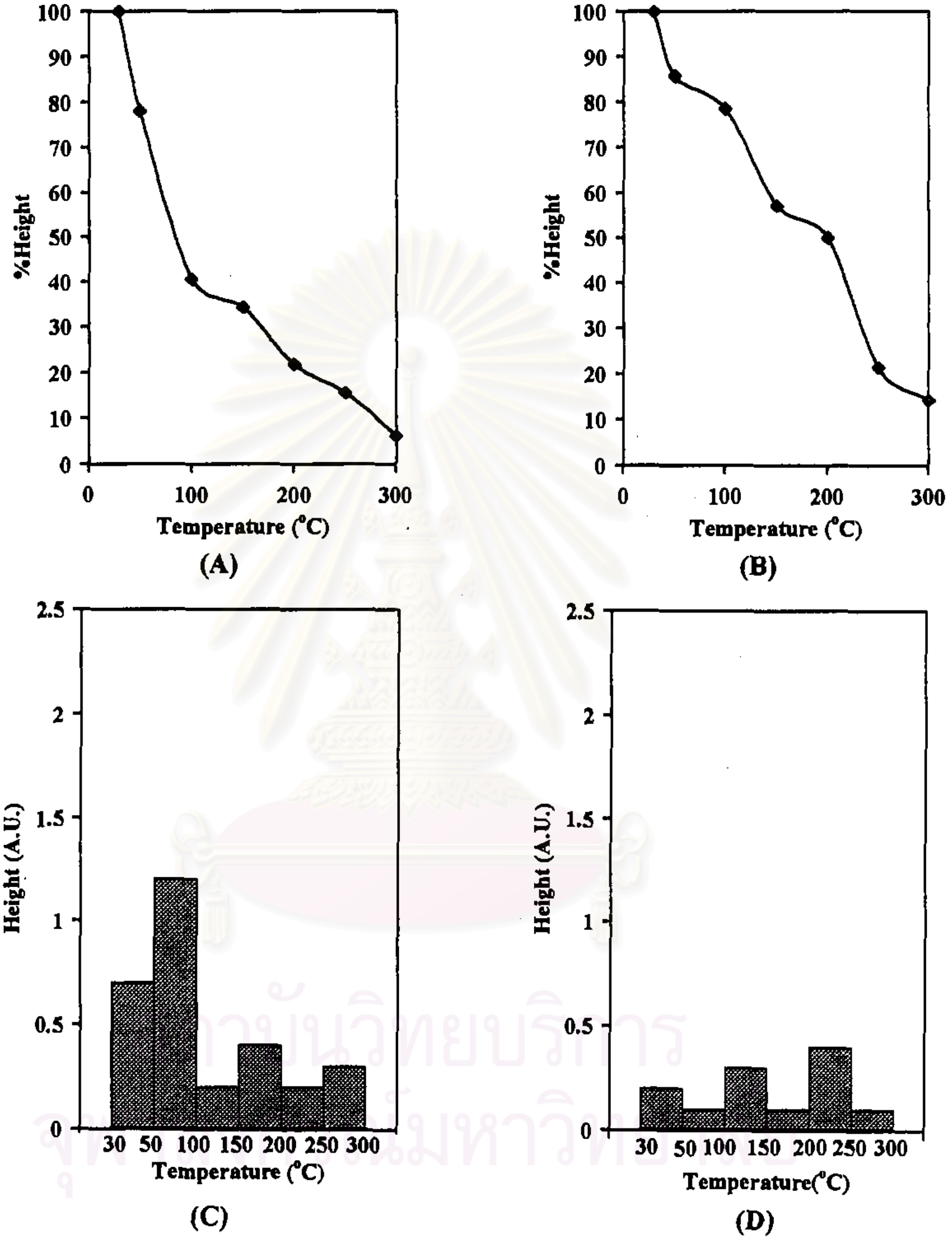

Figure 5.38 The percentage of the band height of pyridine adsorbed on Lewis (A) and Brönsted (B) acid site and the amount of pyridine desorbed from Lewis (C) and Brönsted (D) acid site on spent 25wt%V_2O_5/TiO_2 without SO_2 at 450 °C

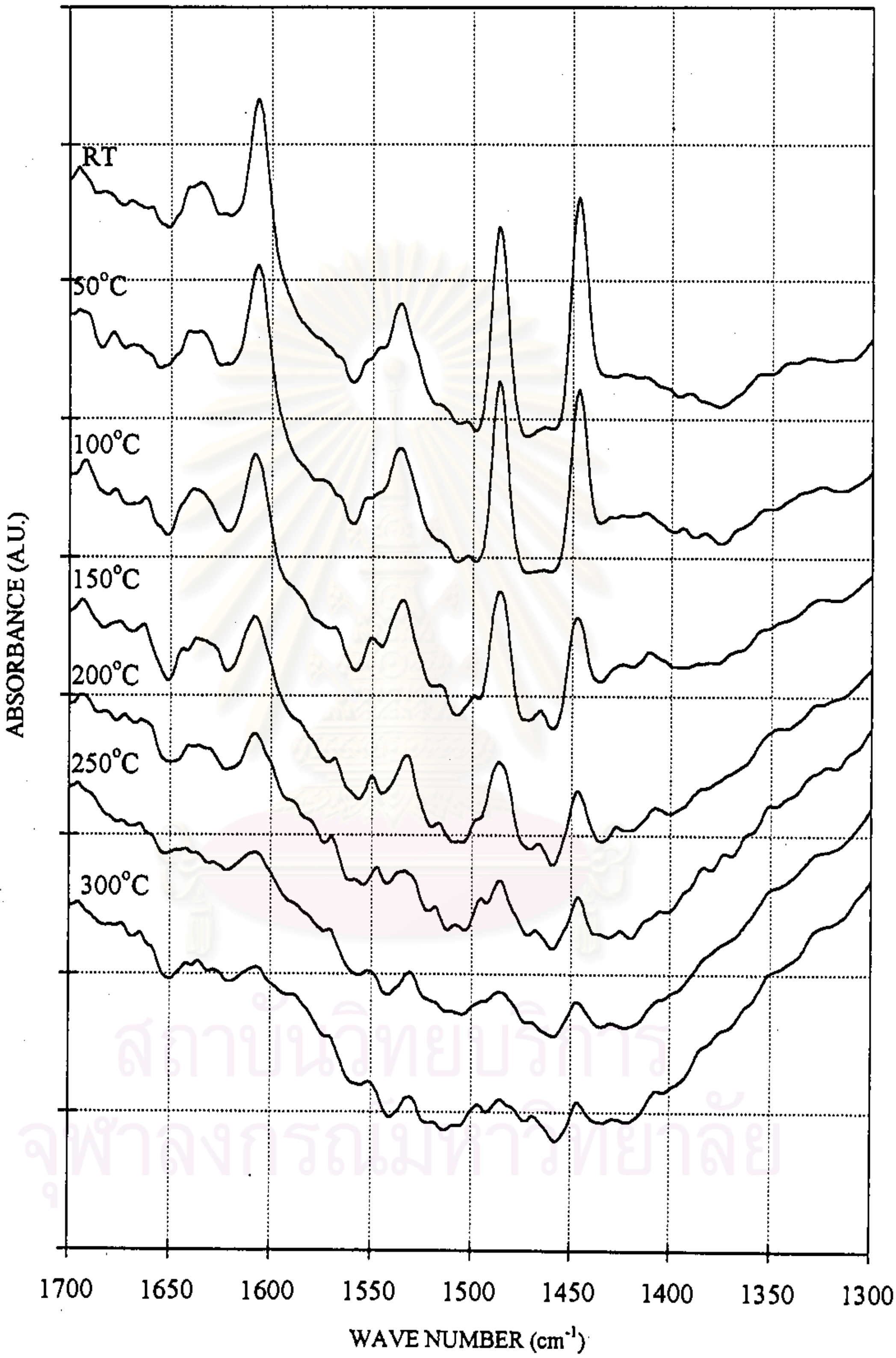

Figure 5.39 Pyridine adsorption on spent 25wt%V_2O_5/TiO_2 with SO_2 at 200°C

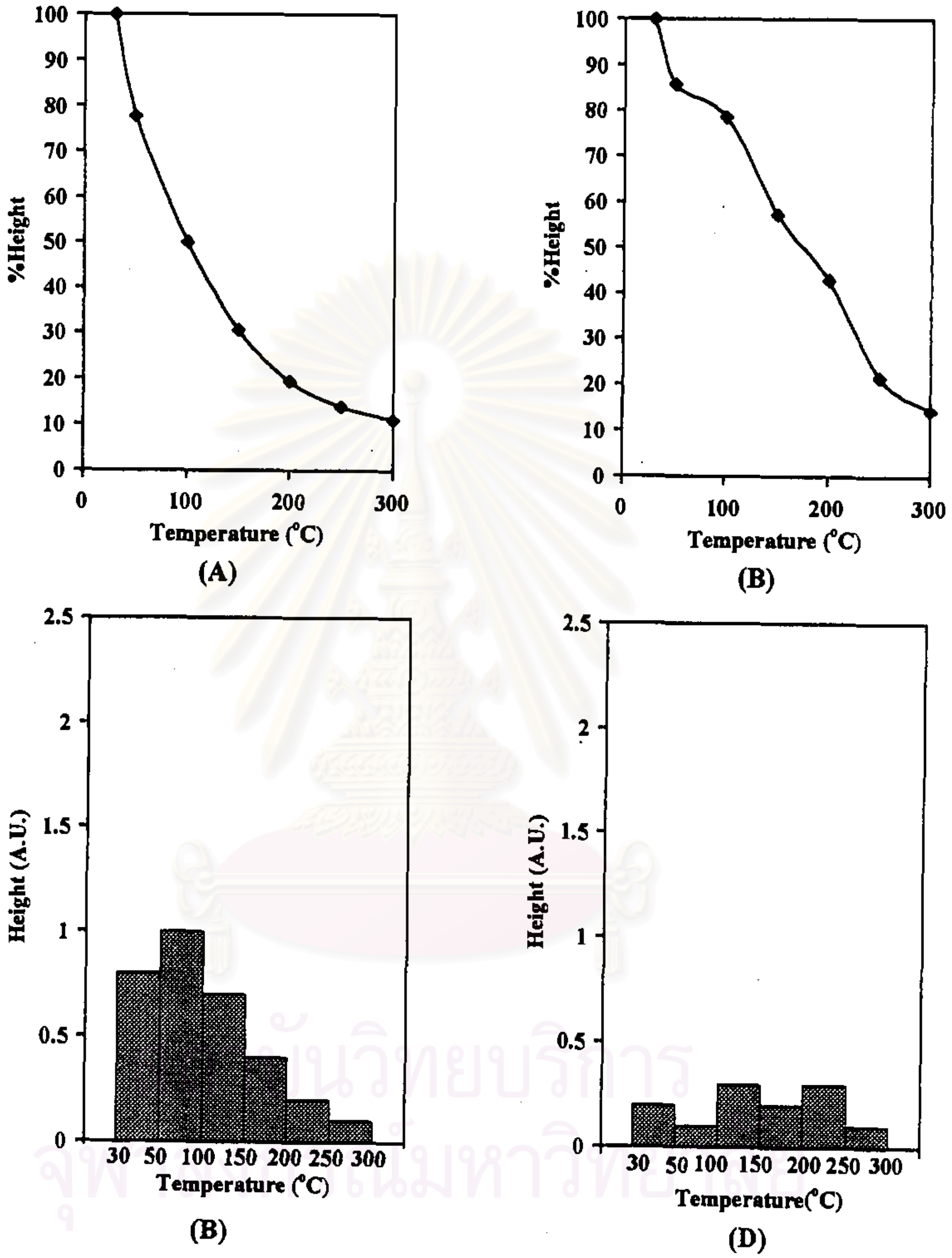

Figure 5.40 The percentage of the band height of pyridine adsorbed on Lewis (A) and Brönsted (B) acid site and the amount of pyridine desorbed from Lewis (C) and Brönsted (D) acid site on spent 25wt%V_2O_5/TiO_2 with SO_2 at 200°C

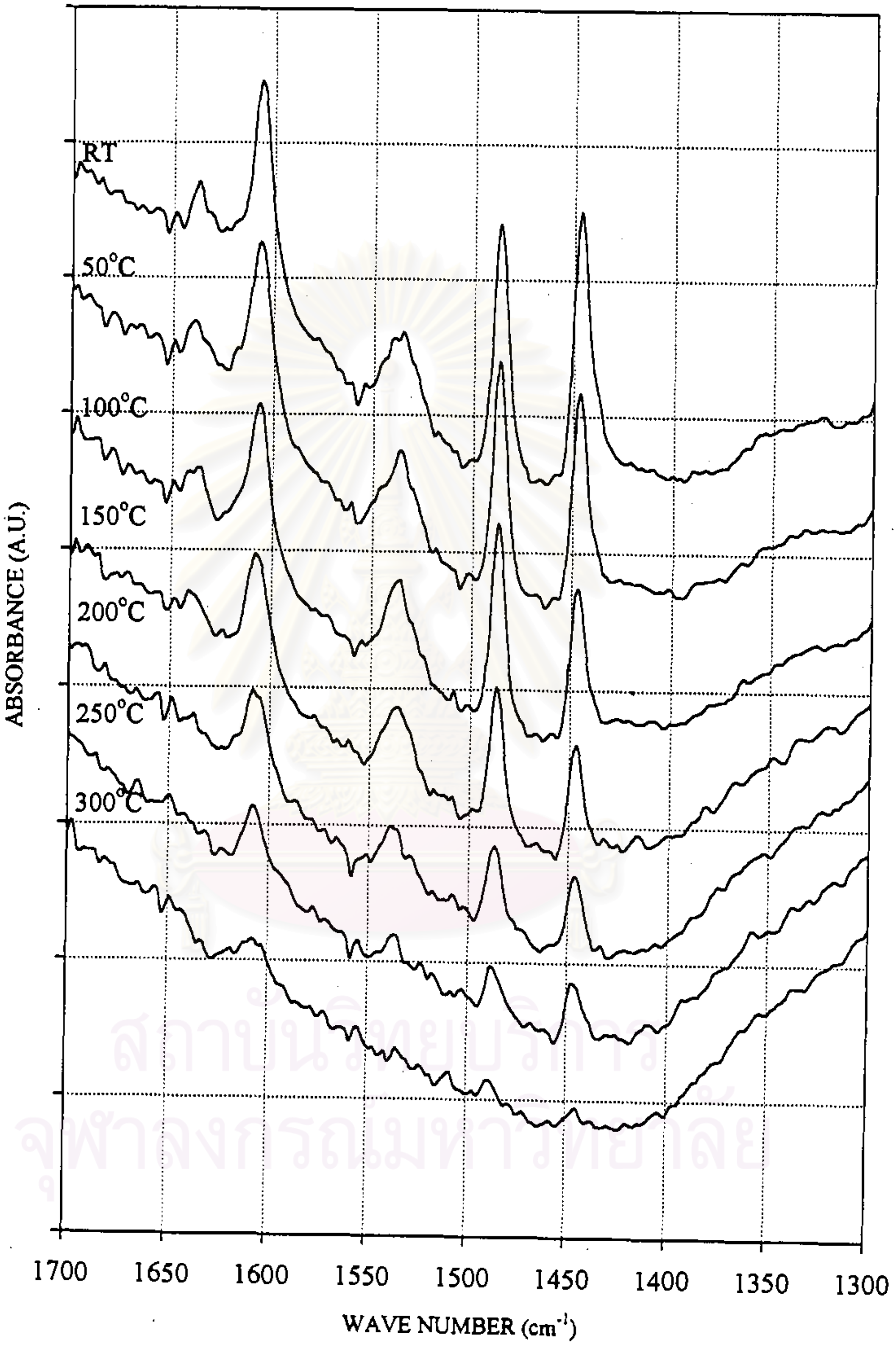

Figure 5.41 Pyridine adsorption on spent 25wt%V_2O_5/TiO_2 with SO_2 at 450°C

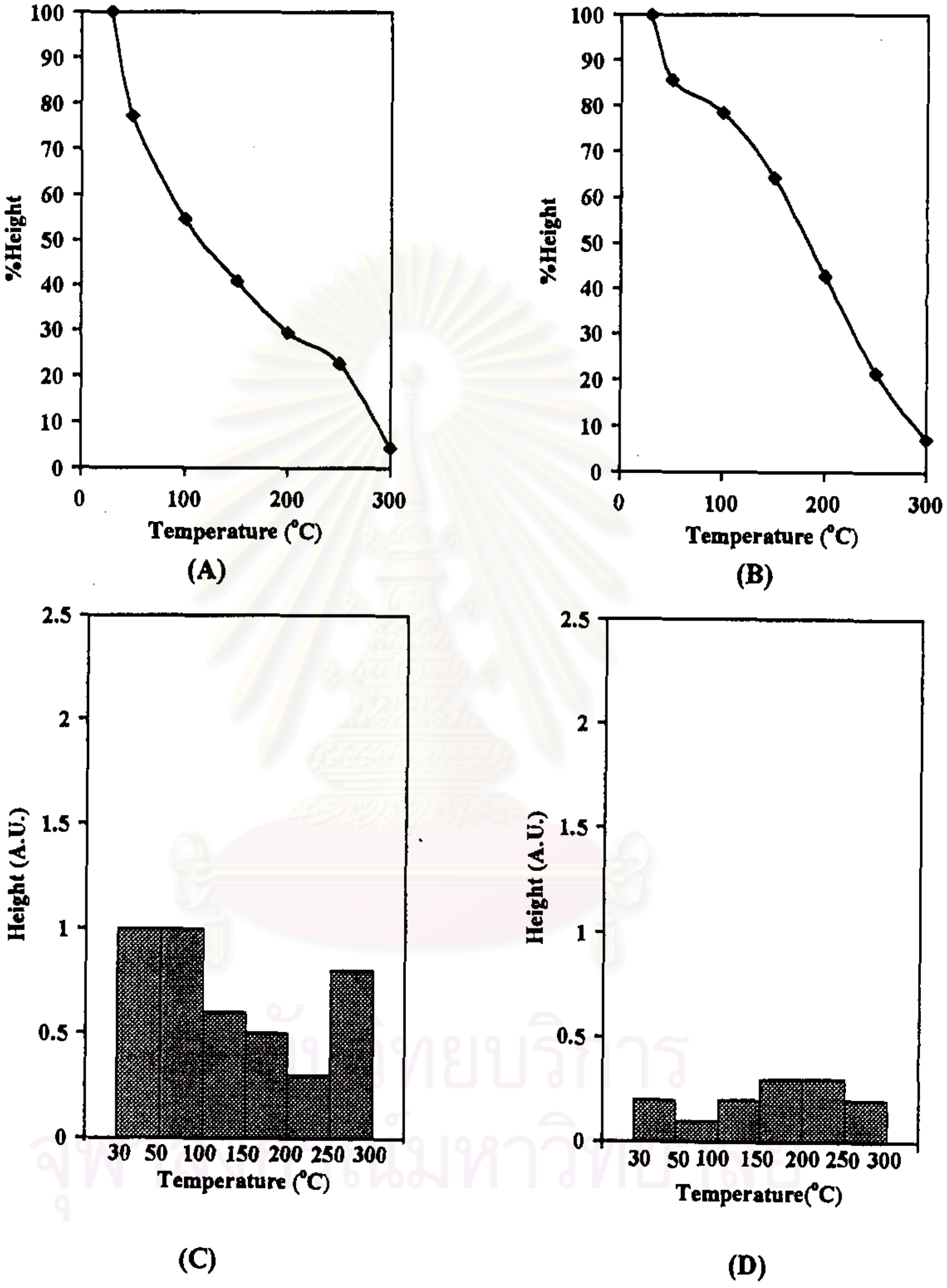

Figure 5.42 The percentage of the band height of pyridine adsorbed on Lewis (A) and Brönsted (B) acid site and the amount of pyridine desorbed from Lewis (C) and Brönsted (D) acid site on spent 25wt%V_2O_5/TiO_2 with SO_2 at 450 °C

Table 5.2 Comparison of the amount and strength of acid sites on 25wt%V_2O_5/TiO_2 catalysts at various reaction temperatures.

Comparison of catalysts	Lewis acid site			Brönsted acid site		
	Total	weak	strong	Total	weak	strong
200°C/fresh	constant	constant	constant	constant	constant	constant
450°C/fresh	constant	↓	↑	constant	constant	constant
450°C/200°C	constant	↓	↑	constant	constant	constant
200°C with SO_2/fresh	↑	↓	↑	constant	constant	constant
450°C with SO_2/fresh	↑↑↑	↑	↑↑↑	constant	↓	↑
450°C with SO_2/200°C with SO_2	↑↑↑	constant	↑↑↑	constant	constant	constant
200°C with SO_2/200°C	↑	↑	constant	constant	constant	constant
450°C with SO_2/450°C	↑↑↑	↑↑	↑↑↑	constant	↓	↑

↑ < ↑↑ < ↑↑↑ and ↓↓↓ > ↓↓ > ↓

- **5wt%W-25wt%V_2O_5/TiO_2**

Figure 5.43 shows the SCR activity on 25wt%V_2O_5/TiO_2 in the presence and absence of SO_2 from 50 °C to 500 °C. At reaction temperature below 350 °C and without SO_2 in feed component, it is found that NO conversion is higher than NO conversion of reaction with SO_2. At reaction temperature higher than 300 °C and without SO_2, NO conversion rapidly decreases but in the reaction with SO_2, it can retain a constant maximum NO conversion about 90%, until 400 °C before decreasing. In the case of reaction without SO_2, NO conversion slightly increases up to 98% at 300 °C but it gradually declines in the temperature range of 300 – 400 °C before rapidly decreasing at higher temperature. It can be explained that SO_2 in this reaction suppresses the SCR reaction at low temperature and the NH_3 oxidation at high temperature. Like the case of 25wt%V_2O_5/TiO_2, the effect of SO_2 on 5wt%W-25wt%V_2O_5/TiO_2 is explained by using changing value of acidity at reaction temperatures at 200 °C and 450 °C. Acidity measurement in the reaction without SO_2 shows that the amount of Lewis and Brönsted acid site of spent of 5wt%W-25wt%V_2O_5/TiO_2 at 200 °C (as shown in figures 5.44 and 5.45) is higher than that of the spent catalyst at 450 °C (as shown in figures 5.46 and 5.47). Comparing of both spent catalysts with fresh 5wt%W-25wt%V_2O_5/TiO_2 (see figure 5.19), The fresh catalyst has the highest amount of Lewis and Brönsted acid site. Thus, it can be concluded that the amount of acid site depends on reaction temperature that when reaction temperature increases, the amount of acid site decreases. The amount of acid site of the spent catalyst with SO_2 at reaction temperature of 200 °C and 450 °C is shown in figures 5.48 - 5.49, and figures 5.50 – 5.51. The amount and strength of Lewis acid site of the spent 5wt%W-25wt%V_2O_5/TiO_2 at 450 °C is more than that of the spent catalyst at 200 °C in vice versa the amount and strength of Brönsted acid site. From this result it can be concluded that the reaction with SO_2 makes variation of the amount and strength of Lewis and Brönsted acid site with temperature.

The results of acidity modification of the spent 5wt%W-25wt%V_2O_5/TiO_2 at various temperatures from the reaction with and without SO_2 can be used to explain the SCR activity of 5wt%W-25wt%V_2O_5/TiO_2. It is said that NO conversion of

5wt%W-25wt%V_2O_5/TiO_2 without SO_2 is higher than that of the reaction with SO_2 at reaction temperature below 350 °C (see figure 5.43). From the difference in activity of 5wt%W-25wt%V_2O_5/TiO_2 at reaction temperature 200 °C and in the reaction with and without SO_2, it is found that in the reaction without SO_2 the amount of weak Lewis acid site is higher than that of the reaction with SO_2. Both spent catalysts have the same amount of Brönsted acid site but the strength of Brönsted acid site of the catalyst with SO_2 is much higher. Thus, it can conclude that at the reaction temperature below 350 °C, SO_2 decreases Lewis acid site which results in the decrease of activity of the SCR reaction. This result supports the previously described experimental results, which show that in the case of 25wt%V_2O_5/TiO_2 Lewis acid site is an active center.

As for high temperature, NO conversion of the reaction with SO_2 is more slightly decreased than that of the reaction without SO_2. From changing acidity result of the spent catalyst at 450 °C, it is found that in the reaction with SO_2 the amount of weak and strong Lewis acid site is higher than that of the reaction without SO_2. But the amount of strong Brönsted acid site of the spent catalyst in the reaction without SO_2 is higher. Consequently, it can be suggested that at high temperature adding SO_2 increases the amount and strength of Lewis acid site, therefore, NO conversion of the catalyst is slowly decreased. Moreover, the decrease of Brönsted acid site on 5wt%W-25wt%V_2O_5/TiO_2 in the reaction with SO_2 when compared with that without SO_2 might retain NO conversion to slowly decrease. Table 5.3 shows the comparison of the amount and strength of acid sites on 5wt%W-25wt%V_2O_5/TiO_2 catalysts at various reaction temperatures.

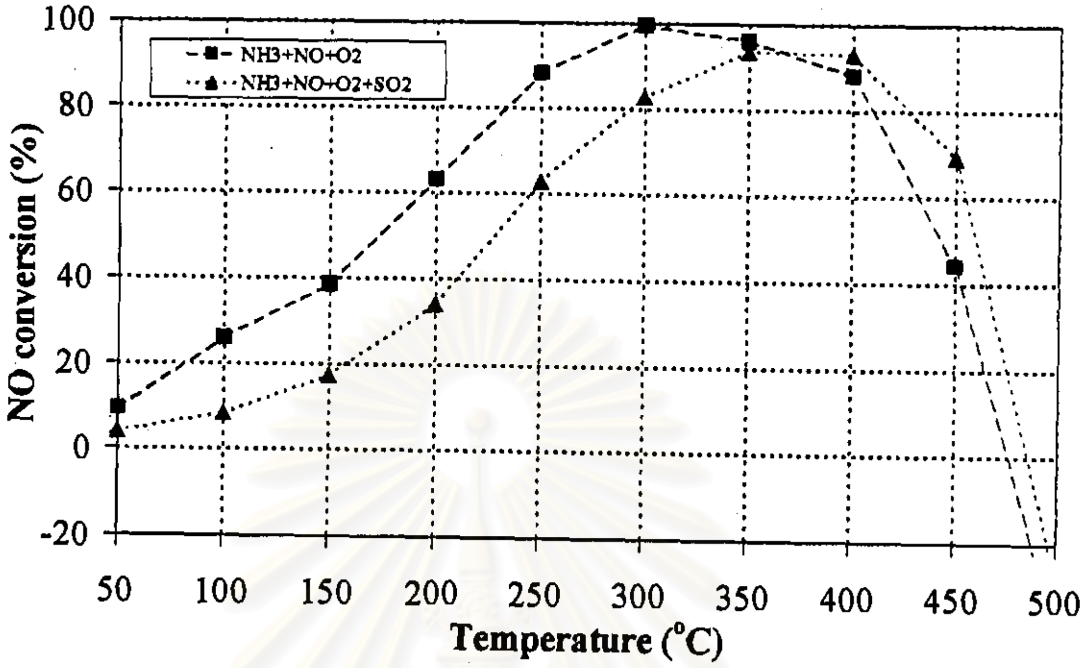

Figure 5.43 SCR activity of 5wt%W-25wt%V_2O_5/TiO_2

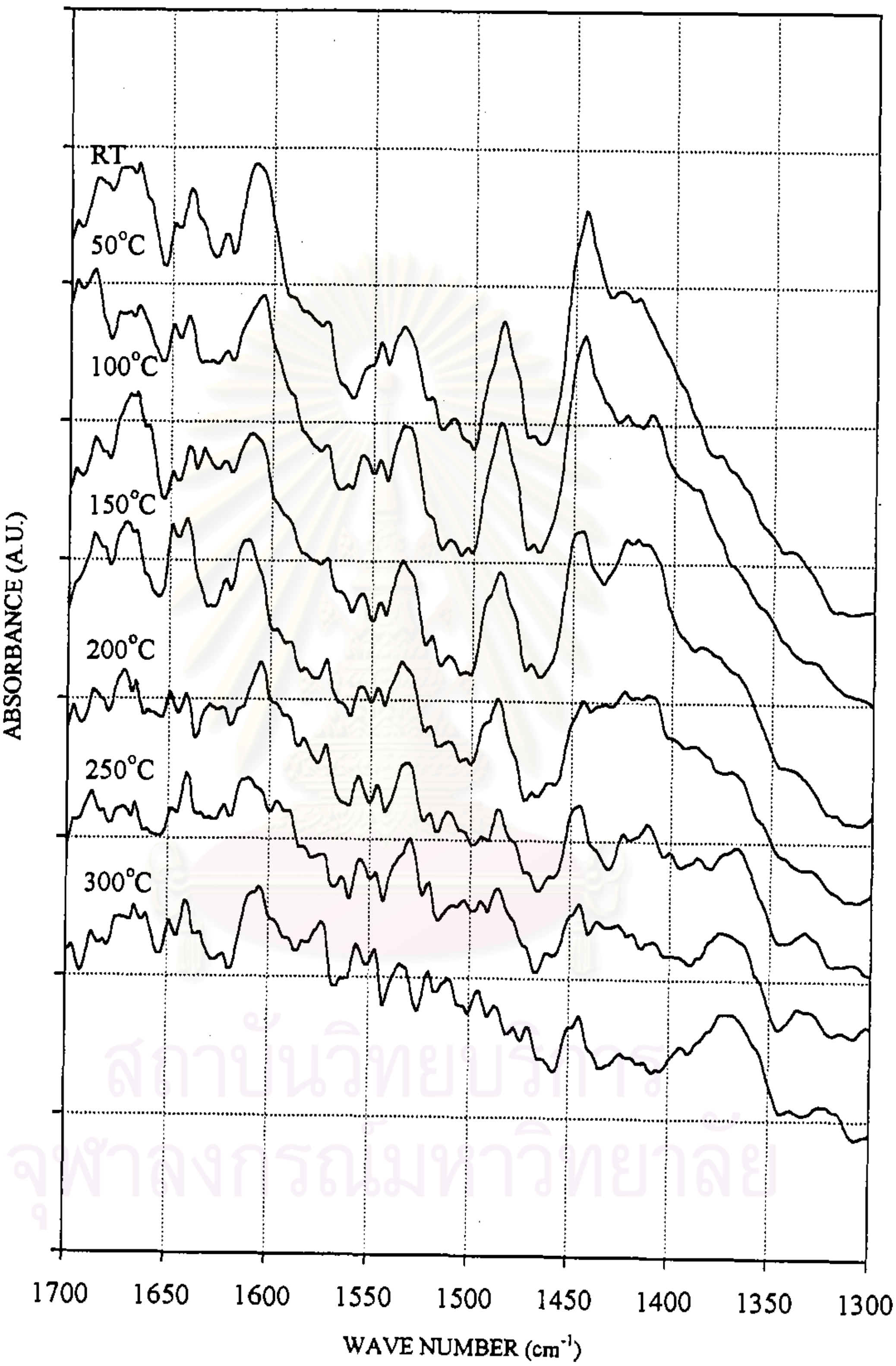

Figure 5.44 Pyridine adsorption on spent 5wt%W-25wt%V_2O_5/TiO_2 without SO_2 at 200°C

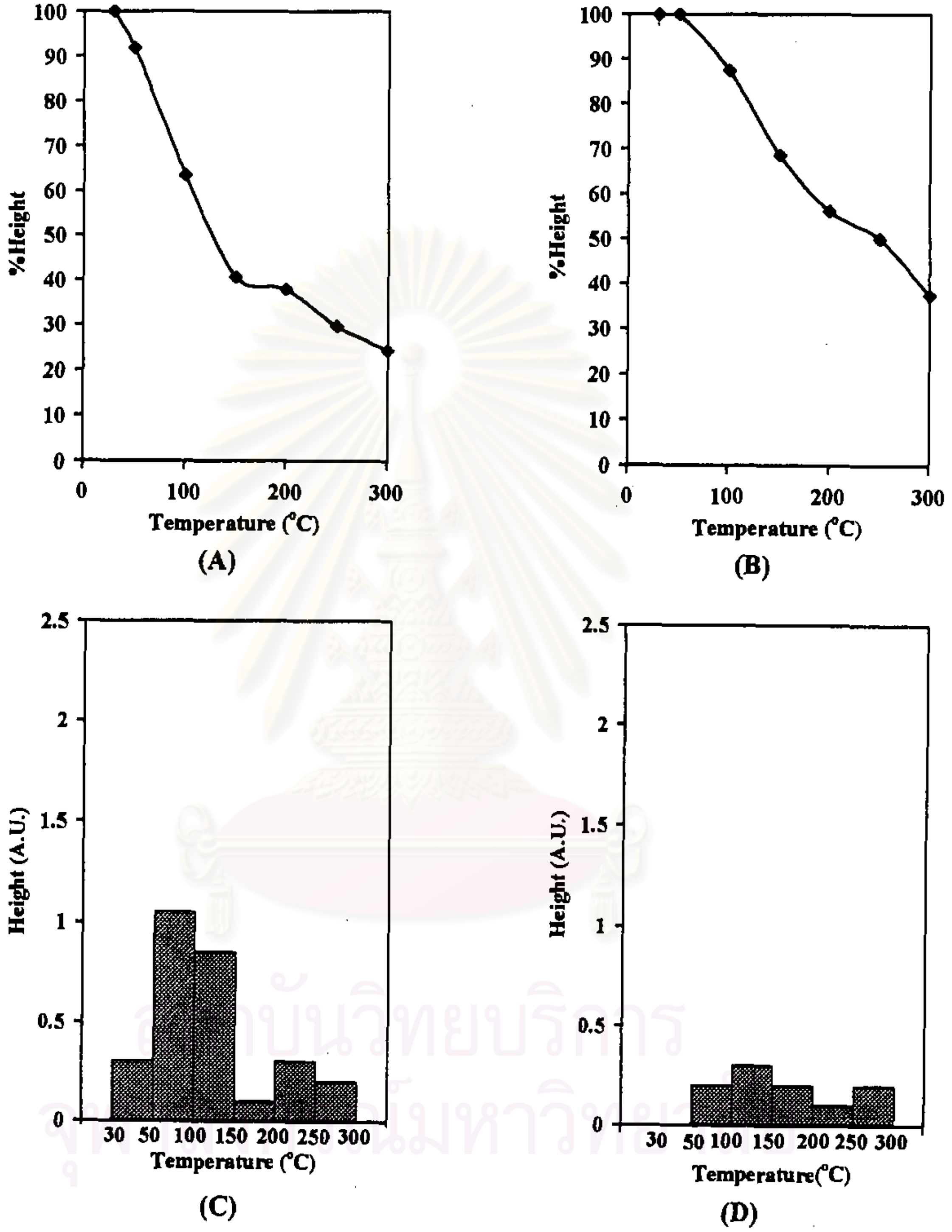

(A) (B) (C) (D)

Figure 5.45 The percentage of the band height of pyridine adsorbed on Lewis (A) and Brönsted (B) acid site and the amount of pyridine desorbed from Lewis (C) and Brönsted (D) acid site on spent 5wt%W-25wt%V_2O_5/TiO_2 without SO_2 at 200 °C

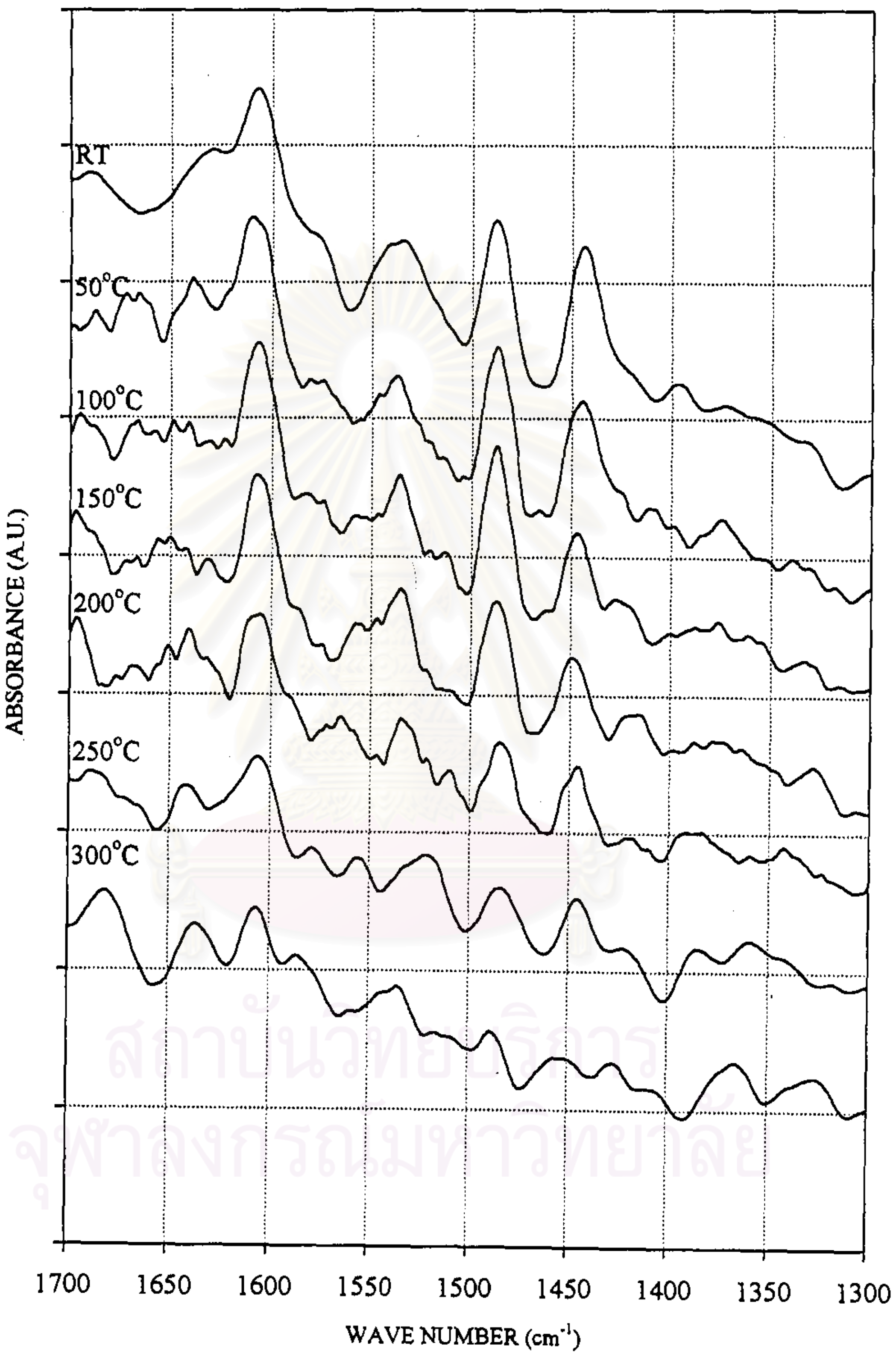

Figure 5.46 Pyridine adsorption on spent 5wt%W-25wt%V_2O_5/TiO_2 without SO_2 at 450°C

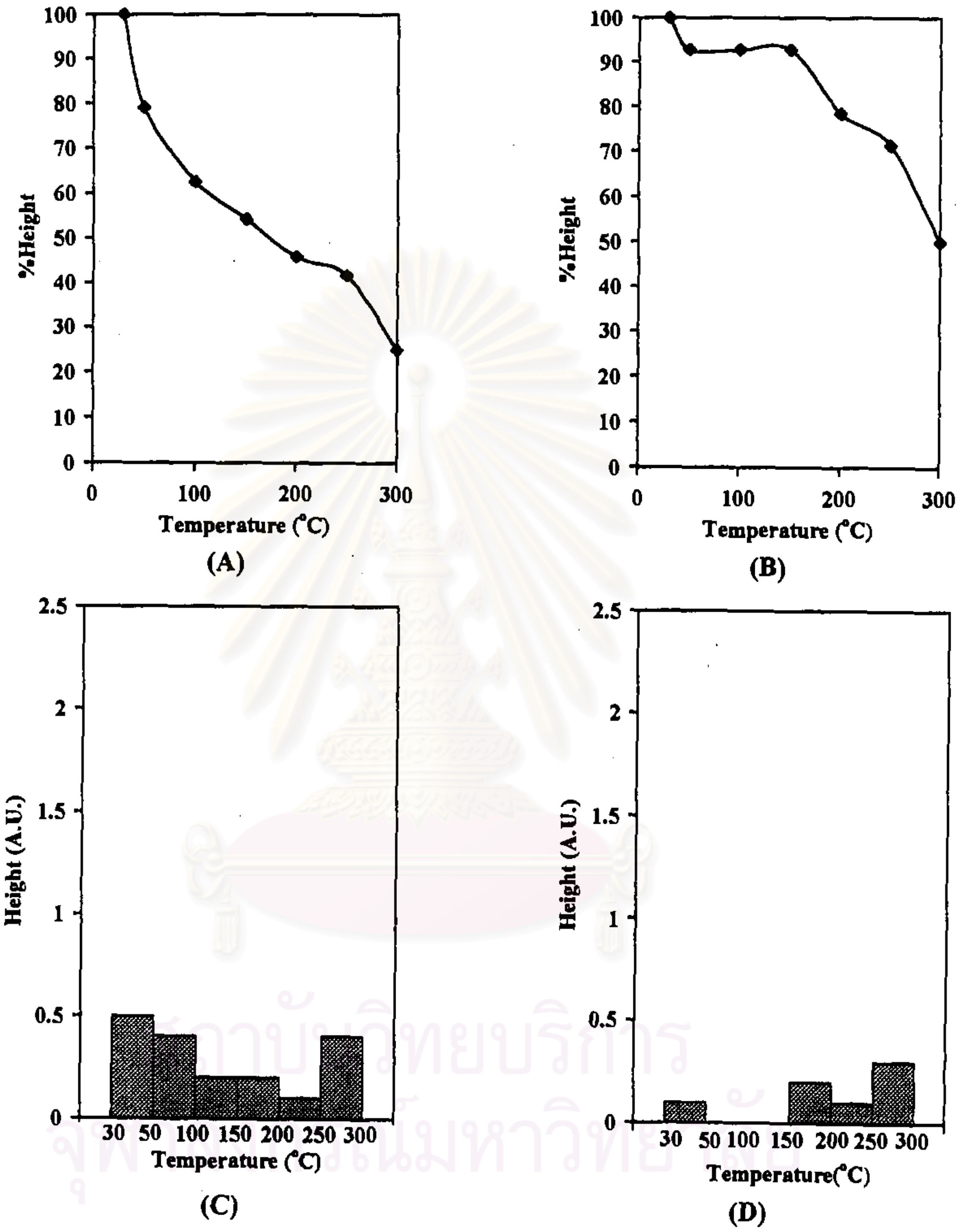

Figure 5.47 The percentage of the band height of pyridine adsorbed on Lewis (A) and Brönsted (B) acid site and the amount of pyridine desorbed from Lewis (C) and Brönsted (D) acid site on spent 5wt%W-25wt%V_2O_5/TiO_2 without SO_2 at 450 °C

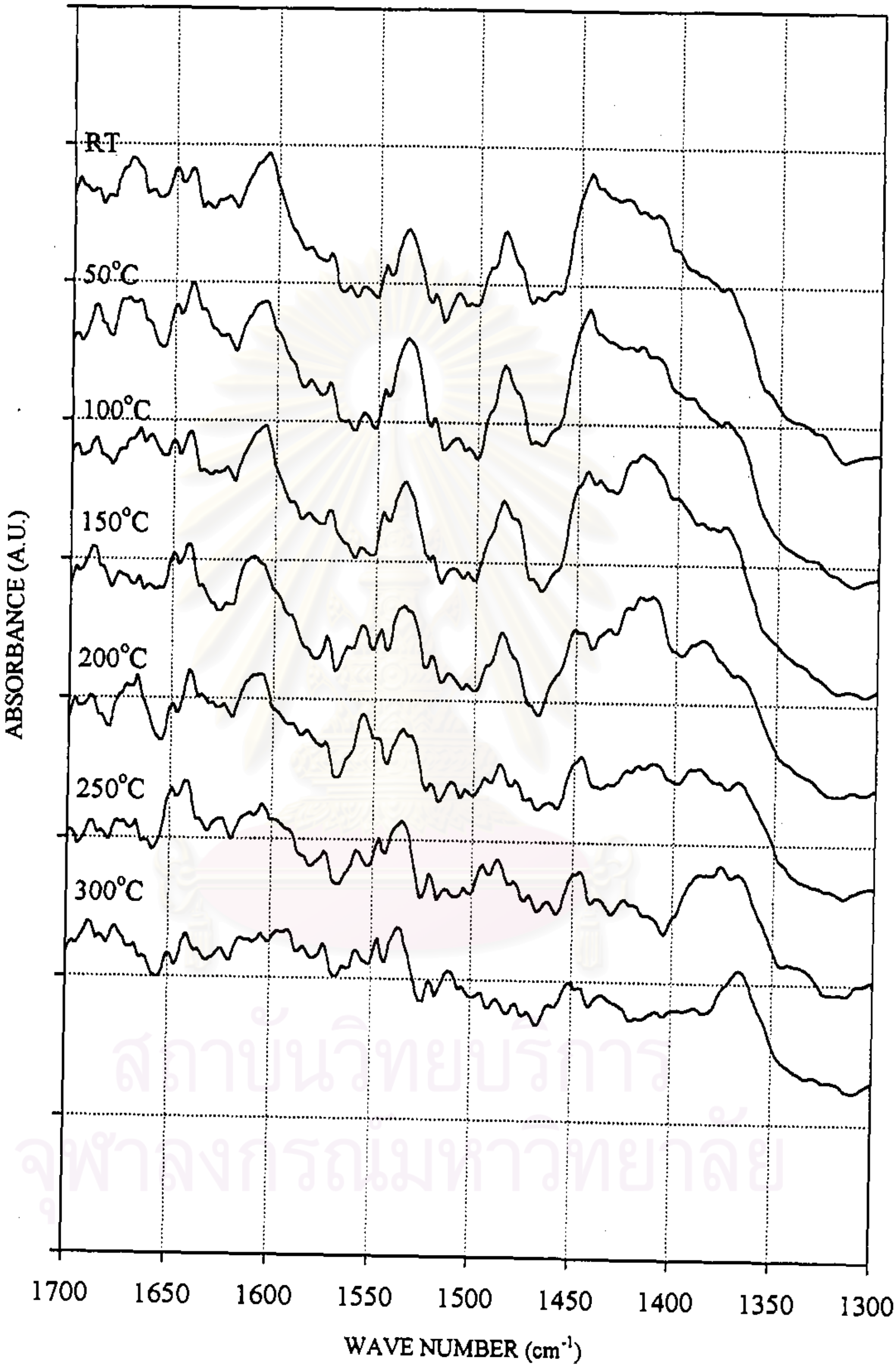

Figure 5.48 Pyridine adsorption on spent 5wt%W-25wt%V_2O_5/TiO_2 with SO_2 at 200°C

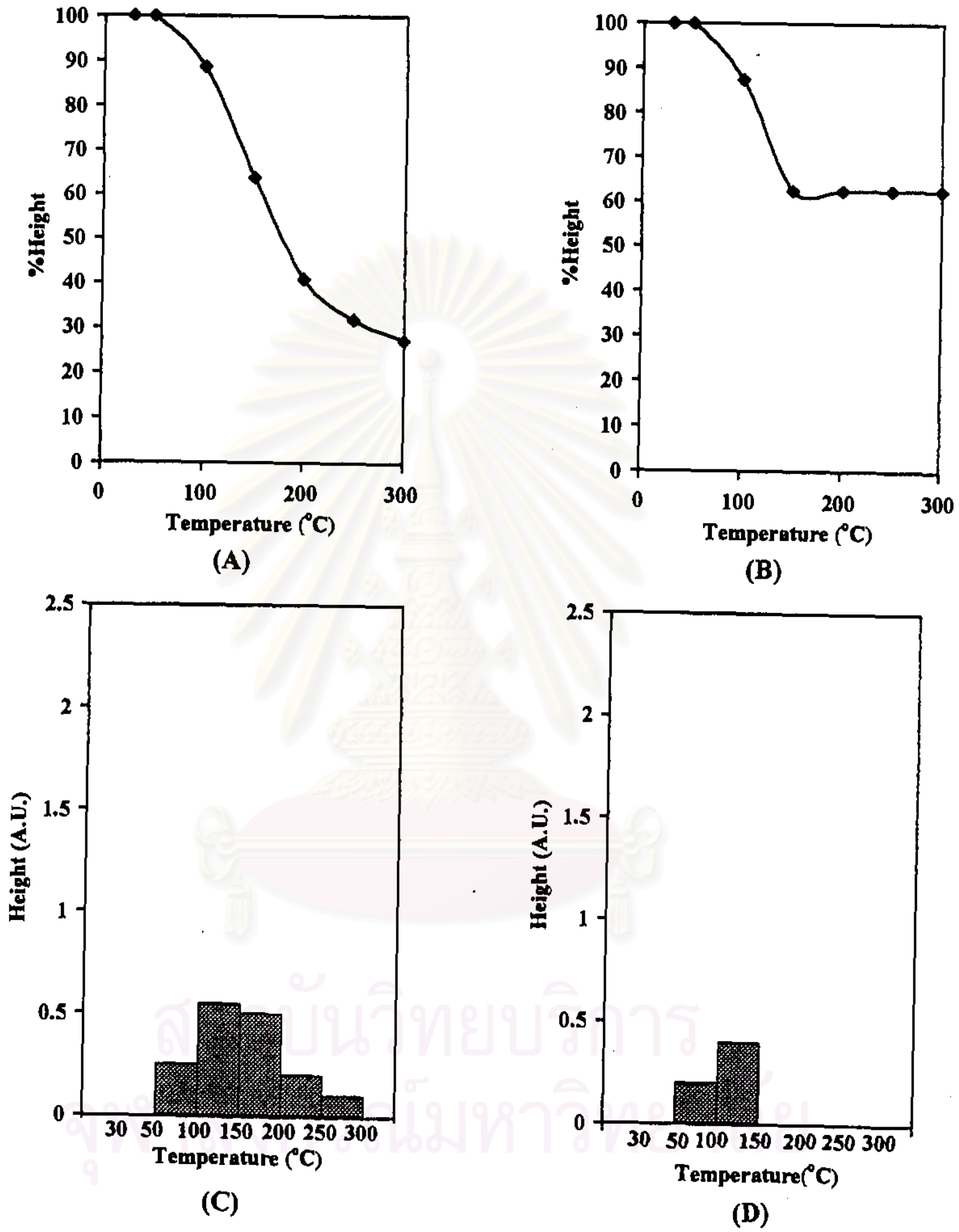

(A) (B)

(C) (D)

Figure 5.49 The percentage of the band height of pyridine adsorbed on Lewis (A) and Brönsted (B) acid site and the amount of pyridine desorbed from Lewis (C) and Brönsted (D) acid site on spent 5wt%W-25wt%V_2O_5/TiO_2 with SO_2 at 200 °C

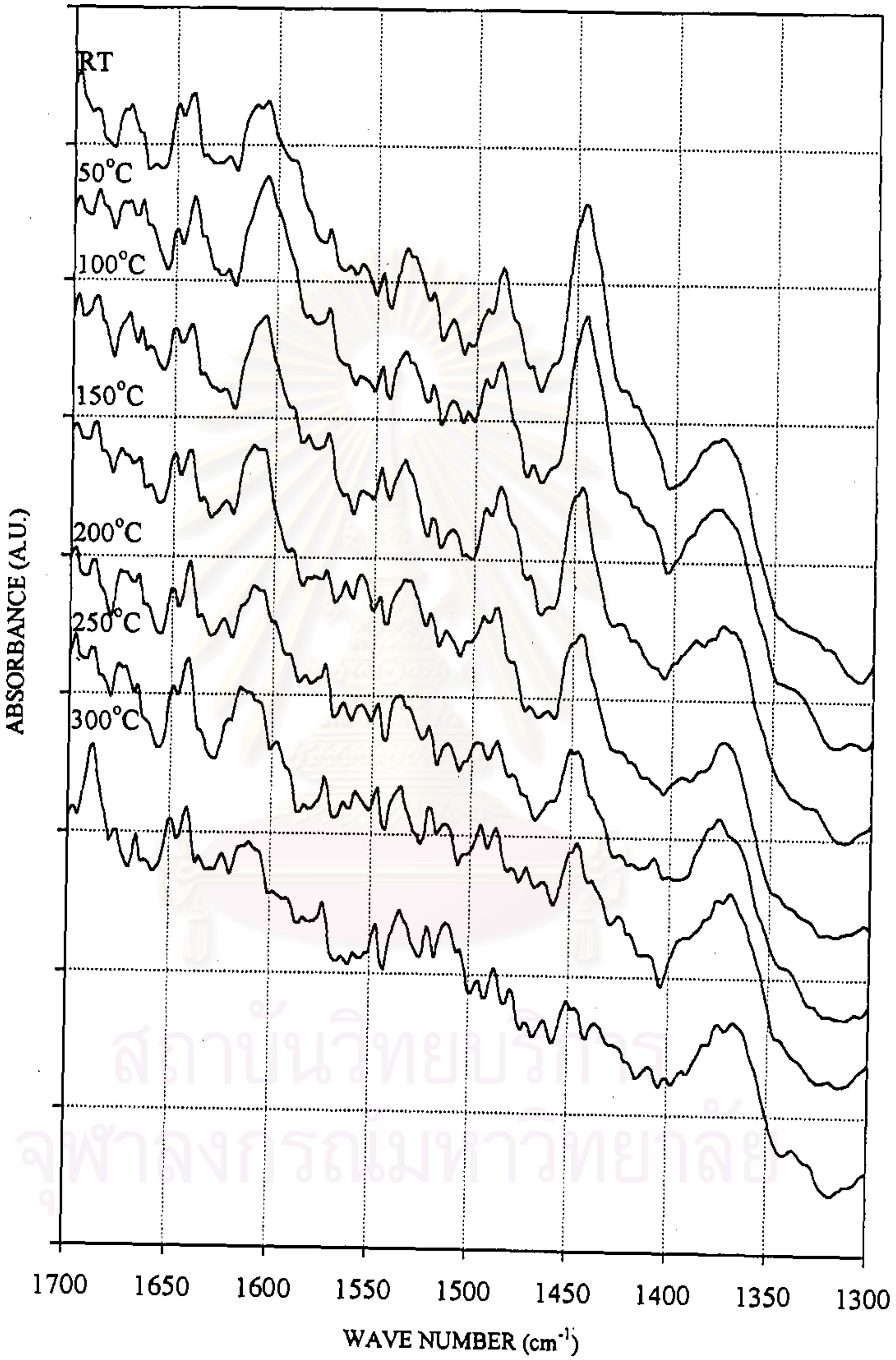

Figure 5.50 Pyridine adsorption on spent 5wt%W-25wt%V_2O_5/TiO_2 with SO_2 at 450°C

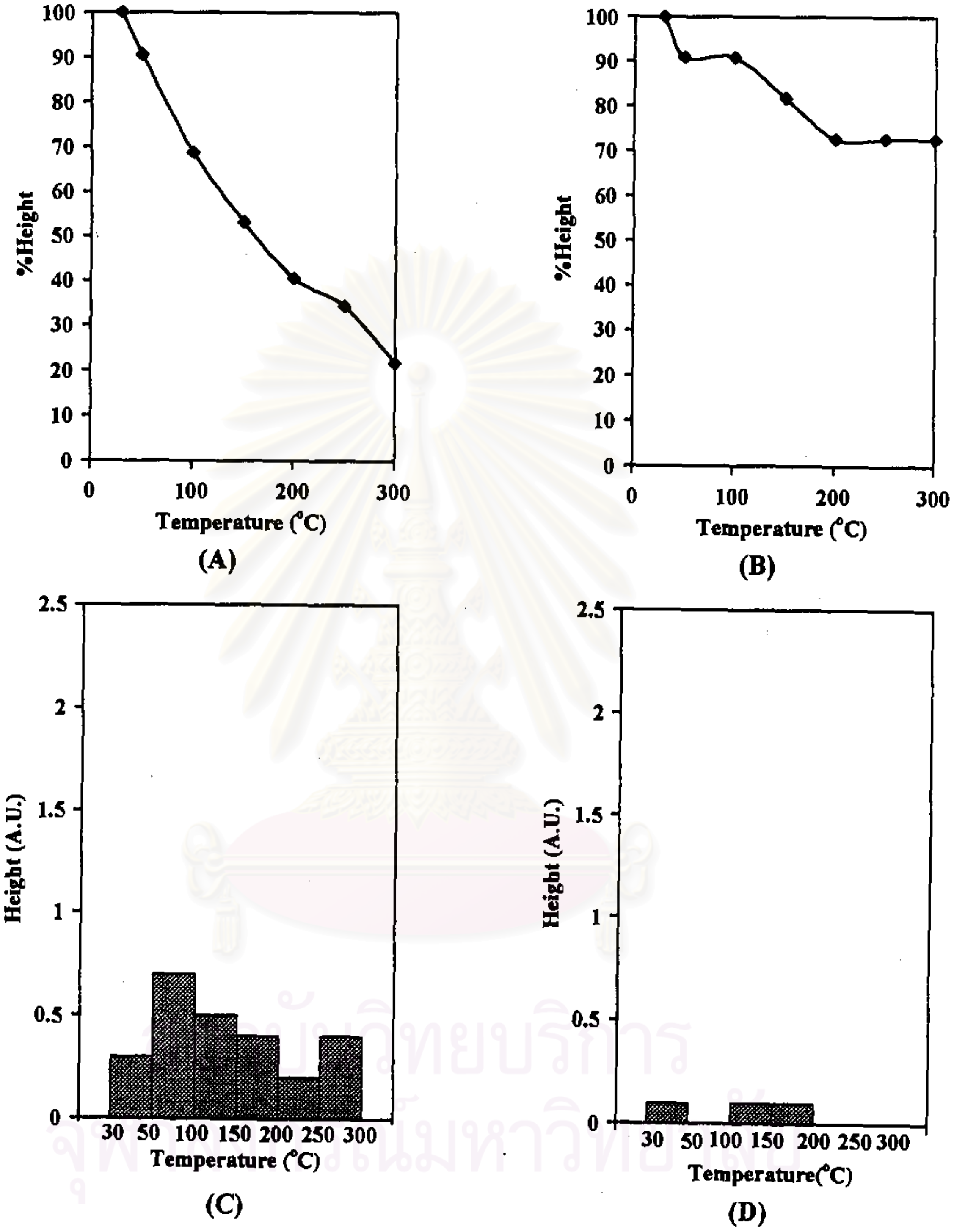

Figure 5.51 The percentage of the band height of pyridine adsorbed on Lewis (A) and Brönsted (B) acid site and the amount of pyridine desorbed from Lewis (C) and Brönsted (D) acid site on spent 5wt%W-25wt%V_2O_5/TiO_2 with SO_2 at 450 °C

Table 5.3 Comparison of the amount and strength of acid sites on 5wt%W-25wt%V_2O_5/TiO_2 catalysts at various reaction temperatures.

Comparison of catalysts	Lewis acid site			Brönsted acid site		
	Total	weak	strong	Total	weak	strong
200°C/fresh	↓↓↓	↓↓↓	↓↓	↓↓↓	↑	↓↓↓
450°C/fresh	↓↓↓	↓↓↓	↓↓	↓↓	↓	↓
450°C/200°C	↓↓	↓↓	↑	↑↑	↓	↑↑
200°C with SO_2/fresh	↓↓↓	↓↓↓	↓↓	↓↓	↑↑	↓↓↓
450°C with SO_2/fresh	↓↓	↓↓↓	constant	↓↓	constant	↓↓
450°C with SO_2/200°C with SO_2	↑↑	↑↑	constant	↓	↓	constant
200°C with SO_2/200°C	↓↓	↓↓	constant	↓↓	↑	↓↓
450°C with SO_2/450°C	↑↑	↑↑	↑↑	↓↓	↑	↓↓

↑ < ↑↑ < ↑↑↑ and ↓↓↓ > ↓↓ > ↓

- **3wt%K-25wt%V_2O_5/TiO_2**

Figure 5.52 shows NO conversion of 3wt%K-25wt%V_2O_5/TiO_2 in the reaction with and without SO_2 in feed gas. It is observed that in the reaction with SO_2 at the temperature below 300 °C NO conversion is higher than that of the reaction without SO_2. In case of reaction temperature higher than 300 °C, in the reaction with SO_2 NO conversion significantly decreases. The reasons are that SO_2 improves the SCR reaction at temperature below 300 °C and suppresses the SCR reaction at high temperature.

To clarify the effect of SO_2 on the SCR activity of 3wt%K-25wt%V_2O_5/TiO_2, acidity measurement of the spent 3wt%K-25wt%V_2O_5/TiO_2 at 200 °C and 450 °C in the reaction with and without SO_2 is performed to explain changing of acidity on the SCR activity. The acidity measurement in the reaction without SO_2 shows that the amount of Lewis acid site on the spent 3wt%K-25wt%V_2O_5/TiO_2 at reaction temperature 200 °C (as shown in figures 5.54-55) is lower than that obtained from reaction at 450 °C (see figures 5.55-5.56). While Brönsted acid site of the spent 3wt%K-25wt%V_2O_5/TiO_2 can be neglected because of a little amount. When compare this spent catalyst with fresh 3wt%K-25wt%V_2O_5/TiO_2 it can be seen that the spent catalyst has lower amount of Lewis acid site. In case of the reaction with SO_2, figures 5.57-5.58 and 5.59-5.60 show the amount of Lewis and Brönsted acid site of the spent 3wt%K-25wt%V_2O_5/TiO_2 at reaction temperatures of 200 °C and 450 °C, respectively. The amount of Lewis acid site at 200 °C is lower than that at 450 °C and is similar to that of fresh 3wt%K-25wt%V_2O_5/TiO_2.

It has been previously said that in the reaction with SO_2 at temperature below 300 °C NO conversion is higher. The effect of changing activity of the spent catalyst at 200 °C shows that in case of the reaction with SO_2 the spent catalyst has higher amount of Lewis acid site. Thus, it can be concluded that at low temperature SO_2 increases Lewis acid site and enhances the SCR reaction. In the reaction with SO_2 at high temperature, NO conversion is more decreased but in the reaction without SO_2 NO conversion is increased slowly. From acidity data, it is found that in the presence of SO_2 in reaction the amount and strength of Lewis acid site is much higher than that the absence of SO_2. When the spent catalyst from the reaction with SO_2 is characterized by using FT-IR, no new band (of NH_4SO_4 or $(NH_4)_2SO_2$) can be observed (as shown in appendix B). Thus, it can be suggested that in the reaction with SO_2 at high temperature, the increase of the amount and strength of Lewis acid site on 3wt%K-25wt%V_2O_5/TiO_2 promotes NH_3 oxidation which results in a fast drop in NO conversion. It is relevant to the case of 25wt%V_2O_5/TiO_2 in the reaction with SO_2 that SO_2 improves the amount and strength of Lewis acid site of the catalyst at high temperature since NH_3 oxidation reaction highly occurs too. Comparison of the amount and strength of acid sites on 3wt%K-25wt%V_2O_5/TiO_2 catalysts at various temperatures are summarized in Table 5.4.

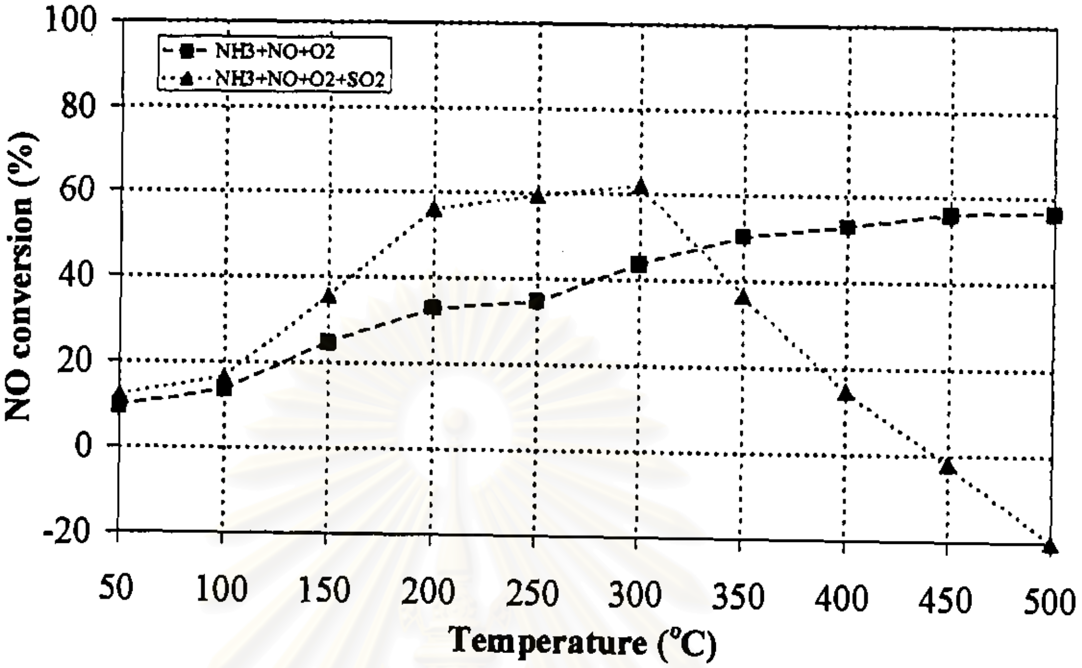

Figure 5.52 SCR activity of 3wt%K-25wt%V_2O_5/TiO_2

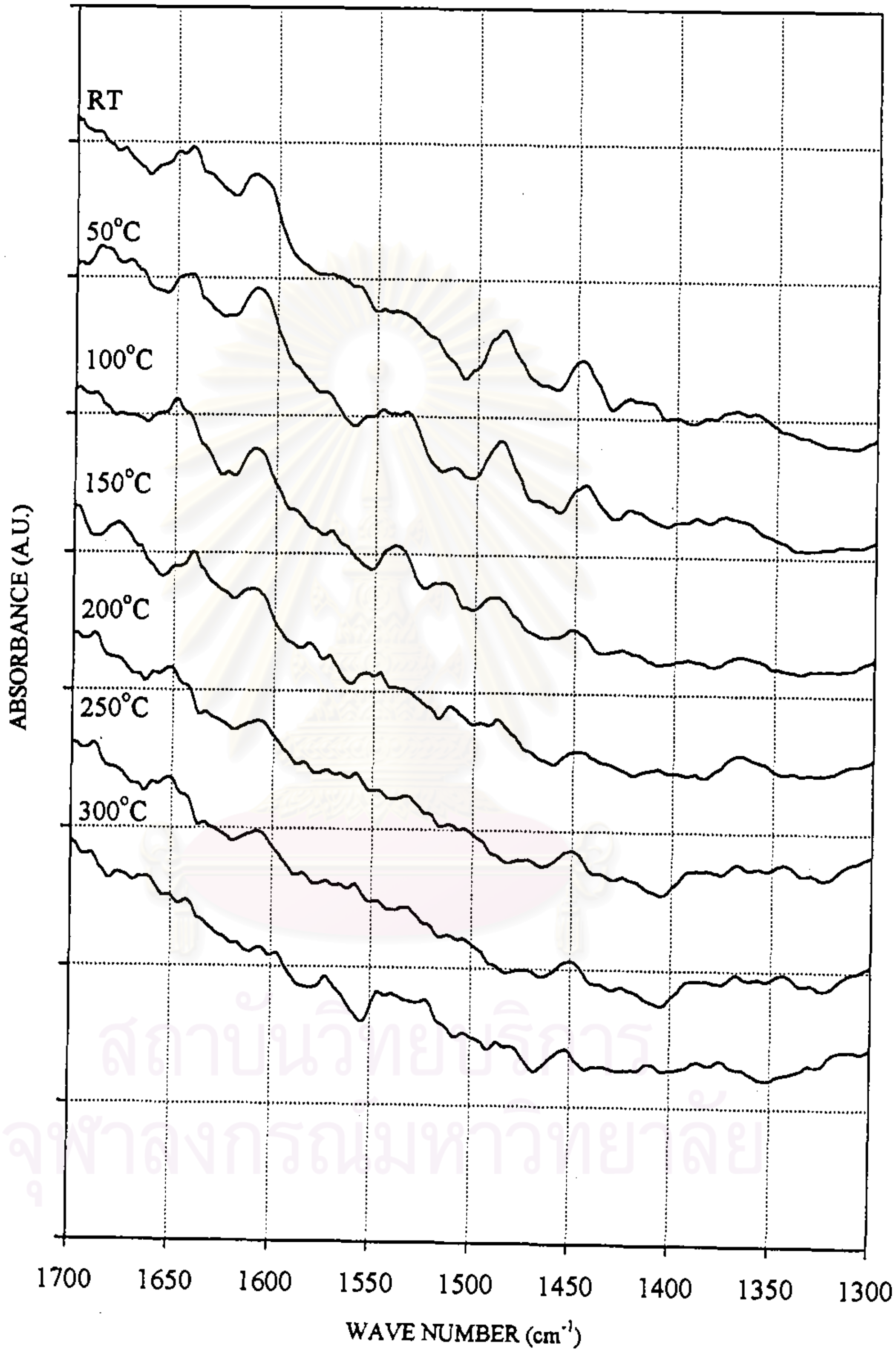

Figure 5.53 Pyridine adsorption on spent 3wt%K-25wt%V_2O_5/TiO_2 without SO_2 at 200°C

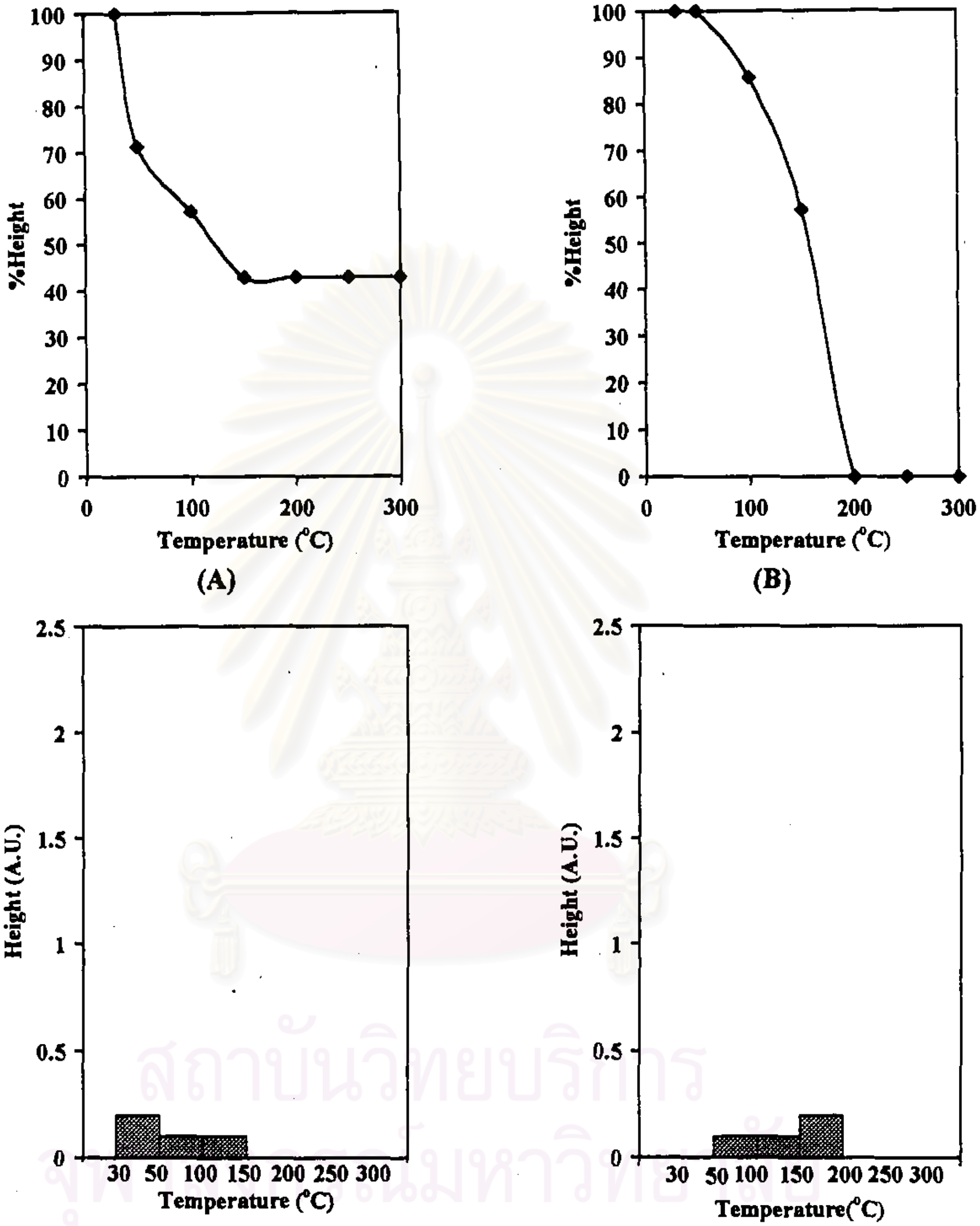

(A) (B)

(C) (D)

Figure 5.54 The percentage of the band height of pyridine adsorbed on Lewis (A) and Brönsted (B) acid site and the amount of pyridine desorbed from Lewis (C) and Brönsted (D) acid site on spent 3wt%K-25wt%V_2O_5/TiO_2 without SO_2 at 200 °C

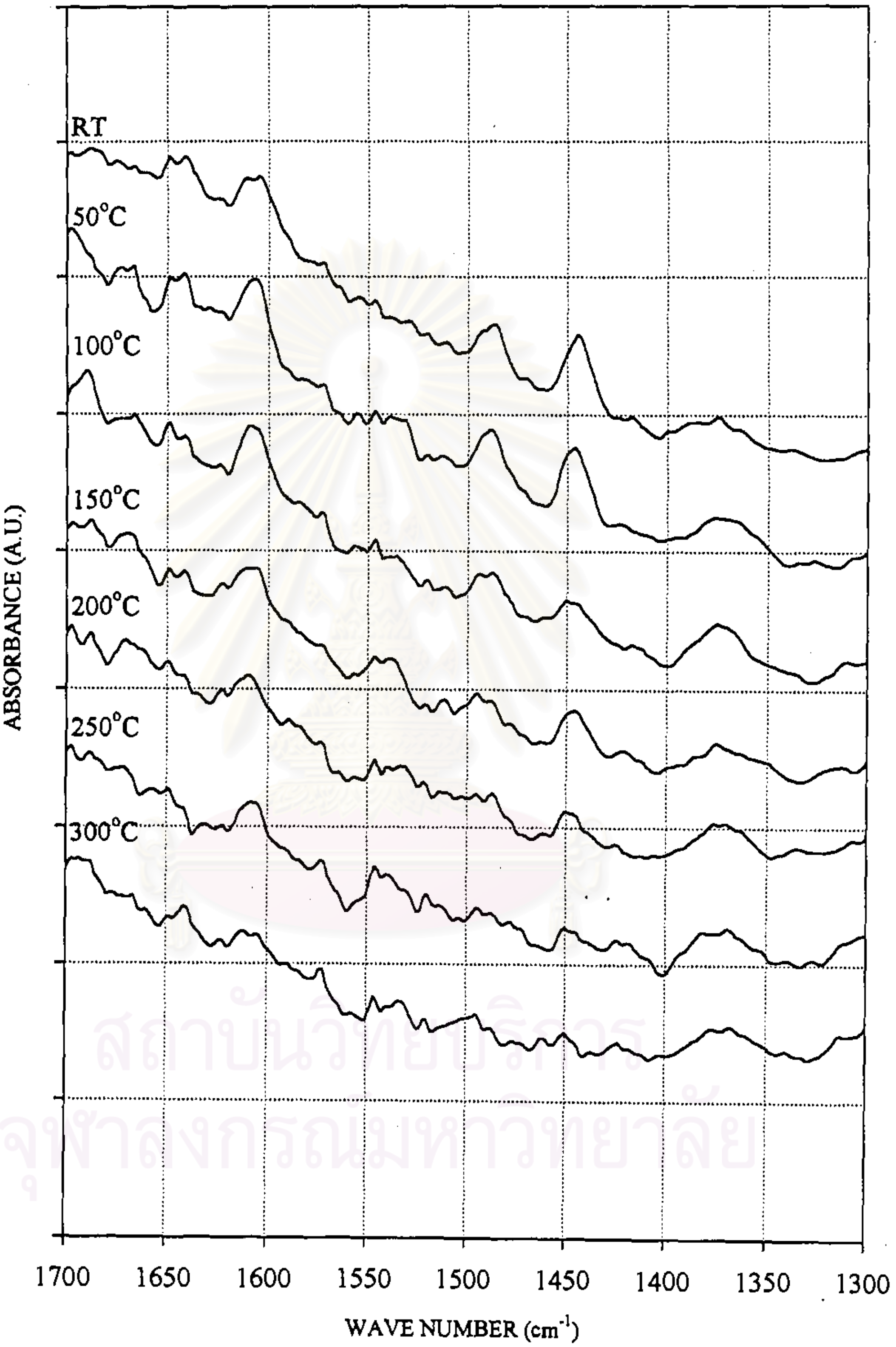

Figure 5.55 Pyridine adsorption on spent 3wt%K-25wt%V_2O_5/TiO_2 without SO_2 at 450°C

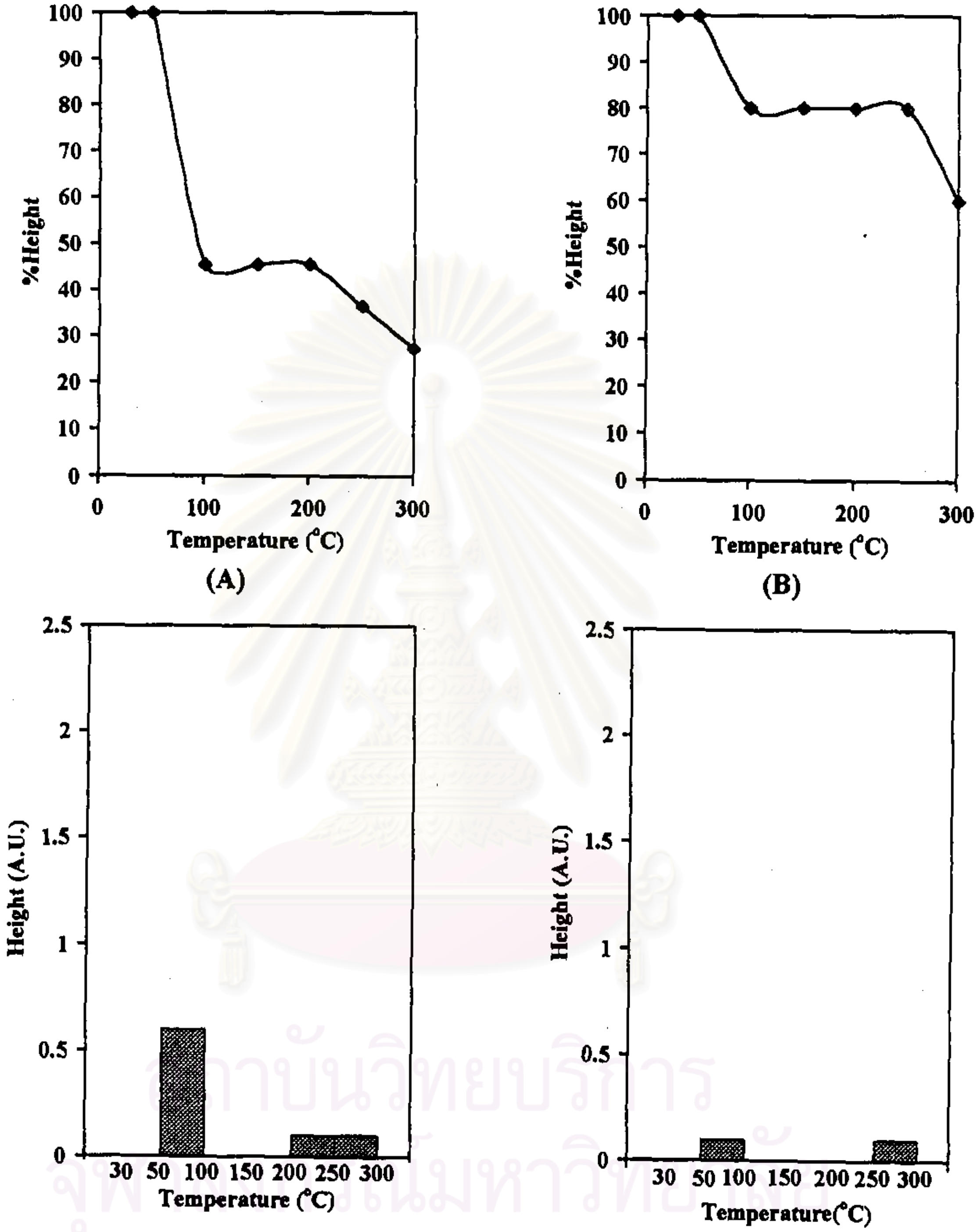

(A) (B)

(C) (D)

Figure 5.56 The percentage of the band height of pyridine adsorbed on Lewis (A) and Brönsted (B) acid site and the amount of pyridine desorbed from Lewis (C) and Brönsted (D) acid site on spent 3wt%K-25wt%V_2O_5/TiO_2 without SO_2 at 450 °C

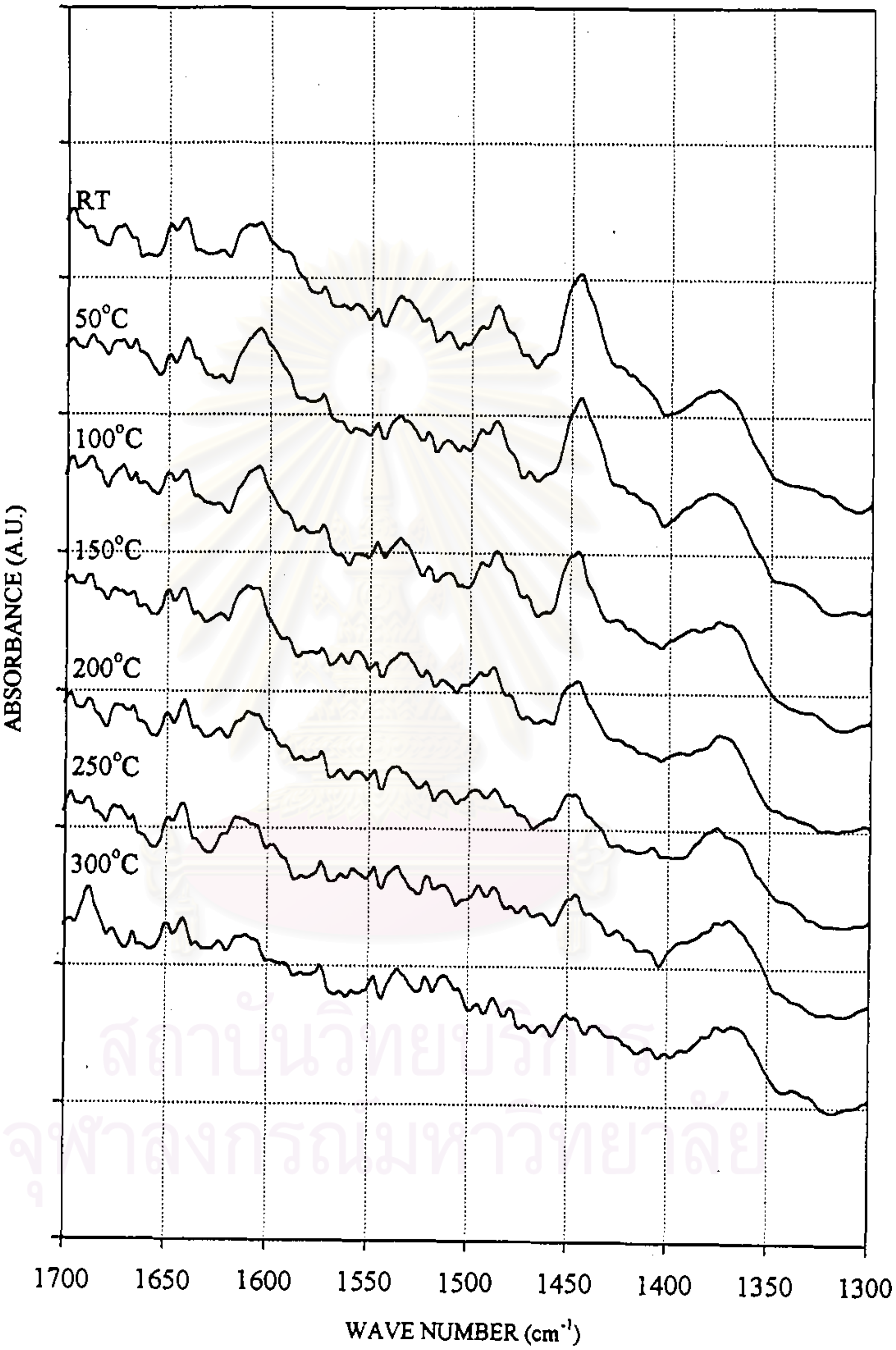

Figure 5.57 Pyridine adsorption on spent 3wt%K-25wt%V_2O_5/TiO_2 with SO_2 at 200°C

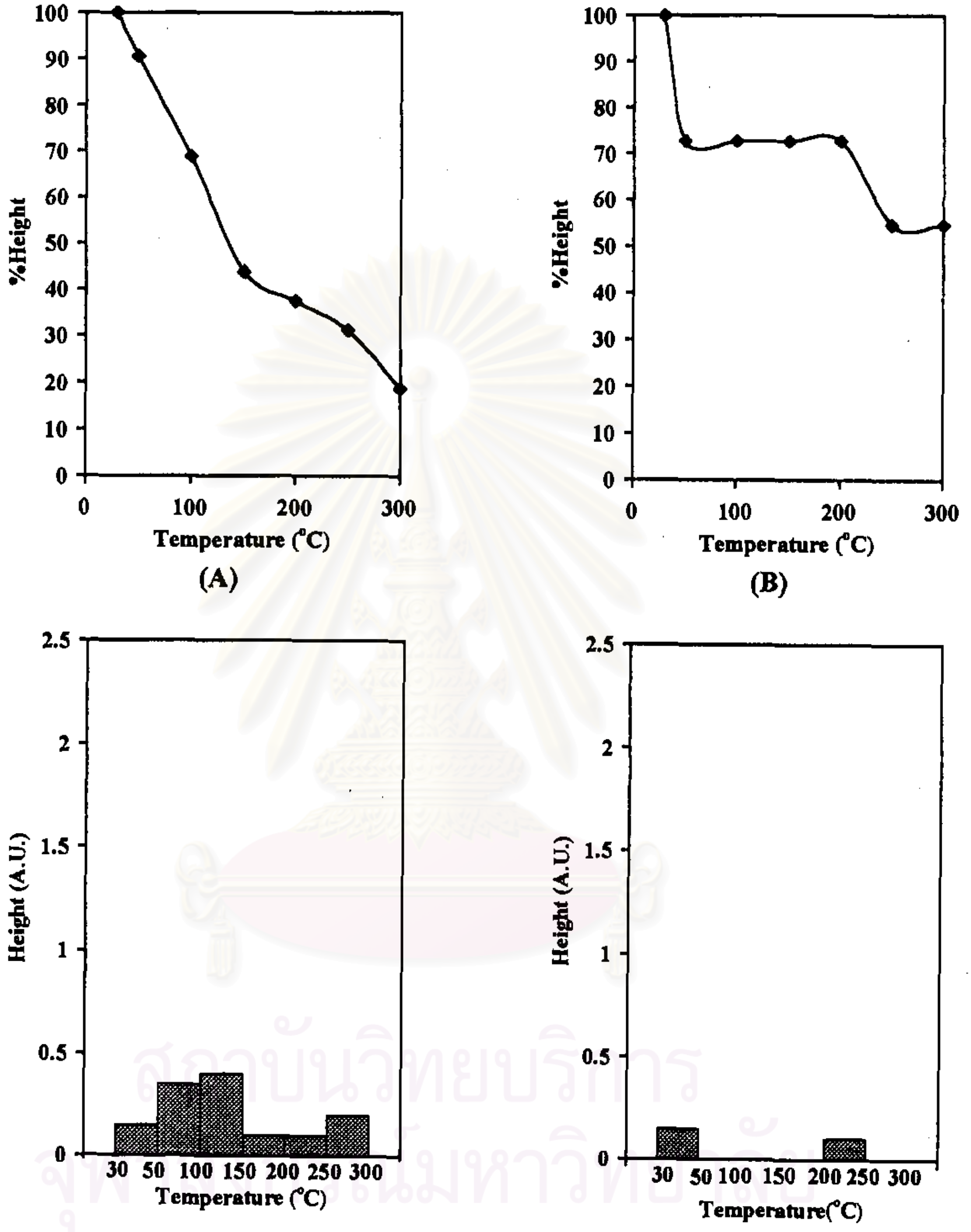

(A)

(B)

(C)

(D)

Figure 5.58 The percentage of the band height of pyridine adsorbed on Lewis (A) and Brönsted (B) acid site and the amount of pyridine desorbed from Lewis (C) and Brönsted (D) acid site on spent 3wt%K-25wt%V_2O_5/TiO_2 with SO_2 at 200 °C

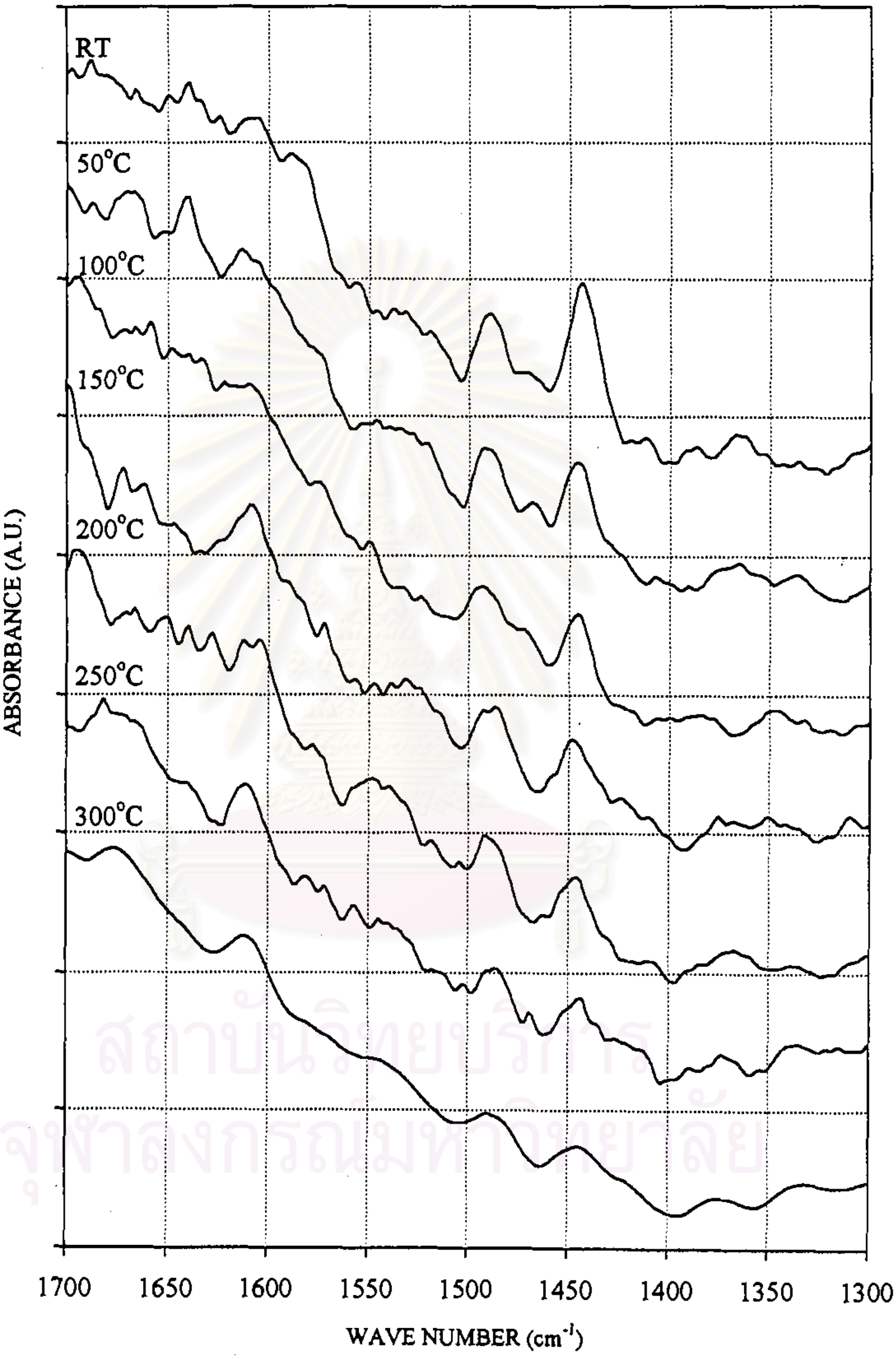

Figure 5.59 Pyridine adsorption on spent 3wt%K-25wt%V_2O_5/TiO_2 with SO_2 at 450°C

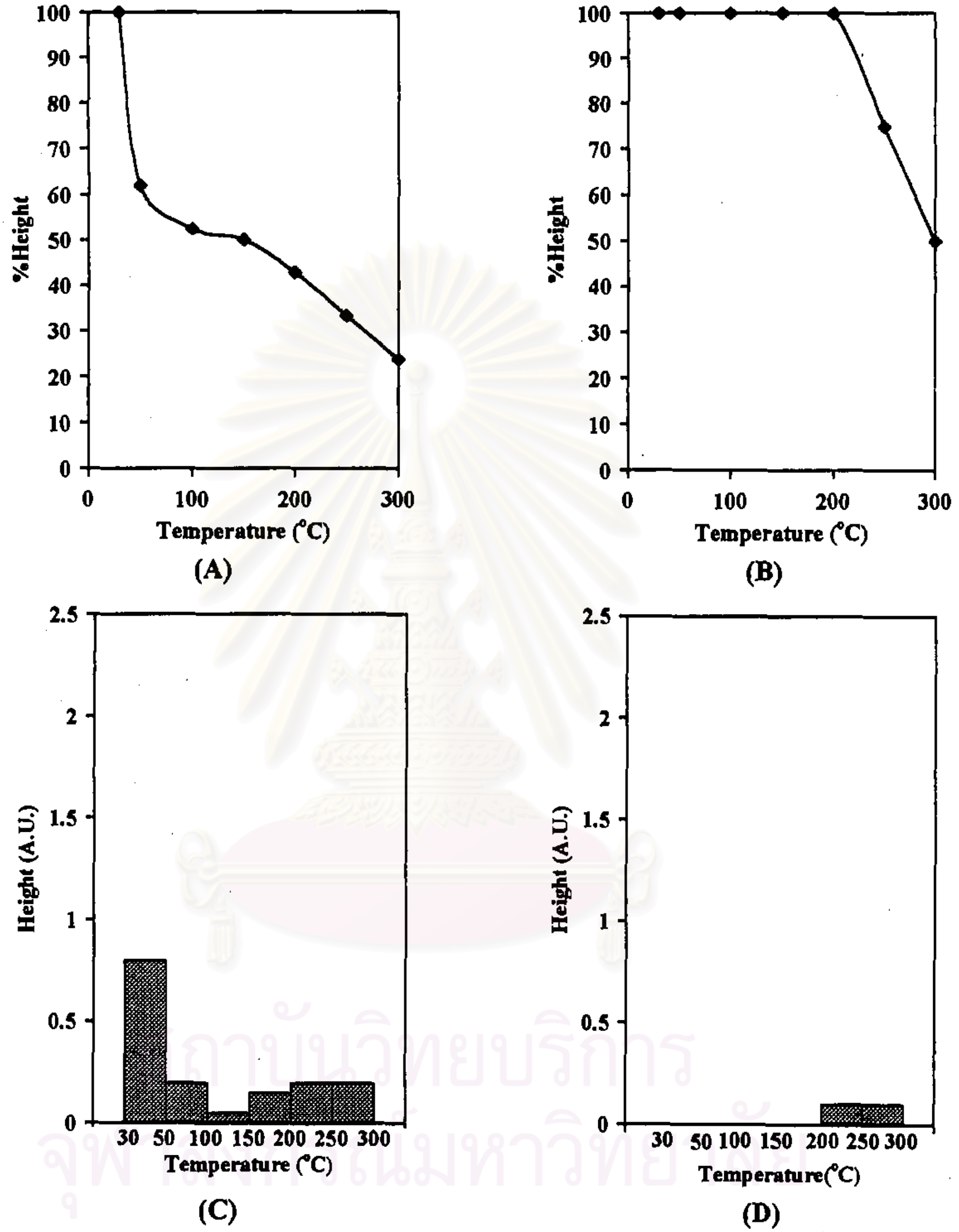

(A)

(B)

(C)

(D)

Figure 5.60 The percentage of the band height of pyridine adsorbed on Lewis (A) and Brönsted (B) acid site and the amount of pyridine desorbed from Lewis (C) and Brönsted (D) acid site on spent 3wt%K-25wt%V_2O_5/TiO_2 with SO_2 at 450 °C

Table 5.4 Comparison of the amount and strength of acid sites on 3wt%K-25wt%V_2O_5/TiO_2 catalysts at various reaction temperatures

Comparison of catalysts	Lewis acid site			Brönsted acid site		
	Total	weak	strong	Total	weak	strong
200°C/fresh	↓↓	↓↓	↓↓	-	-	-
450°C/fresh	↓↓	↓↓	↓	-	-	-
450°C/200°C	↑↑	↑	↑	-	-	-
200°C with SO_2/fresh	↓	↓	↑	-	-	-
450°C with SO_2/fresh	↑	↓	↑	-	-	-
450°C with SO_2/200°C with SO_2	↑↑	↑	↑↑	-	-	-
200°C with SO_2/200°C	↑↑	↑↑	↑↑	-	-	-
450°C with SO_2/450°C	↑↑	↑↑	↑↑	-	-	-

↑ < ↑↑ < ↑↑↑ and ↓↓↓ > ↓↓ > ↓